Supporting Information

Design and Synthesis of 'Chloropicolinate Amides and Urea Derivatives' as Novel Inhibitors for *Mycobacterium Tuberculosis*

Srihari Konduri[§], Dodda Bhargavi [§], Jyothi Prashanth[†], Vagolu Siva Krishna[‡], Dharmarajan Sriram[‡], and Koya Prabhakara Rao [§*]

[§]*New Generation Materials Lab (NGML), Department of Science and Humanities, Vignan's Foundation for Science Technology and Research (VFSTR) (Deemed to be University), Vadlamudi-522 213, Guntur, Andhra Pradesh, India*
[†]*Department of physics, Kakatiya University, Warangal-506009, Telangana, India*
[‡]*Department of Pharmacy, Birla Institute of Technology & Amp; Science-Pilani, Hyderabad Campus, Shameerpet, Jawaharnagar, Hyderabad-500 078, India.*

∗Corresponding author. Tel.: +91-967-715-7858; fax: +91-863-253-4468; e-mail: drkpr_sh@vignan.ac.in ; kprao2005@gmail.com

Syntheses

Synthesis of 6-bromo-3-chloropyridine-2-carboxylic acid (2).

To a stirred solution of 3, 6-dichloropyridine-2-carboxylic acid (5.0 g, 26.04 mmol) in acetic acid (10.0 mL), added HBr (33 %) in acetic acid (1.2 mL, 6.51mmol). The whole reaction mixture was pre-heated to 110 ^{o}C, and added HBr (33 %) in acetic acid (9.0 mL, 49.48 mmol). The reaction mixture was stirred at the same temperature over a period of 24 hrs. Later the product was cooled to room temperature and poured into ice water. After filtration, compound **2**, off-white solid with good yield.[1,2]

Synthesis of methyl 6-bromo-3-chloropyridine-2-carboxylate (3).

To compound **2**, (4.3 g, 18.19 mmol) in methanol (25 mL), added slowly dropwise sulphuric acid (2.91 mL, 54.56 mmol) and refluxed for 6 hrs. The reaction mixture was concentrated and added water (70 mL). Filtered the product to get compound **3**, off-white solid.[1,2]

Synthesis of* methyl 6-bromo-3-chloropyridine-2-carboxylate-N-oxide *(4).

Compound **3**,(3.9 g, 15.57 mmol) in trifluoroacetic acid (7.7 mL, 99.65 mmol) was cooled to 5-10 °C. Later to this reaction mixture, added slowly trifluoroacetic anhydride (4.0 mL, 28.03 mmol) and 50% H_2O_2 (1.6 mL, 15.57 mmol) simultaneously. The whole reaction mixture heated to 80 ^{0}c for 3 hrs. After completion of the reaction, the product was poured into a mixture of ice and sodium bisulfite solution. The compound **4**, was filtered and dried to get off-white solid.[1,2]

Synthesis of methyl 6-bromo-4-nitro-3-chloropyridine-2-carboxylate-N-oxide (5).

To a stirred solution of nitric acid(11.7 mL, 262 mmol) and sulfuric acid (11.7 mL, 219.3 mmol) was cooled to 0-10 ^{0}c and added portions wise **4**, (3.5 g, 13.3 mmol). The whole reaction mixer was stirred at 70 ^{0}c for 4 hrs. After completion of the reaction, the product was poured into ice and extracted with ethyl acetate. The ethyl acetate layers were washed water and brine, dried with Na_2SO_4 and distilled out under reduced pressure conditions to get pale yellow color solid.[1,2]

Synthesis of methyl 4-amino-6-bromo-3-chloropyridine-2-carboxylate (6).

To the mixture of **5** (3.0 g, 9.63 mmol) in methanol (40 mL) in to hydrogenation partiaker, aadded Raney-Ni (0.8 g) and flush with nitrogen for two times and then applied

hydrogen pressure (60 psi). The whole reaction mixture was stirred at 45 ^{0}c for 8 hrs. After completion of the reaction, passed the nitrogen gas and filter through hyflo by washing with methanol. Distil out the methanol under vacuum to get the crude product. The product was purified using column chromatography with EtOAc: *n*-Hexane (30:70), to get **6** (1.7 g, 66 %). ^{1}H NMR (300 MHz, DMSO) δ 6.95 (s, 1H), 5.11 (s, 2H), 3.97 (s, 3H); ^{13}C NMR (75 MHz, DMSO) δ 165.1, 150.9, 147.3, 138.3, 114.7, 53.1; MS: *m/z* 265.40 $[M+H]^{+}$.

Synthesis of methyl 4-amino-6-(2-aminophenyl)-3-chloropyridine-2-carboxylate (7).

The compound **6** (1.5 g, mmol) in Ethanol/Toluene (1:1) (20 ml) was degassed with nitrogen. Later, 2-amino phenylboronic acid (1.0 g, 7.34 mmol), K_2CO_3 (1.17 g, 8.47 mmol), and Pd(dppf)Cl_2 (0.21 g, 0.28 mmol) were added to the reaction mixture and stirred for 3 h at 90 ^{o}C. The crude product was filtered to remove the catalyst and washed with water. Later from the mixture, the product was extracted with ethyl acetate (2x10ml). The organic layer was washed water and brine, dried over Na_2SO_4 and distilled out under reduced pressure conditions. The product was purified by column chromatography (Ethyl acetate: Hexane, 75:25) to afford scaffold, methyl 4-amino-6-(2-aminophenyl)-3-chloropyridine-2-carboxylate[12] off white solid (0.91 g, 57 %); ^{1}H NMR (300 MHz, DMSO) δ 7.32 (m, 1H), 7.11 (s, 1H), 7.08 (m, 1H), 6.72 (d, J= 8.1 Hz, 1H), 6.69 (s, 2H), 6.60 (m, 1H), 6.27 (s, 2H), 3.88 (s, 3H); ^{13}C NMR (75 MHz, DMSO) δ 165.3, 156.1, 152.0, 147.2, 146.0, 129.5, 128.4, 119.4, 116.3, 115.6, 110.1, 107.7, 52.4; HRMS: *m/z* 278.0695 $[M+H]^{+}$.

***In-vitro* anti-tubercular activity determination**

Anti-mycobacterial activity against *Mycobacterium tuberculosis* minimum inhibitory concentrations (MIC) values for the most potent inhibitors were obtained using the microplate alamar blue assay (MABA) method. The Mt cultures, H37Rv in Middlebrook 7H9 broth with 10 % OADC (0.5 % glycerol, 0.1 % casitone, supplemented oleic acid, dextrose, albumin and catalase) (Himedia make) having OD590 1.0 were diluted to 1:20, of which 100 µL culture was used as inoculum for the screening. Moreover, the stock solutions of each test compound were diluted to four times in Middlebrook 7H9 broth and also the maximum concentration used in any test was 100 µM. Compounds used for the test were successively diluted using 100 µL Middlebrook 7H9 broth in sterile 96-well microtiter plates. For all the compounds the sampling were performed in triplicate. The assay readings were compared against the well-known reference TB drugs such as rifampicin (Rif), isoniazid (INH) and ethambutol. The sterile water

into all the boundary wells of each plate was employed in order to retain the humidity during the incubation at 37 °C, over a period of 7 days. After completion of the incubation period, 30 µL of Alamar blue solution was added to each test well, and all the plates were pre-incubated again for 12 h. The cell growth was monitored, which indicated a color change from a blue to pink with the lowermost concentration of the particular compound that did not change color recorded as its MIC value.

Nutrient starvation assay (NSA) model

In the NSA model, a *M. tuberculosis* H37Rv (O.D. of 0.8–1.0) culture was grown in Middlebrook 7H9 medium supplemented with OADC mixture was pelleted and washed twice with PBS solution. Later, the pellet was suspended in PBS in sealed bottles and incubated at 37 °C over a period of 6 weeks. Aliquots of these cultures were then treated with the lead compounds of 10 µM for the compounds **10**, **14**, **16**, **19**, **22** and **28** (i.e. ~10 µg mL^{-1}) and standard TB drugs such as, INH, Rif and moxifloxacin for 7 days. For this purpose, all the cell suspensions were diluted with 10 % OADC to 10-fold using Middlebrook 7H9 broth. Each dilution with 100 µL was plated in sterile 48 well plates containing 450 µL of Middlebrook 7H9 broth and these plates were incubated at 37 °C over a period of 4 weeks. These experiments were performed in triplicate. The wells with illusory bacterial growth were counted as positive, and the most probable number (MPN) values were determined using standard statistical methods (SSM).

Cytotoxicity determination

The cell toxicity of all the thirty compounds, **8-37,** were tested by an inhibition assay method using mouse macrophage cell lines (RAW 264.7). To do this, various concentrations of the compound under test was added to sterile 96 well microtiter plate 5×103 cells and incubated at 37 °C over a period of 48 h. After completion of the incubation period, 10 µL of 3-(4,5-dimethylthiazol-2-yl)-2,5-diphenyltetrazolium bromide (MTT reagent) (5 mg mL^{-1}) was added and then incubated again for 3 h. Later, after removing the, 100 µL of DMSO solvent was added to each well. The DMSO solvent dissolves the formazan crystals grown in the wells. Using this solution the absorbance was measured at 560 nm against the blank using Perkin Elmer Victor X3 microplate reader. The assays were performed in triplicates for each concentration of the samples and represented as % inhibition at each concentration.

Molecular docking studies

Molecular docking analyses of all the thirty compounds, **8-37**, were carried out in order to understand the most active sites of protein receptors. The Three-dimensional (3D) structures of all the ligand compounds were generated using Gauss view 5.0. The molecular geometry of the ligand compounds were optimized using the standard density functional triply-parameter hybrid model DFT/RPM6 employing the ZDO basis set with Gaussian 09w. MurB is a key enzyme that mobilizes the reduction of enolpyruvyl uridine diphosphate N-acetyl glucosamine (EP-UNAG), an intermediate in the assembly of the UNAM-pentapeptide (m-A2pm) portion to uridine diphosphate N-acetyl muramic acid (UNAM), of cell wall precursor. Mur proteins (Mur A-F, Y and G) catalyze more than 10 biosynthetic transformations involved in the formation of the peptidoglycan layer of the cell walls of bacteria and they are also conserved among several bacterial strains. UDP-N-acetylglucosamine-enolpyruvate reductase (MurB) also plays an important part in the binding of EP-UDPGIcNAc or NADPH in E. coil MurB. Due to this cause, we choose the MurB enzyme as a target receptor. The crystallographic 3D structure of UDP-N-acetylglucosamine-enolpyruvate reductase (MurB) protein was downloaded from the Protein Data Bank, RCSB (www.rscb.org) with structure id, PDB ID: 5JZX for S. Areus Murb. From the structure of S. Areus Murb proteins, all the previously associated ligands and water molecules were eliminated using UCSF chimera 1.10.1 software. The molecular docking computational analyses were carried out using Auto Dock Tools (ADT) version 1.5.6 and Auto Dock 4.2 package suite. The output results of docking studies were graphically examined and illustrated by Discovery Studio 4.1.0 software. To confirm the relation between *in vitro* antimicrobial findings and binding affinities of the inhibitors docking analysis of the titled, **8-37**, analogs against UDP-N-acetylglucosamine-enolpyruvate reductase (MurB) was performed using the Auto Dock program.

X-ray structure refinement

Single crystals of compounds **15** and **18** were mounted on a loop, and data were collected with a Bruker AXS-KAPPA Apex II diffractometer equipped with a normal focus, 2.4 kW sealed-tube X-ray source (Mo-$K\alpha$ radiation, = 0.71073 Å) operating at 50 kV and 30 mA. An empirical absorption correction based on symmetry-equivalent reflections was applied using SADABS. The structures were solved by the WINGX suit of programs using the program SHELXS-97 and refined against $F2$ using SHELXL-97. All non-hydrogen atoms were located in Fourier map and

refined anisotropic thermal parameters and hydrogen atoms were introduced in calculated positions and refined isotropically. The crystal structure refinement parameters for compounds **15** and **18** are given in Table S1.

References

1. Fields, S. C.; Alexander, A. L.; Balko, T. W.; Bjelk, L. A.; Buysse, A. M.; Keese, R. J.; Krumel, K. L.; William Lo, C. –L.; lowe, C. T.; Richburg, J. S. et al. 4-Aminopicolinates and their use as herbicides. US 629197 B, October 2, 2001
2. Hartmut, A.; Marco, B.; Hansjörg, D.; Elmar, G.; Isolde, H. –H.; Stefan, L.; Dirk, S. Novel substituted picolinic acids, salts and acid derivatives thereof, and use thereof as herbicides. US2012/157314, February 24, 2015.
3. G. M. Sheldrick, *SADABS Siemens Area Correction Absorption Program*, University of Göttingen, Göttingen, Germany, **1994**.
4. Sheldrick, G. M. *Program for Crystal Structure Solution*; University of Göttingen: Germany, **1997**.
5. Sheldrick, G. M. *Program for Crystal Structure Refinement*; University of Göttingen: Germany, **1997**.
6. Rampersad, S. N. Multiple applications of alamar blue as an indicator of metabolic function and cellular health in cell viability bioassays. *Sensors (Basel)*. **2012,** *12*, 12347–12360.
7. Reddy, K. I.; Chuppala, A.; Manisha, M.; Srihari, K.; Babu, K. S.; Vijayakumar, V.; Sarveswari, S.; Priya, R.; Amrita, A.; Siva. R. Synthesis, DNA binding and in-vitro cytotoxicity studies on novel bis-pyrazoles. *J. Photochem. Photobiol. B: Biology*. **2017**, *168*, 89-97.
8. Frisch, M. J.; Trucks, G. W.; Schlegel, H. B.; Scuseria, G. E.; Robb, M. A.; Cheeseman, J. R.; Scalmani, G.; Barone, V.; Petersson, G. A.; Nakatsuji, H. *et al*, **2009** Gaussian, Inc., Wallingford CT.
9. Farmer, B. T.; Constantine, K. L.; Goldfarb, V.; Friedrichs, M. S.; Wittekind, M.; Yanchunas, J.; Robertson, J. G.; Mueller, L. Localizing the $NADP^+$ binding site on the MurB enzyme by NMR. *Nat. Struct. Biol*. **1996**, *3*, 995-997.
10. San Diego, Calif, USA Accelrys Software Inc. Discovery Studio Modeling Environment, *Release 4.1.0. : Accelrys Software Inc*; **2013**.
11. Ran, Y.; Pei, H.; Xie, C.; Ma, L.; Wu, Y.; Lei, K.; Shao, M.; Tang, M.; Xiang, M.; Peng, A. et al. *Mol. Divers*. **2015**, *19*, 333-346.

Table S1. Crystal data and structure refinement parameters for compounds, **15** and **18.**

Parameters	**15**	**18**
Empirical Formula	$C_{20}H_{14}ClF_3N_4O_3$	$C_{21}H_{16}ClF_2N_3O_4$
Crystal system	Orthorhombic	Monoclinic
Space group	*Pbca*	*P21/c*
Crystal size (mm)	0.18× 0.14 × 0.04	0.26 × 0.21 × 0.17
a (Å)	19.050(3)	6.03(3)
b (Å)	10.875(1)	30.28(16)
c (Å)	19.747(3)	11.18(6)
α (°)	90	90
β (°)	90	104.36(5)
γ (°)	90	90
Volume ($Å^3$)	4091(1)	1979(17)
Z	8	4
Formula mass	450.80	447.82
ρ_{calc} (gcm^{-3})	1.464	1.503
λ *Å*	0.71073 *(MoKα)*	0.71073 *(MoKα)*
μ(mm^{-1})	0.244	0.247
θ range (˚)	2.06 to 28.28	1.35 to 28.48
Total data collected	68316	29366
Unique data	5078	4961
Observed data (I > 2σ(I))	2942	2387
R indexes [I > 2 σ(I)]	R_1 = 0.0524, wR_2 = 0.1091	R_1 = 0.0739, wR_2 = 0.1969
Goodness of fit	1.010	1.027

^{1}H NMR, ^{13}C NMR, and MASS of Synthesized Compounds

^{1}H-NMR

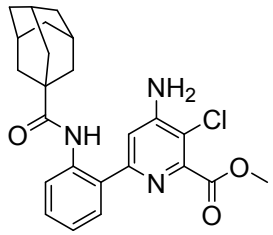

8

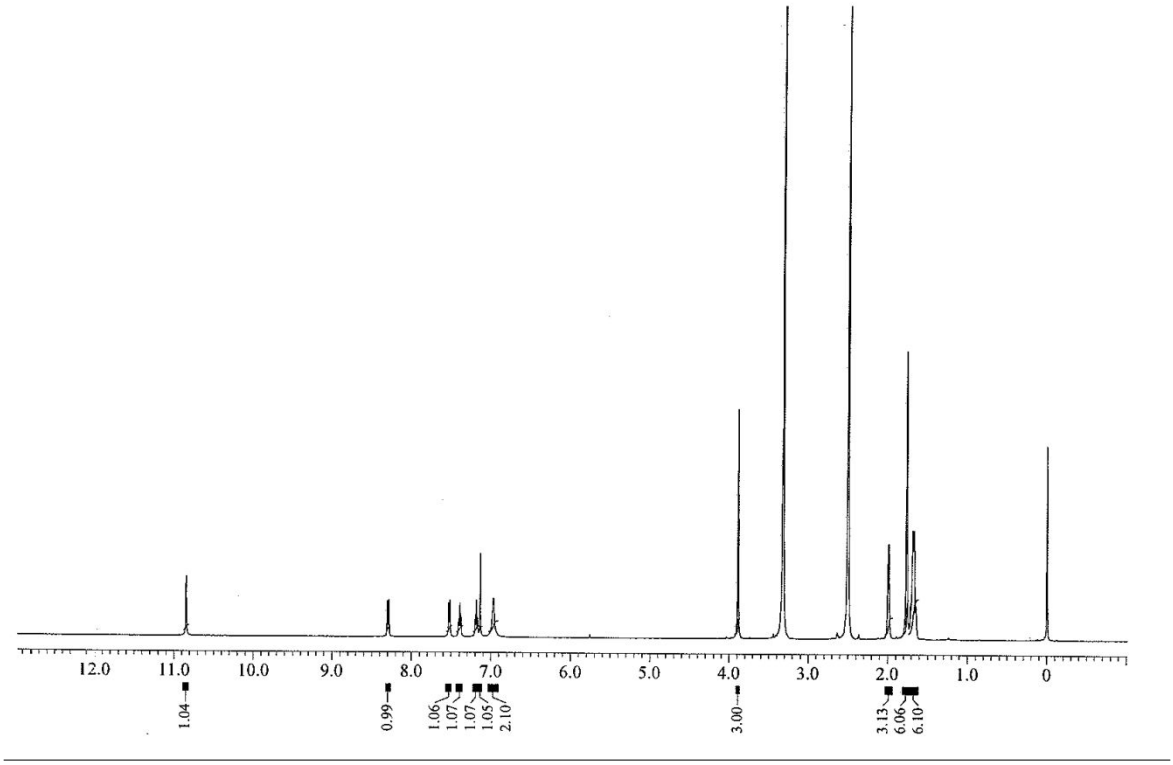

Figure S1: ^{1}H-NMR (300 MHz, DMSO) Methyl-6-(2-(adamantane-1-carboxamido) phenyl)-4-amino-3-chloropicolinate **(8)**.

^{13}C-NMR

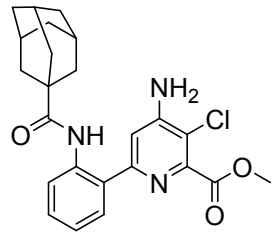

8

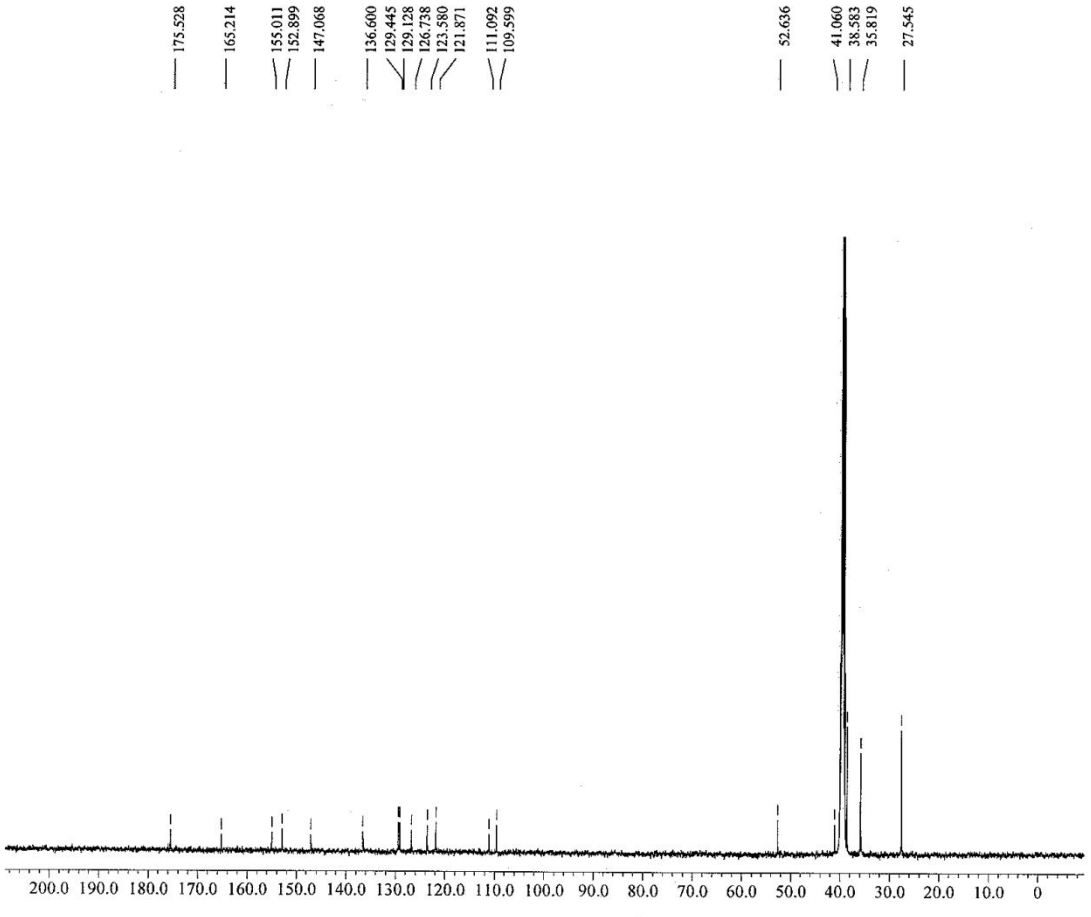

Figure S2: ^{13}C-NMR (75 MHz, DMSO) Methyl-6-(2-(adamantane-1-carboxamido) phenyl)-4-amino-3-chloropicolinate **(8)**.

HRMS

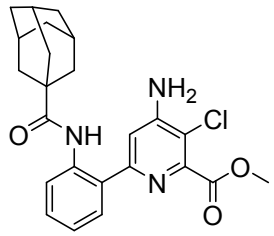

8

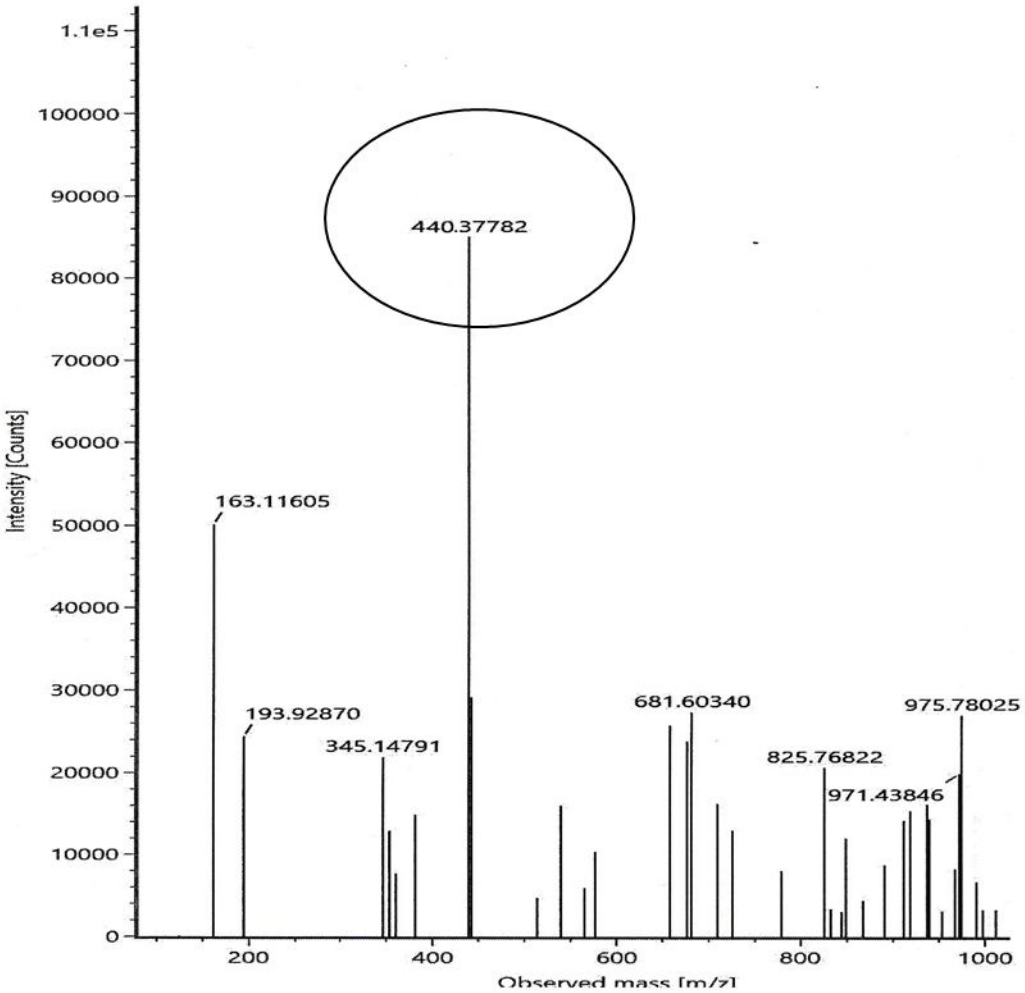

Figure S3: HRMS of Methyl-6-(2-(adamantane-1-carboxamido) phenyl)-4-amino-3-chloropicolinate **(8)**.

^{1}H-NMR

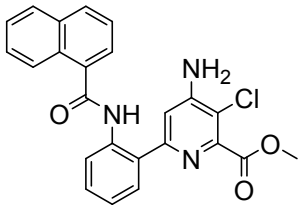

9

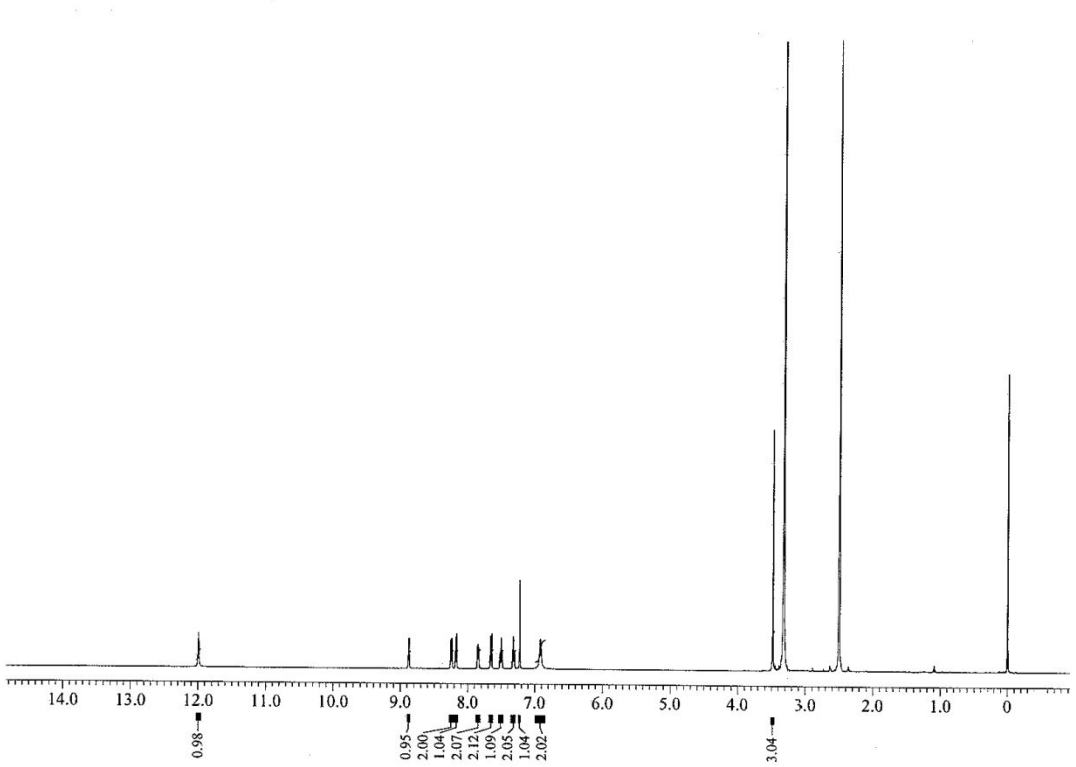

Figure S4: ^{1}H-NMR (300 MHz, DMSO) of Methyl-6-(2-(1-naphthamido) phenyl)-4-amino-3-chloropyridine-2-carboxylate **(9)**.

^{13}C-NMR

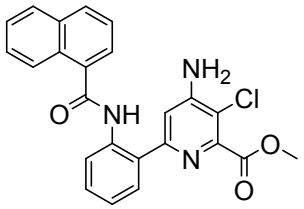

9

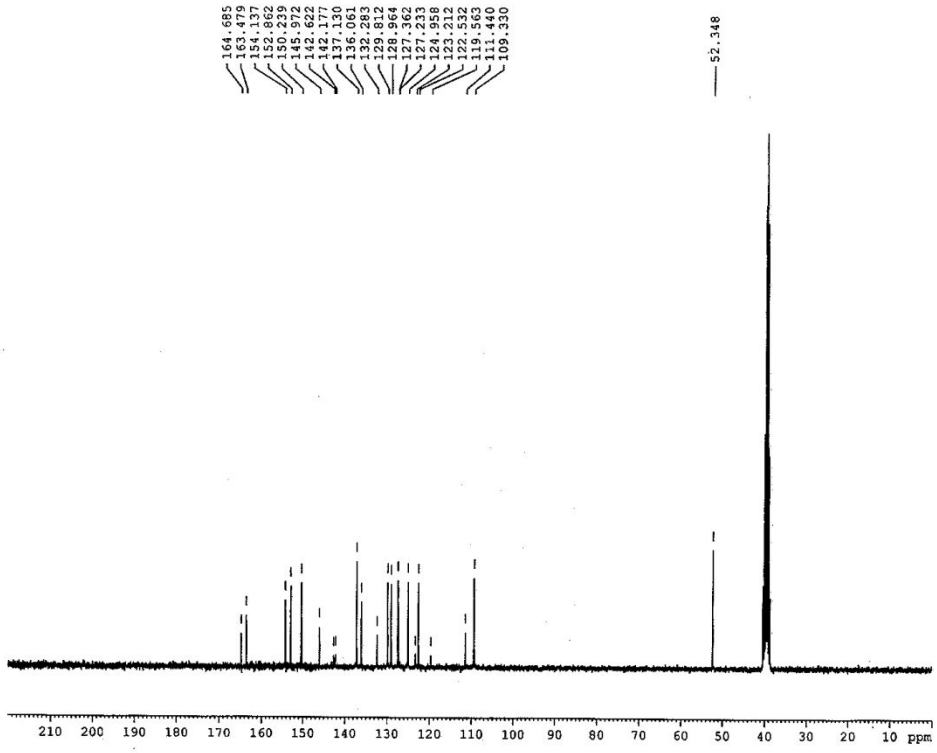

Figure S5: ^{13}C-NMR (**75** MHz, DMSO) of Methyl-6-(2-(1-naphthamido) phenyl)-4-amino-3-chloropyridine-2-carboxylate **(9)**.

HRMS

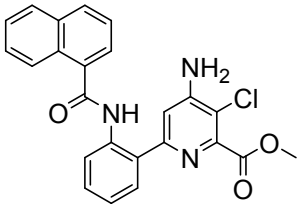

9

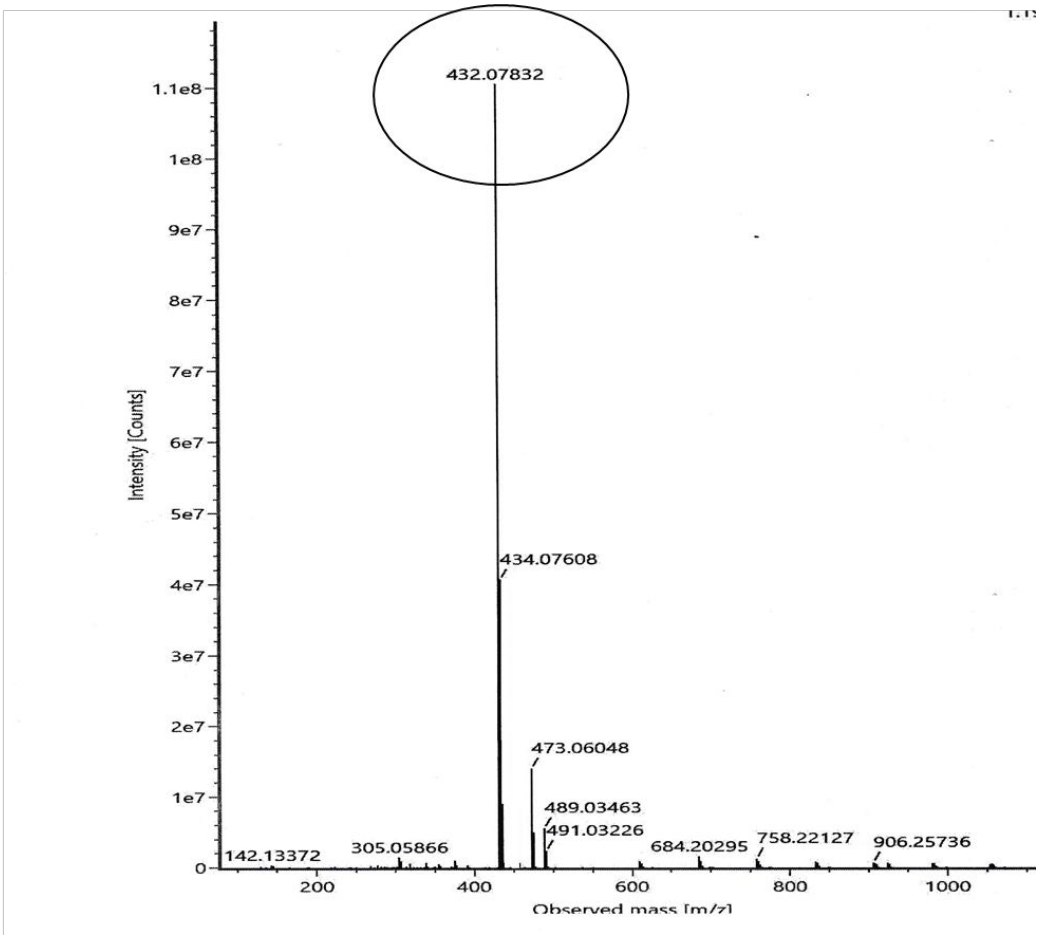

Figure S6: HRMS of Methyl-6-(2-(1-naphthamido) phenyl)-4-amino-3-chloropyridine-2-carboxylate **(9)**.

^{1}H-NMR

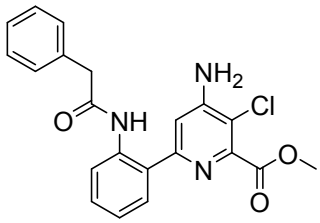

10

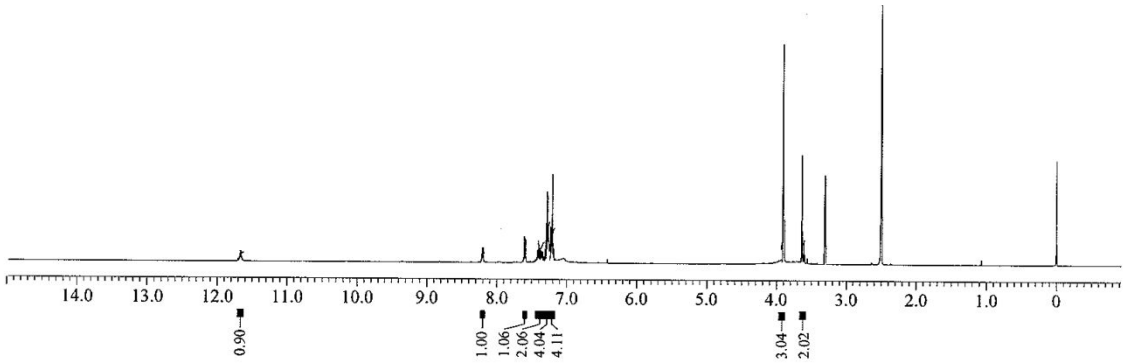

Figure S7: ^{1}H-NMR (300 MHz, DMSO) of Methyl-6-(2-(2-phenylacetamido) phenyl)-4-amino-3-chloropyridine-2-carboxylate **(10)**.

^{13}C-NMR

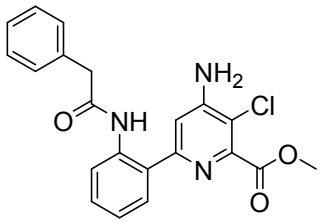

10

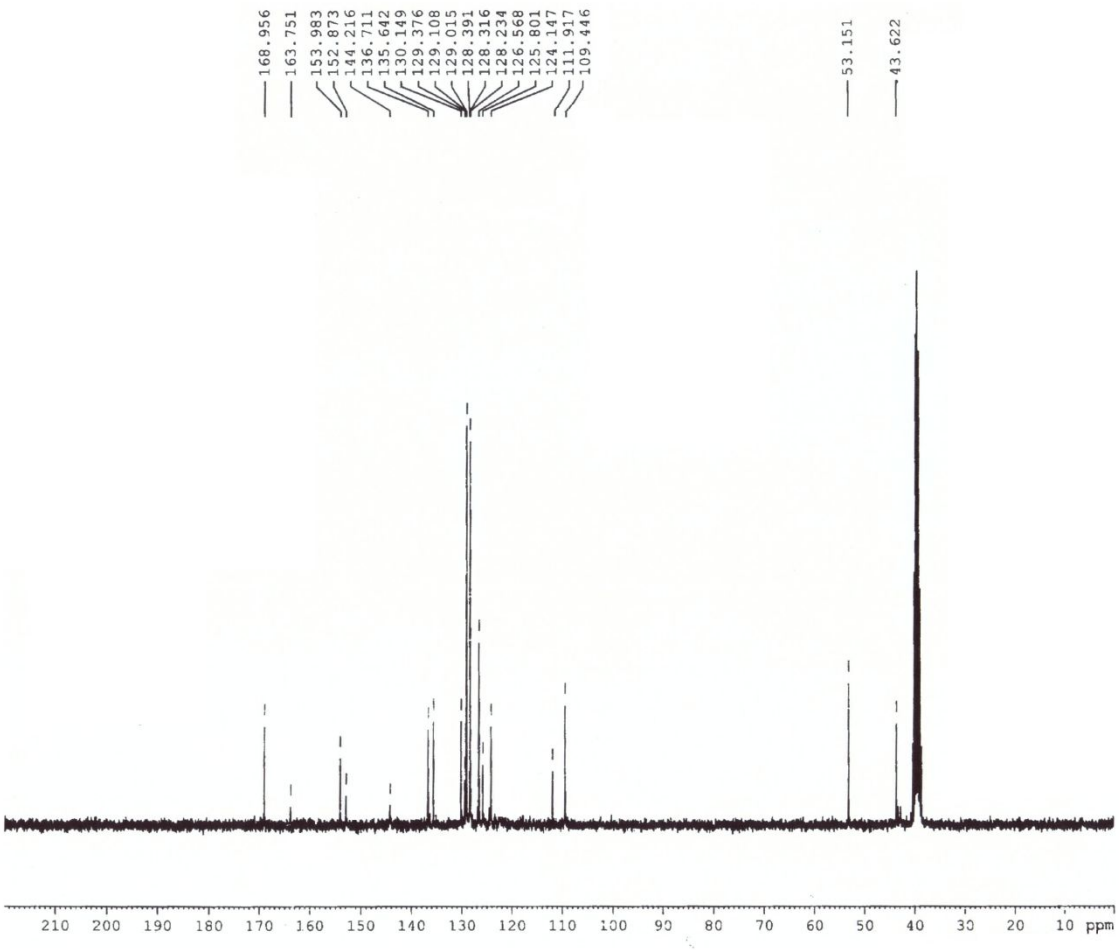

Figure S8: ^{13}C-NMR (**75** MHz, DMSO) of Methyl-6-(2-(2-phenylacetamido) phenyl)-4-amino-3-chloropyridine-2-carboxylate **(10)**.

HRMS

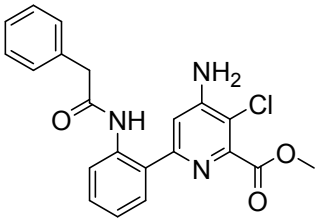

10

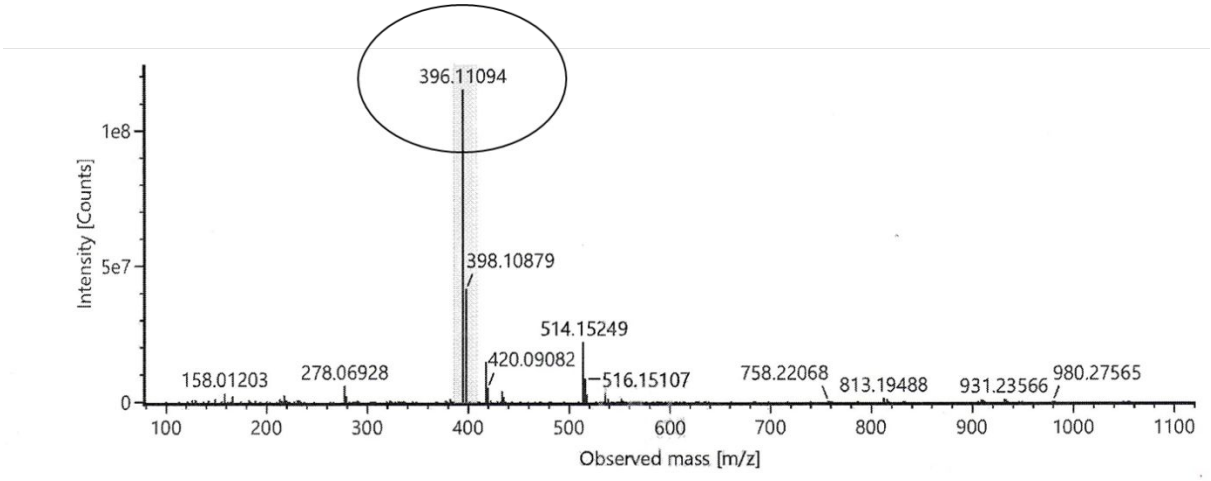

Figure S9: HRMS of Methyl-6-(2-(2-phenylacetamido) phenyl)-4-amino-3-chloropyridine-2-carboxylate **(10)**.

^{1}H-NMR

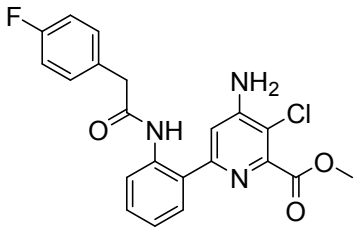

11

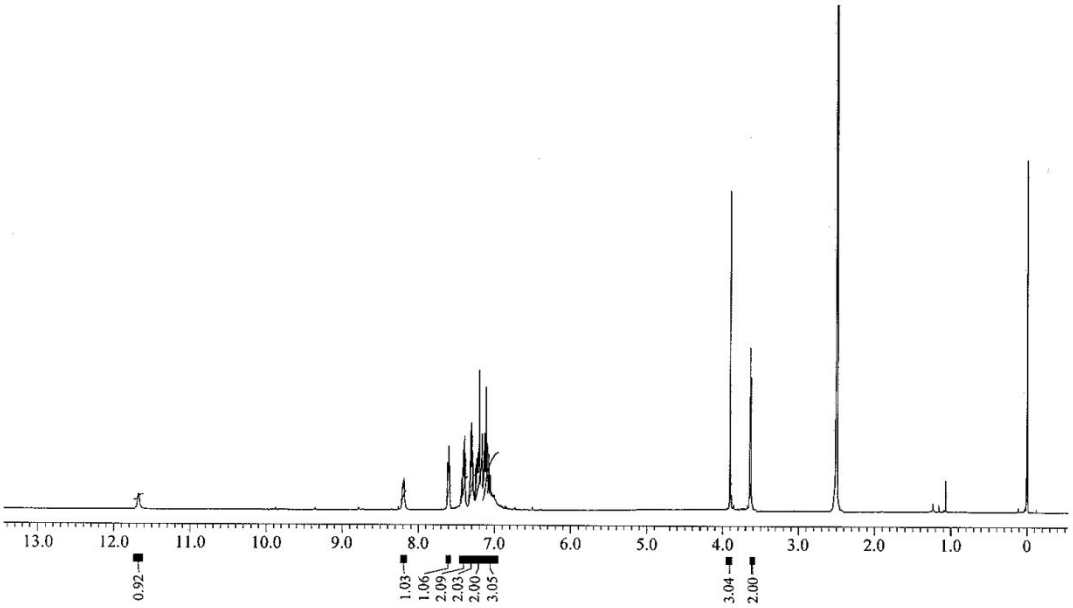

Figure S10: ^{1}H-NMR (**300** MHz, DMSO) of Methyl-6-(2-(2-(4-fluorophenyl) acetamido)phenyl)-4-amino-3-chloropyridine-2-carboxylate **(11)**.

^{13}C-NMR

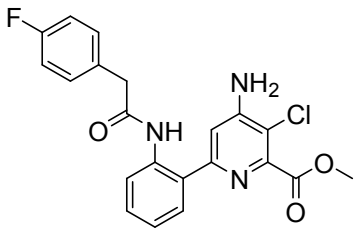

11

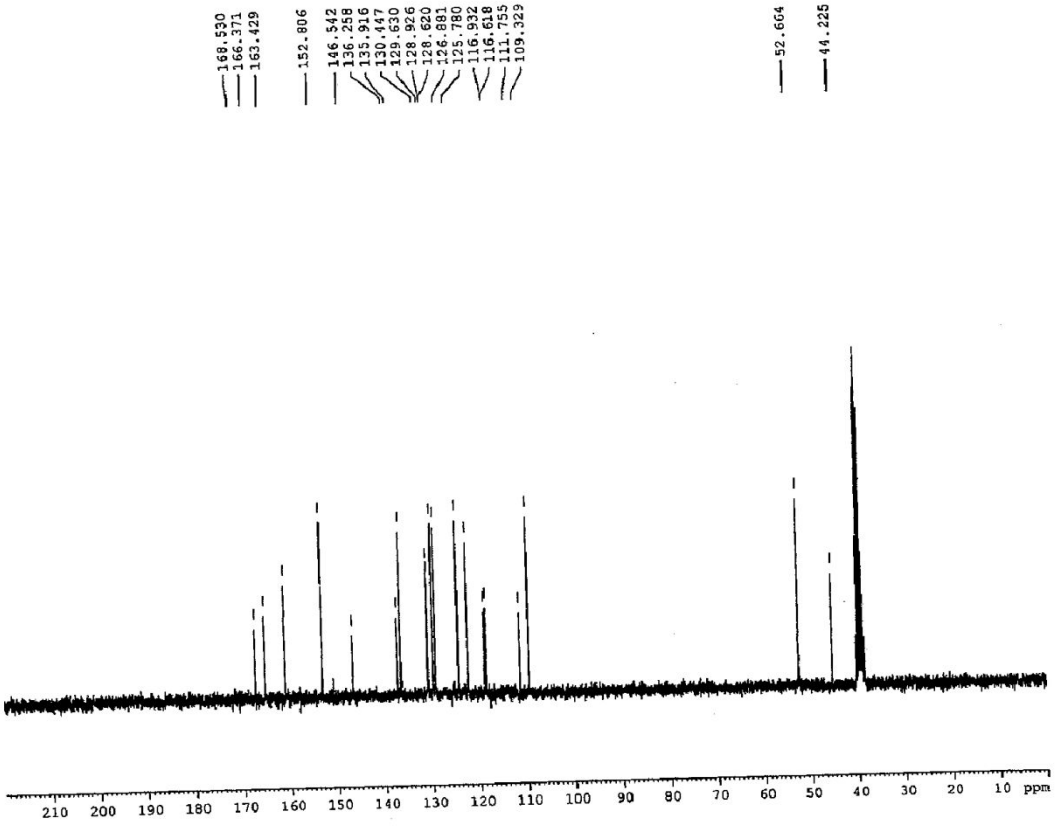

Figure S11: ^{13}C-NMR (**75** MHz, DMSO) of Methyl-6-(2-(2-(4-fluorophenyl) acetamido)phenyl)-4-amino-3-chloropyridine-2-carboxylate **(11)**.

HRMS

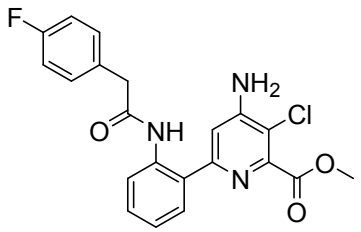

11

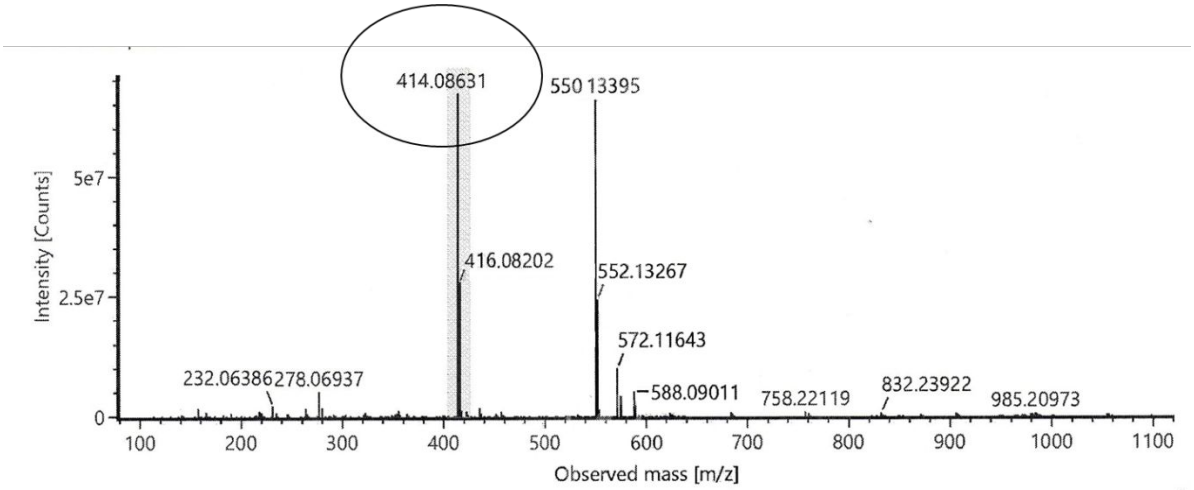

Figure S12: HRMS of Methyl-6-(2-(2-(4-fluorophenyl) acetamido)phenyl)-4-amino-3-chloropyridine-2-carboxylate **(11)**.

^{1}H-NMR

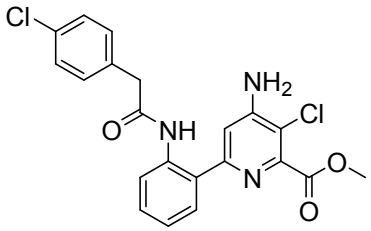

12

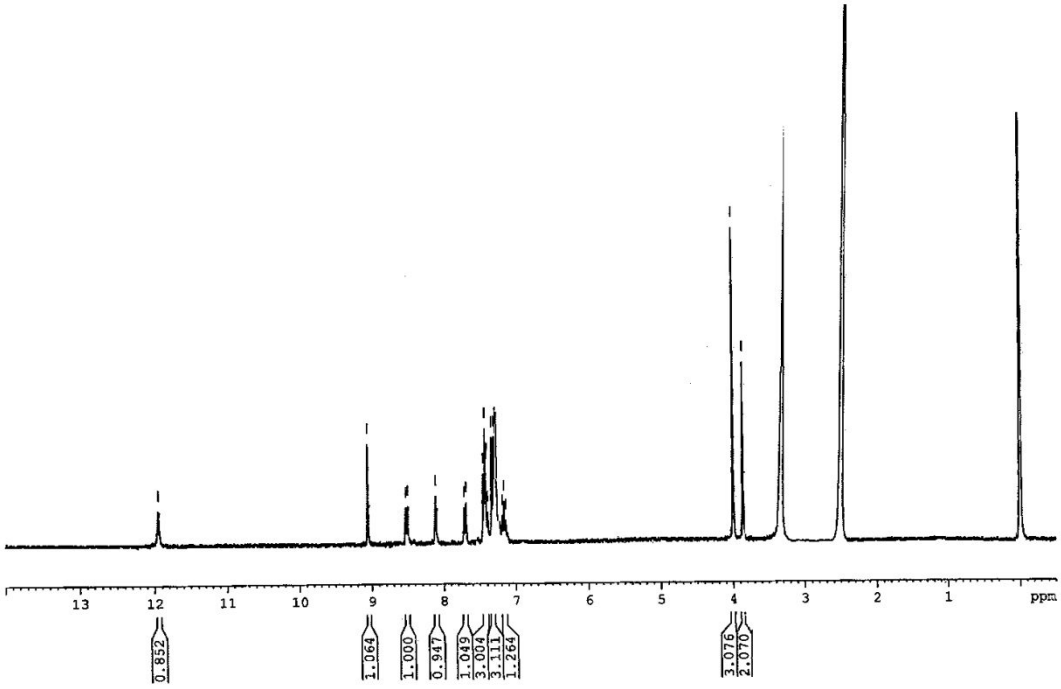

Figure S13: ^{1}H-NMR (300 MHz, DMSO) of Methyl-6-(2-(2-(4-chlorophenyl) acetamido) phenyl)-4-amino-3-chloropyridine-2-carboxylate **(12)**.

^{13}C-NMR

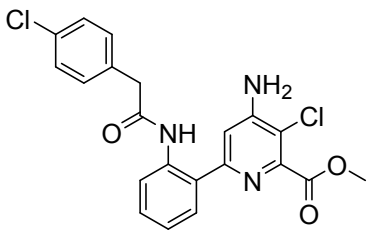

12

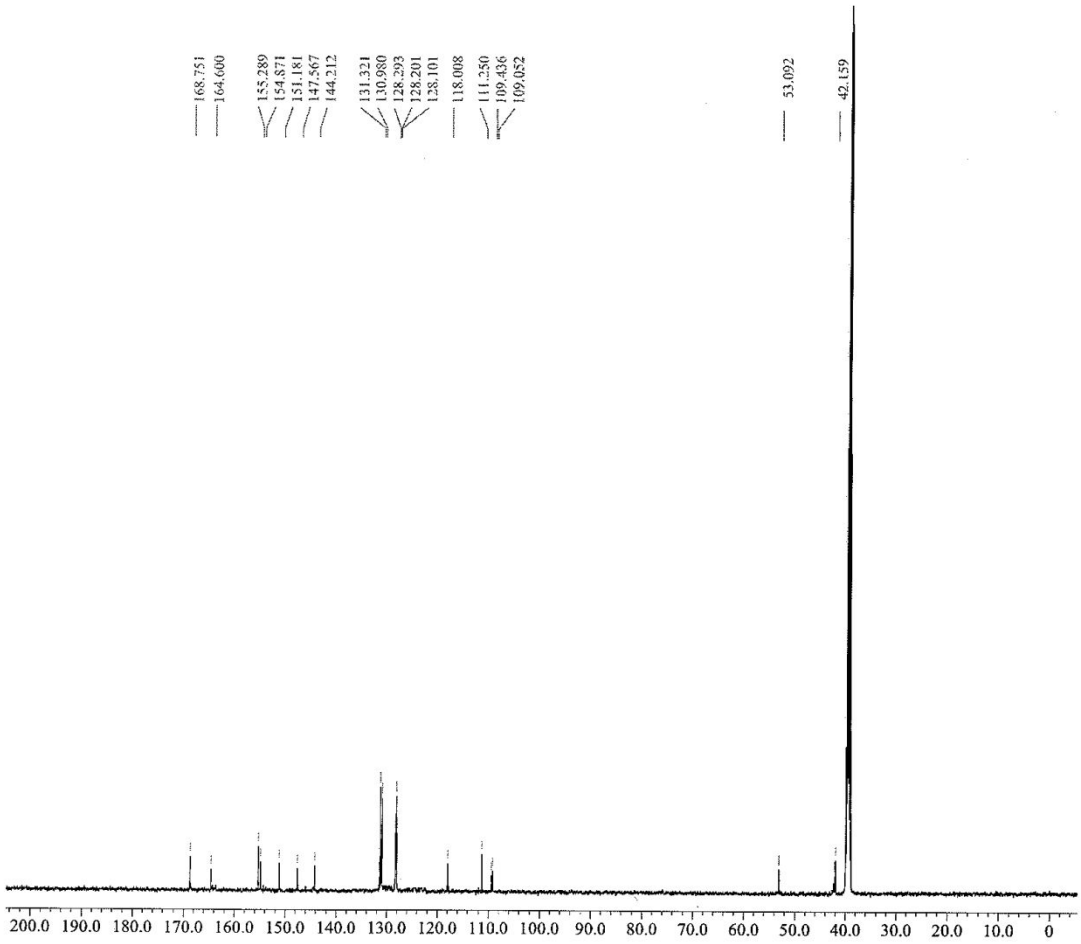

Figure S14: ^{13}C-NMR (**75** MHz, DMSO) of Methyl-6-(2-(2-(4-chlorophenyl) acetamido) phenyl)-4-amino-3-chloropyridine-2-carboxylate **(12)**.

HRMS

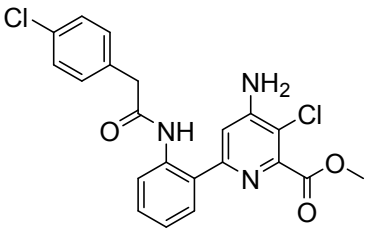

12

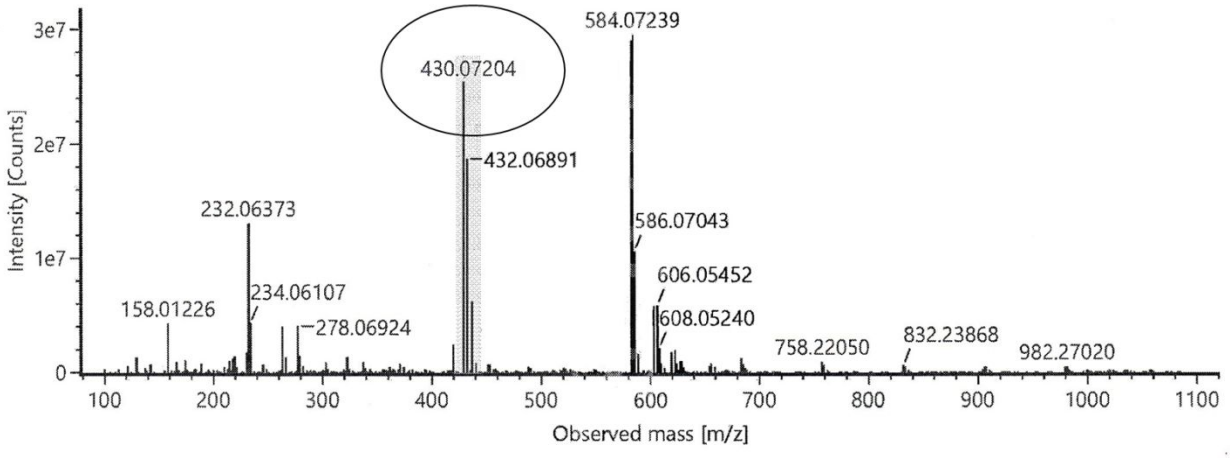

Figure S15: HRMS of Methyl-6-(2-(2-(4-chlorophenyl) acetamido) phenyl)-4-amino-3-chloropyridine-2-carboxylate **(12)**.

^{1}H-NMR

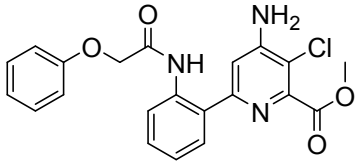

13

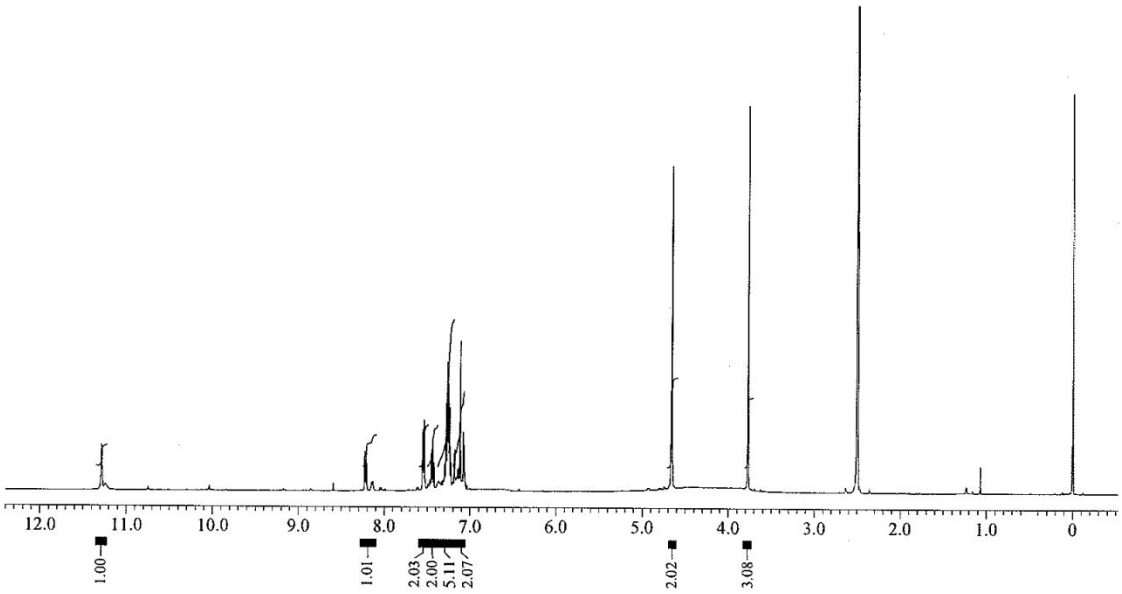

Figure S16: ^{1}H-NMR (300 MHz, DMSO) of Methyl-6-(2-(2-phenoxyacetamido) phenyl)-4-amino-3-chloropyridine-2-carboxylate **(13)**.

^{13}C-NMR

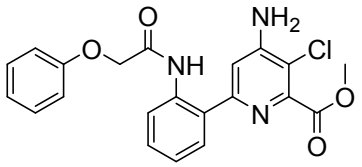

13

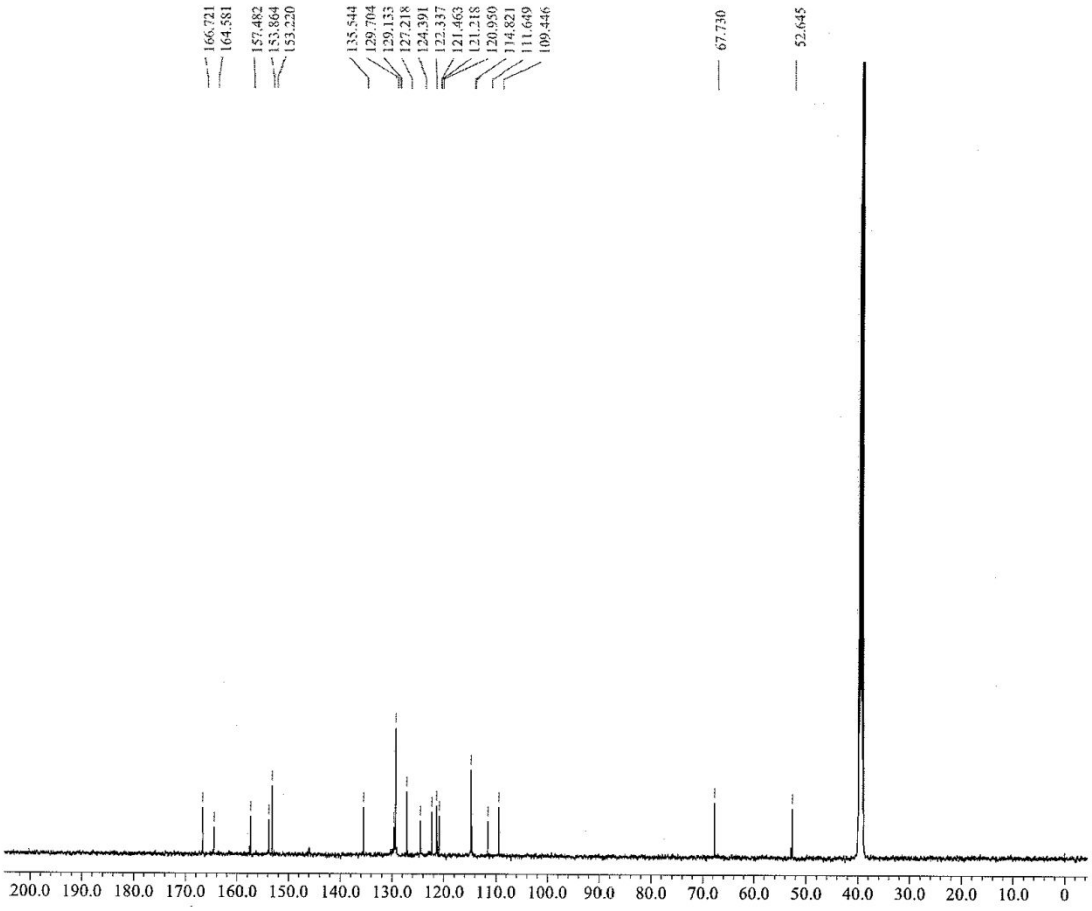

Figure S17: ^{13}C-NMR (**75** MHz, DMSO) of Methyl-6-(2-(2-phenoxyacetamido) phenyl)-4-amino-3-chloropyridine-2-carboxylate **(13)**.

HRMS

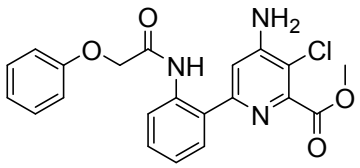

13

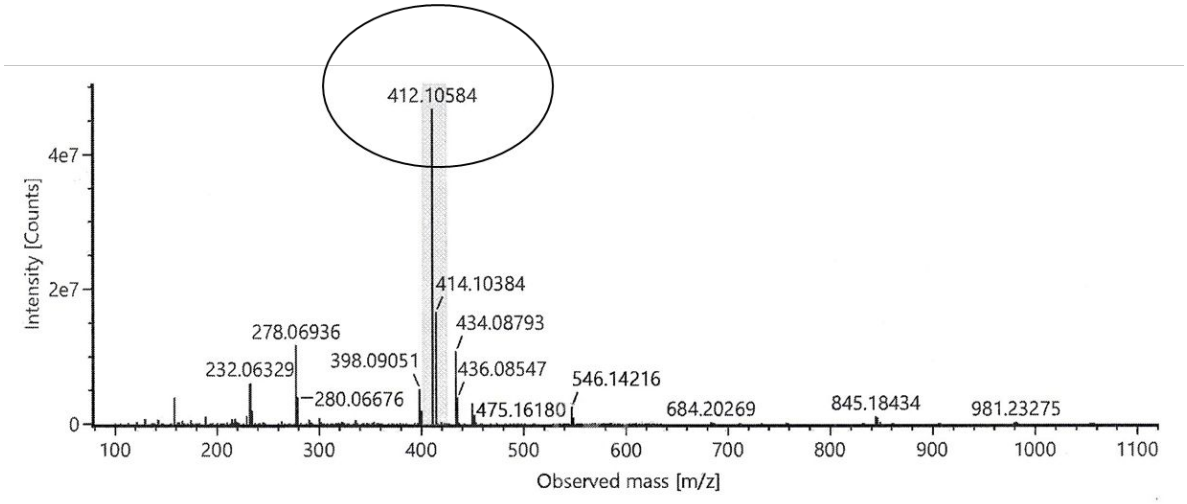

Figure S18: HRMS of Methyl-6-(2-(2-phenoxyacetamido) phenyl)-4-amino-3-chloropyridine-2-carboxylate **(13)**.

^{1}H-NMR

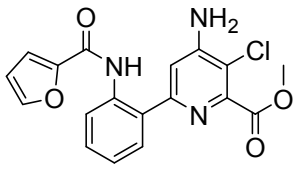

14

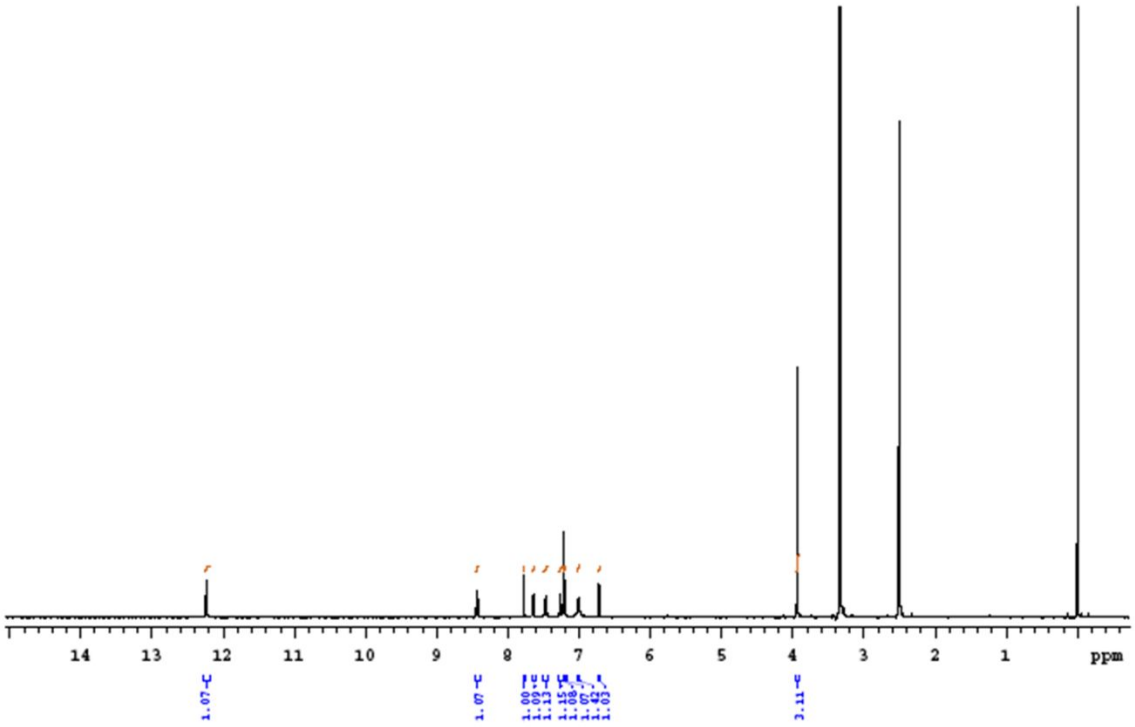

Figure S19: ^{1}H-NMR (400 MHz, DMSO) of Methyl-4-amino-3-chloro-6-(2-(furan-2-carboxamido) phenyl) pyridine-2-carboxylate **(14)**.

^{13}C-NMR

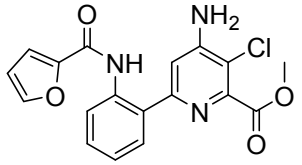

14

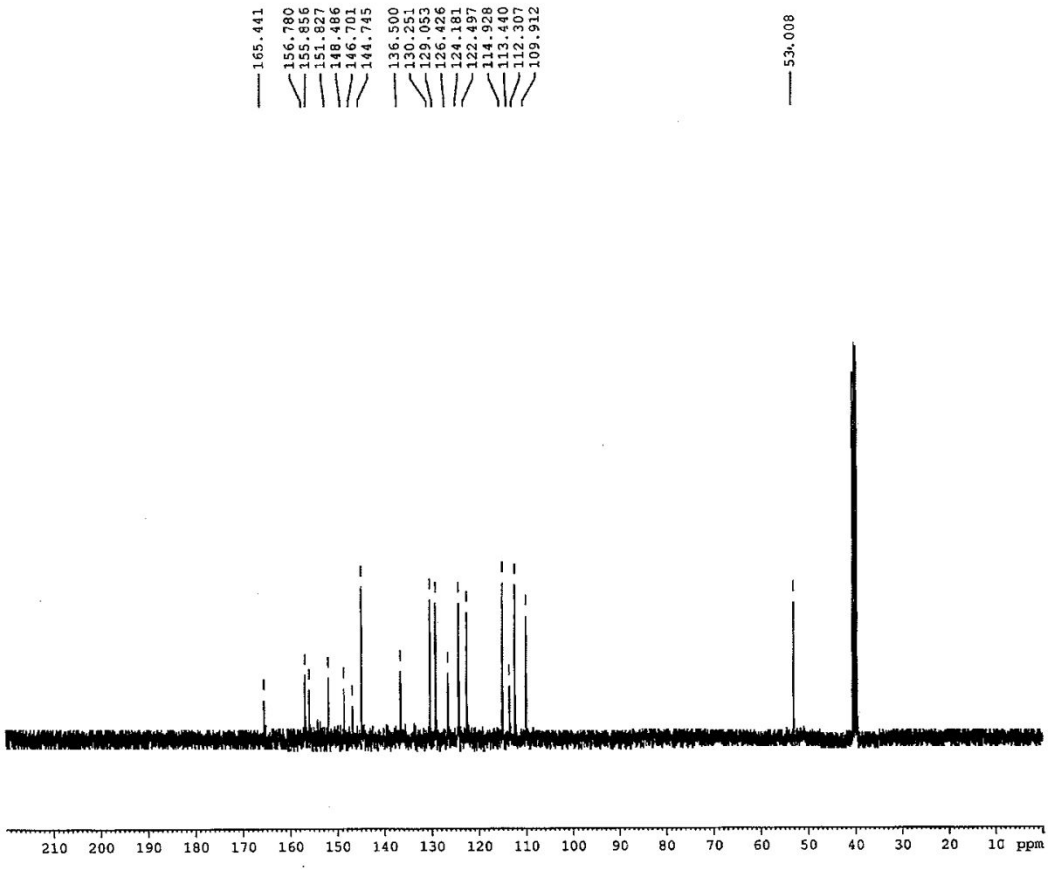

Figure S20: ^{13}C-NMR (75 MHz, DMSO) of Methyl-4-amino-3-chloro-6-(2-(furan-2-carboxamido) phenyl) pyridine-2-carboxylate **(14)**.

HRMS

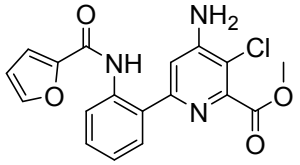

14

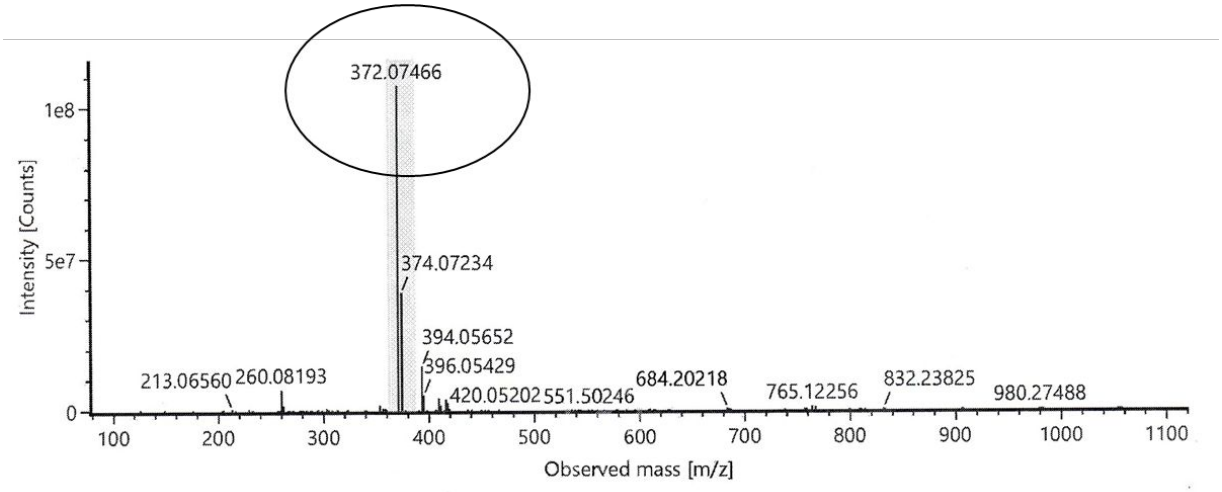

Figure S21: HRMS of Methyl-4-amino-3-chloro-6-(2-(furan-2-carboxamido) phenyl) pyridine-2-carboxylate **(14)**.

^{1}H-NMR

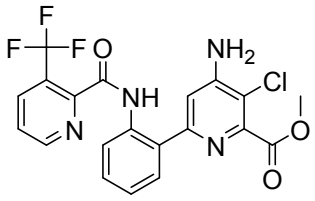

15

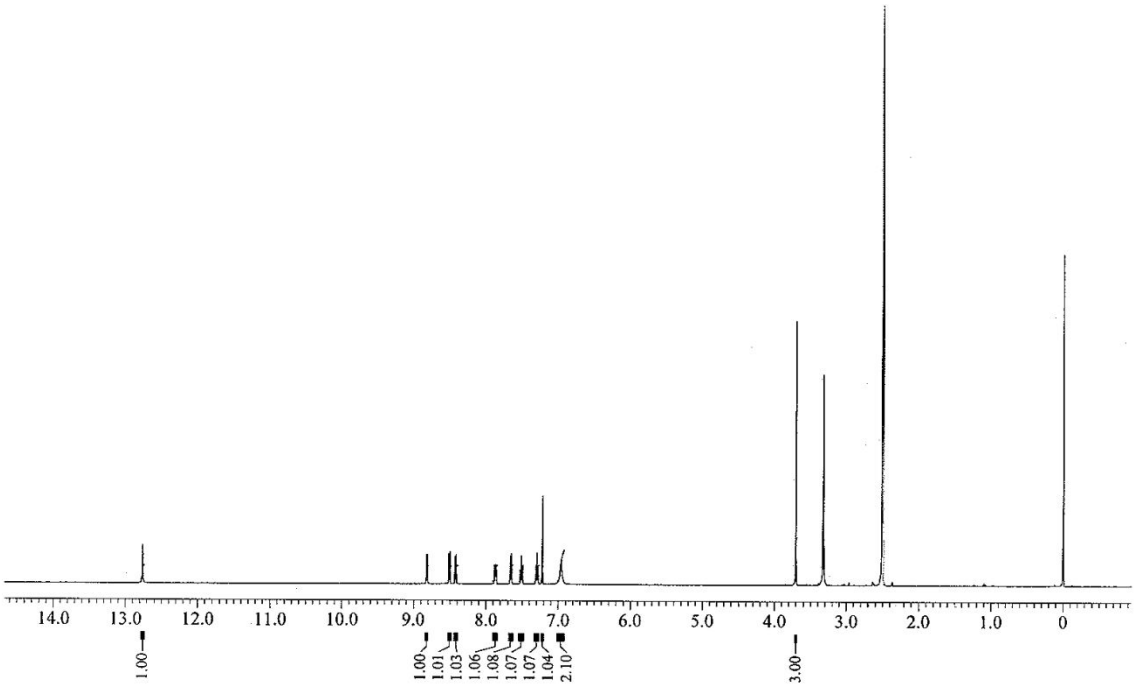

Figure S22: ^{1}H-NMR (300 MHz, DMSO) of Methyl-6-(2-(3-(trifluoromethyl) pyridine-2-carboxamido) phenyl)-4-amino-3-chloropyridine-2-carboxylate **(15)**.

^{13}C-NMR

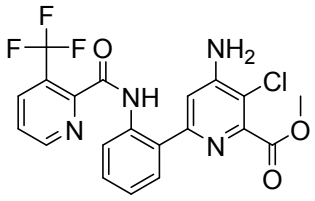

15

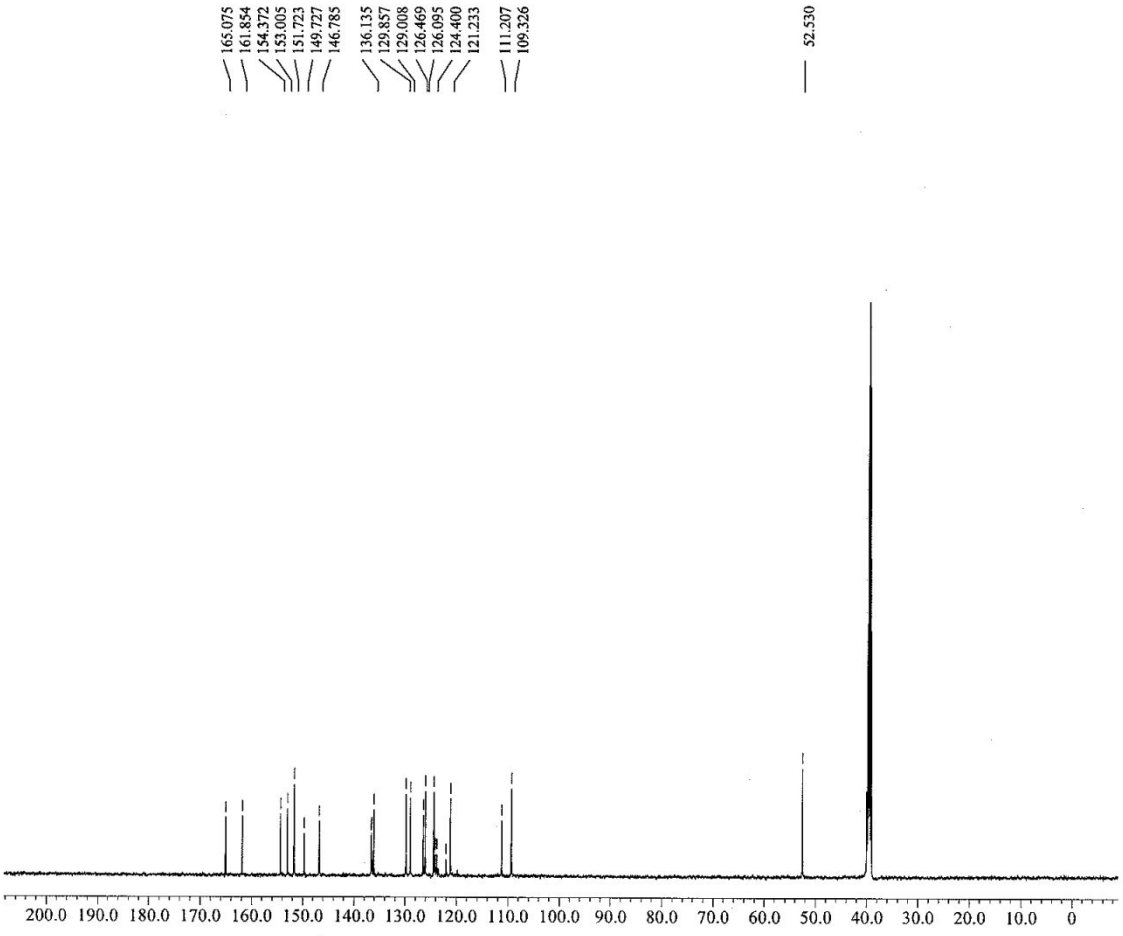

Figure S23: ^{13}C-NMR (75 MHz, DMSO) of Methyl-6-(2-(3-(trifluoromethyl) pyridine-2-carboxamido) phenyl)-4-amino-3-chloropyridine-2-carboxylate **(15)**.

HRMS

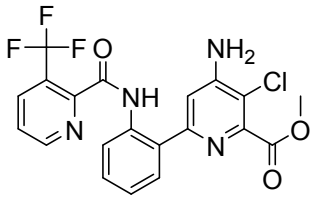

15

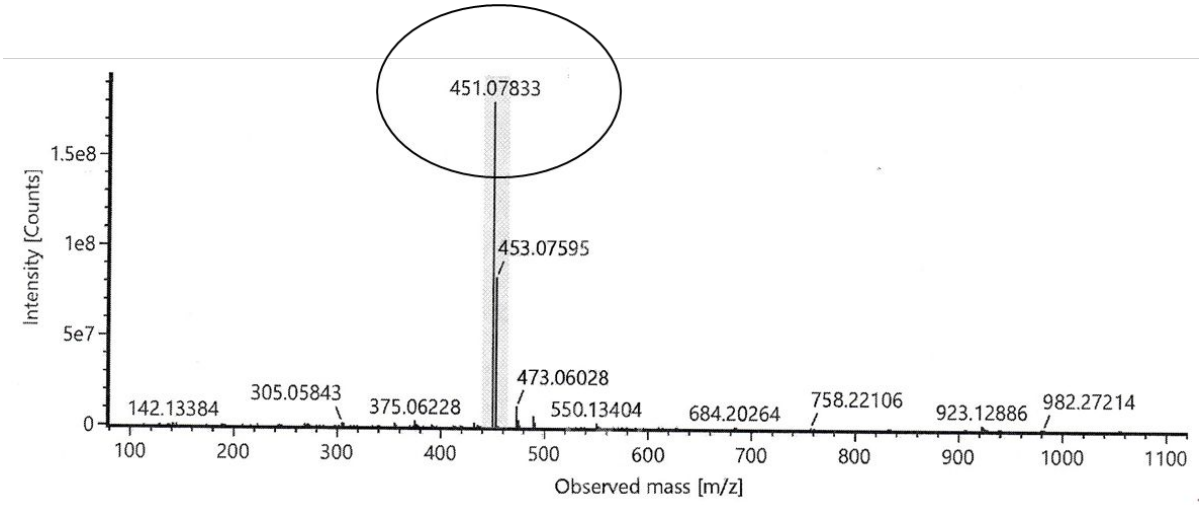

Figure S24: HRMS of Methyl-6-(2-(3-(trifluoromethyl) pyridine-2-carboxamido) phenyl)-4-amino-3-chloropyridine-2-carboxylate **(15)**.

^{1}H-NMR

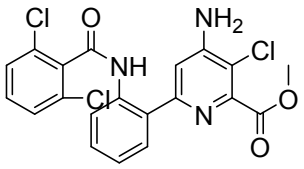

16

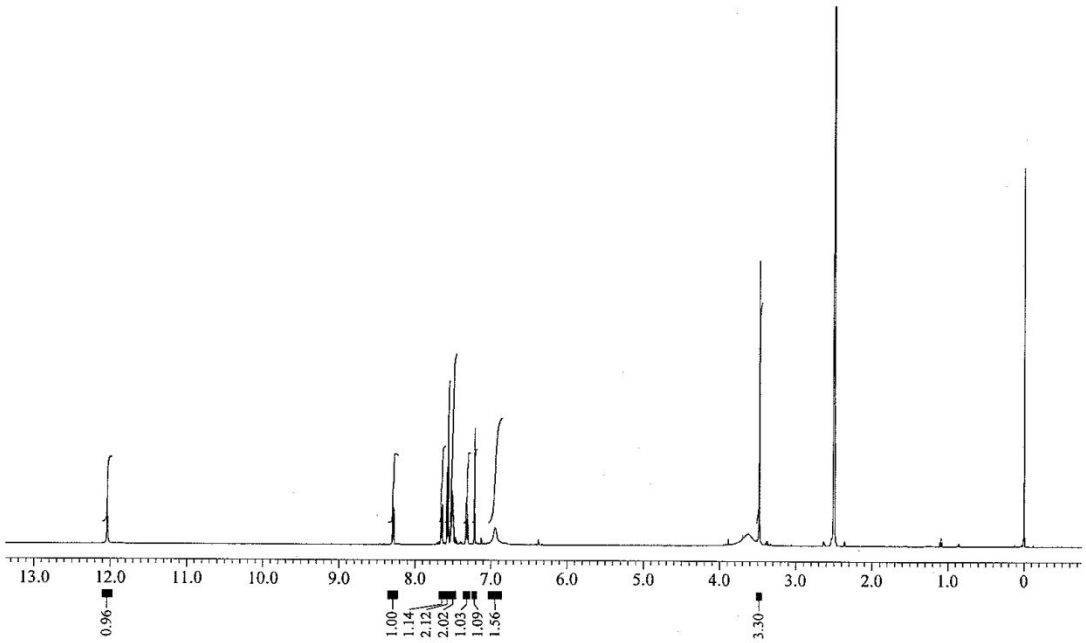

Figure S25: ^{1}H-NMR (300 MHz, DMSO) of Methyl-6-(2-(2,6-dichlorobenzamido)phenyl)-4-amino-3-chloropyridine-2-carboxylate **(16)**.

^{13}C-NMR

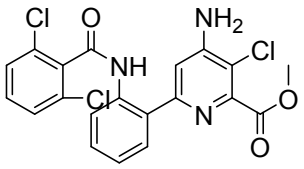

16

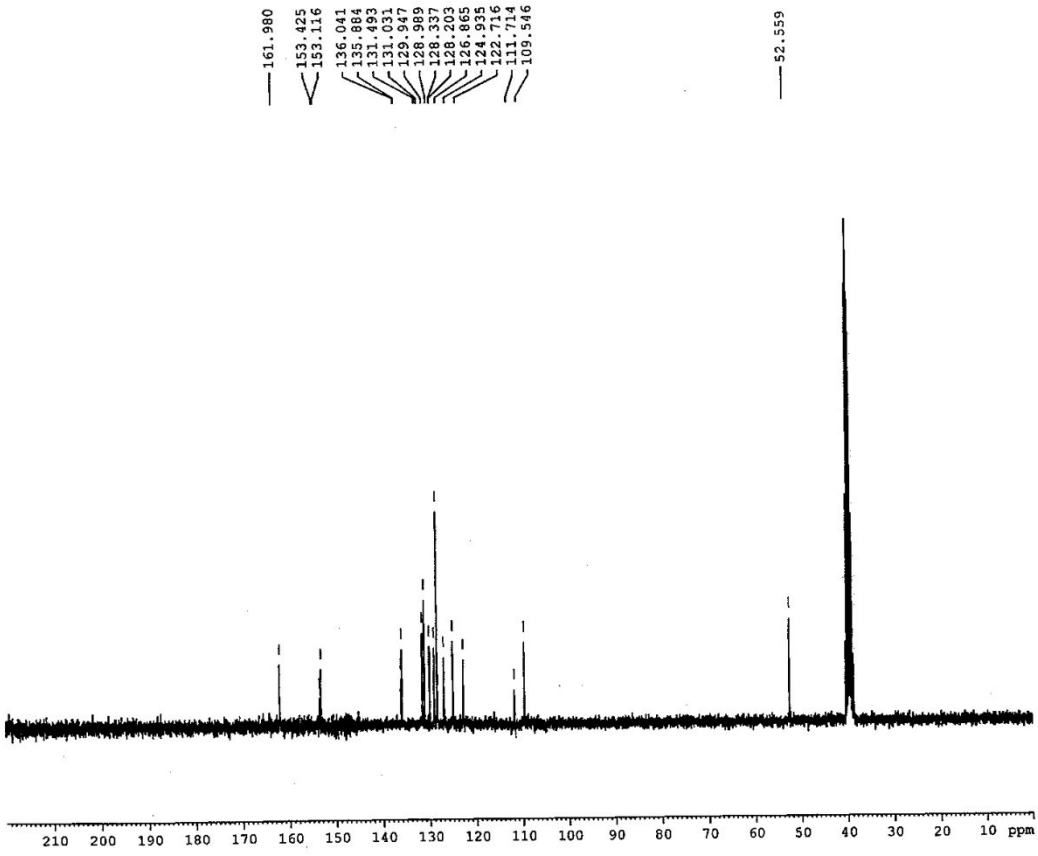

Figure S26: ^{13}C-NMR (75 MHz, DMSO) of Methyl-6-(2-(2,6-dichlorobenzamido)phenyl)-4-amino-3-chloropyridine-2-carboxylate **(16)**.

HRMS

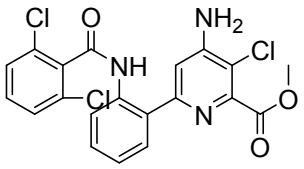

16

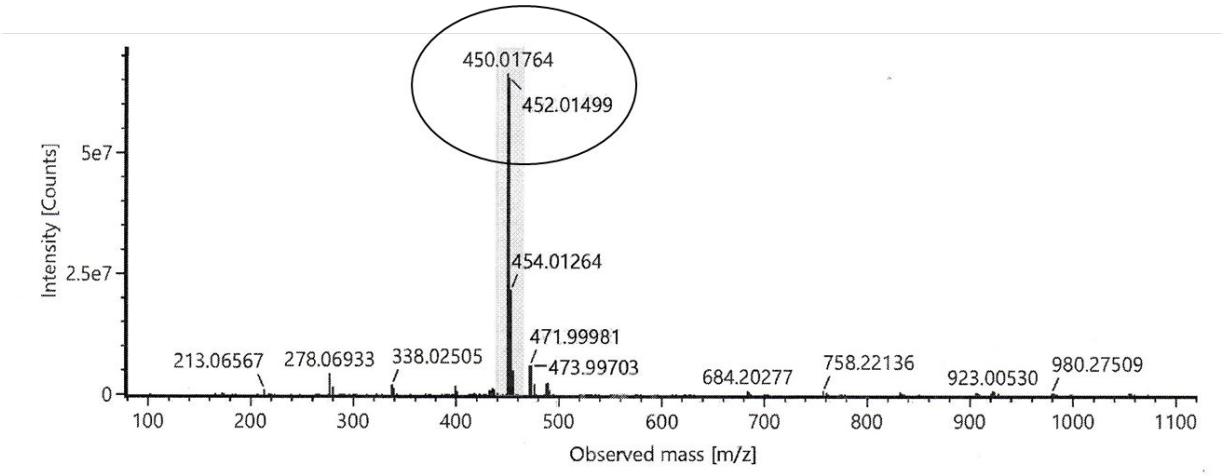

Figure S27: HRMS of Methyl-6-(2-(2,6-dichlorobenzamido)phenyl)-4-amino-3-chloropyridine-2-carboxylate **(16)**.

^{1}H-NMR

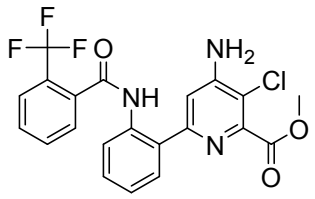

17

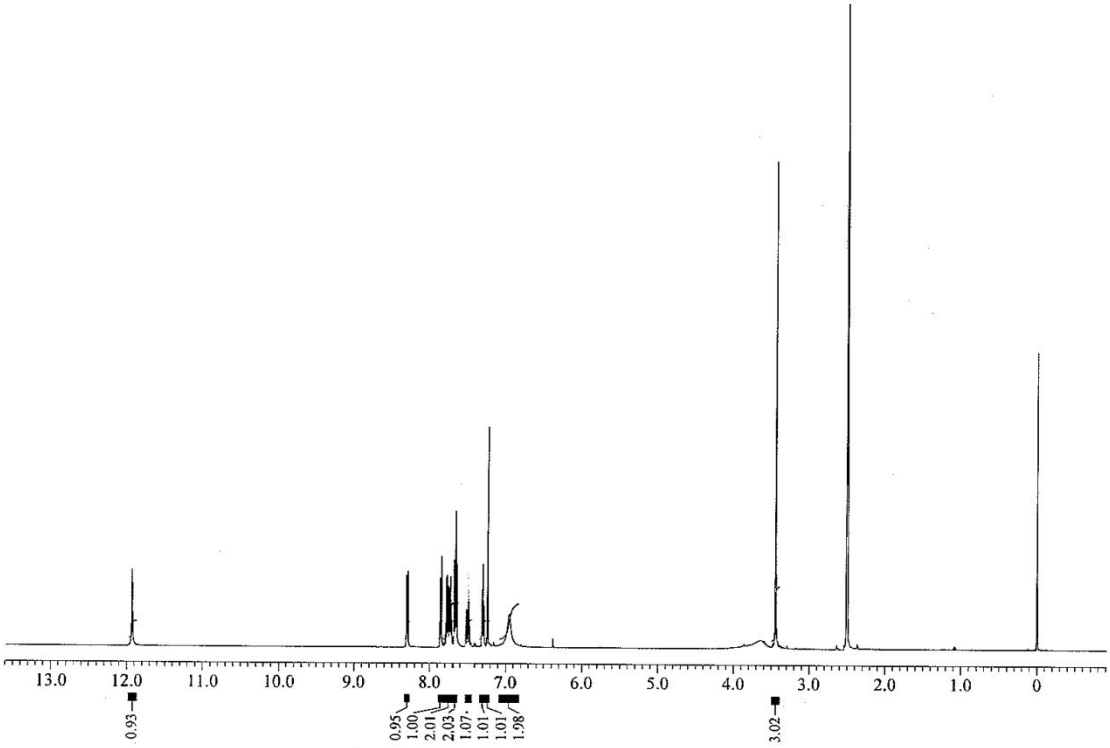

Figure S28: ^{1}H-NMR (300 MHz, DMSO) of Methyl-6-(2-(2-(trifluoromethyl) benzamido) phenyl)-4-amino-3-chloropyridine-2-carboxylate **(17)**.

^{13}C-NMR

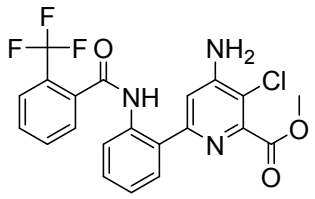

17

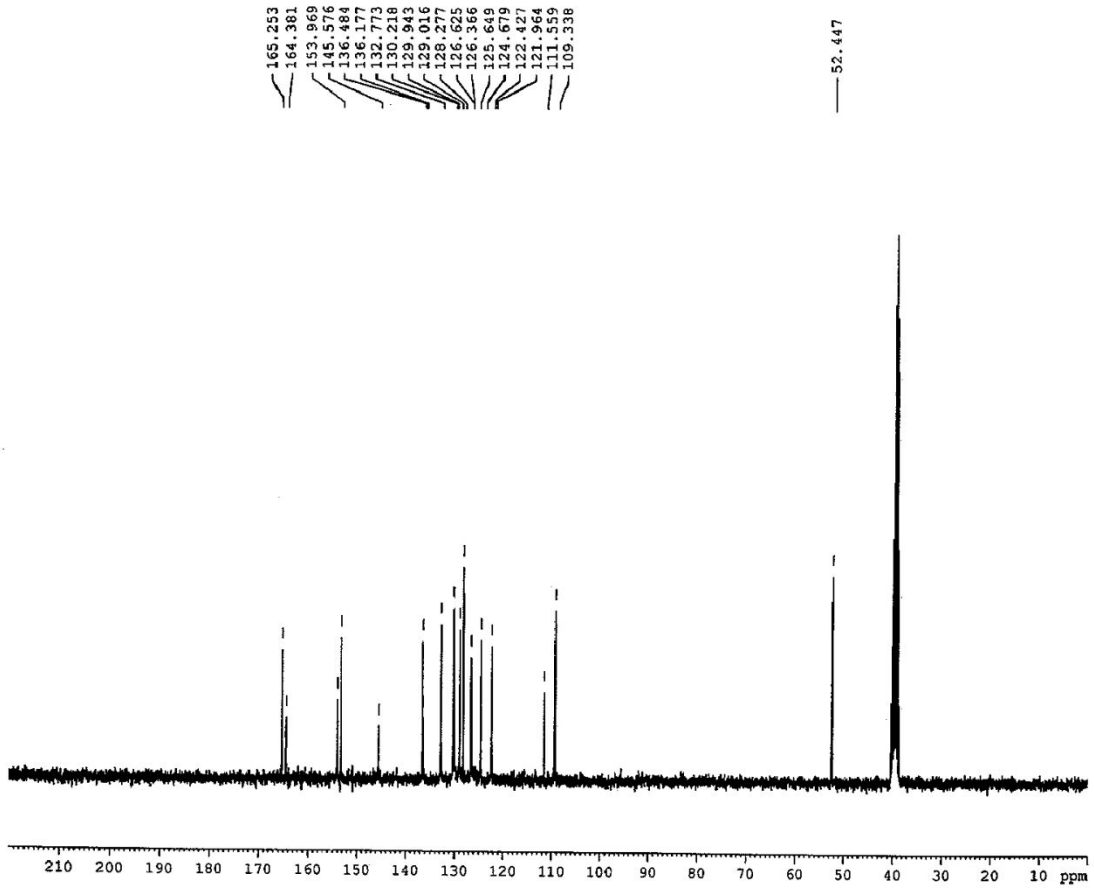

Figure S29: ^{13}C-NMR (75 MHz, DMSO) of Methyl-6-(2-(2-(trifluoromethyl) benzamido) phenyl)-4-amino-3-chloropyridine-2-carboxylate **(17)**.

HRMS

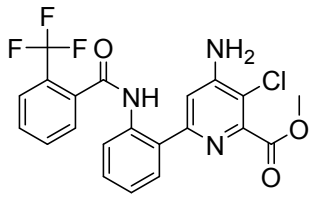

17

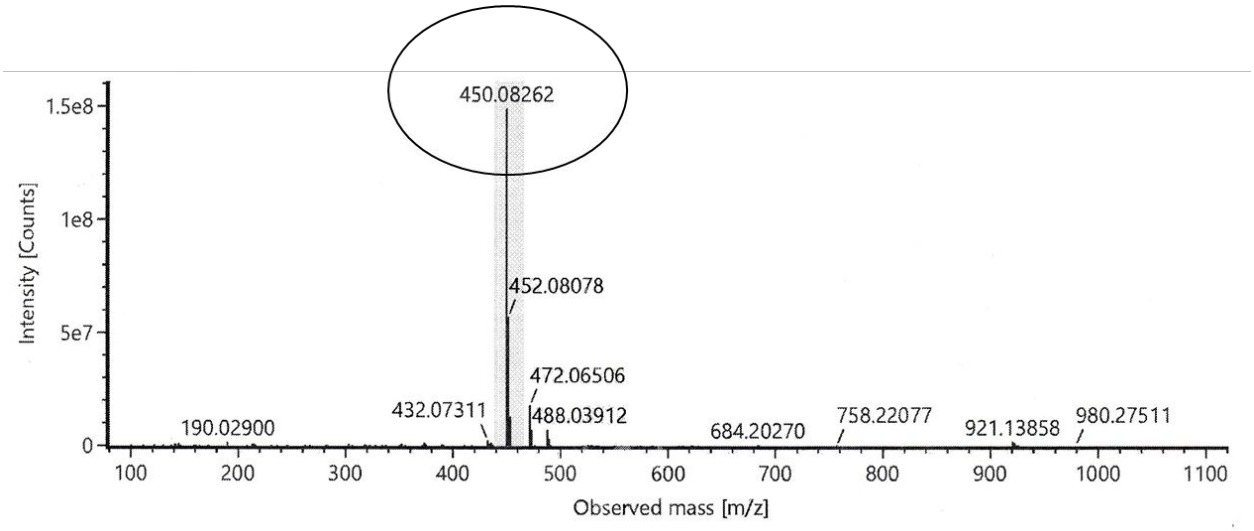

Figure S30: HRMS of Methyl-6-(2-(2-(trifluoromethyl) benzamido) phenyl)-4-amino-3-chloropyridine-2-carboxylate **(17)**.

^{1}H-NMR

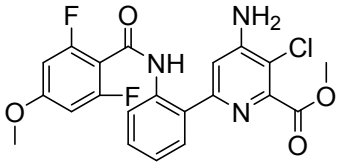

18

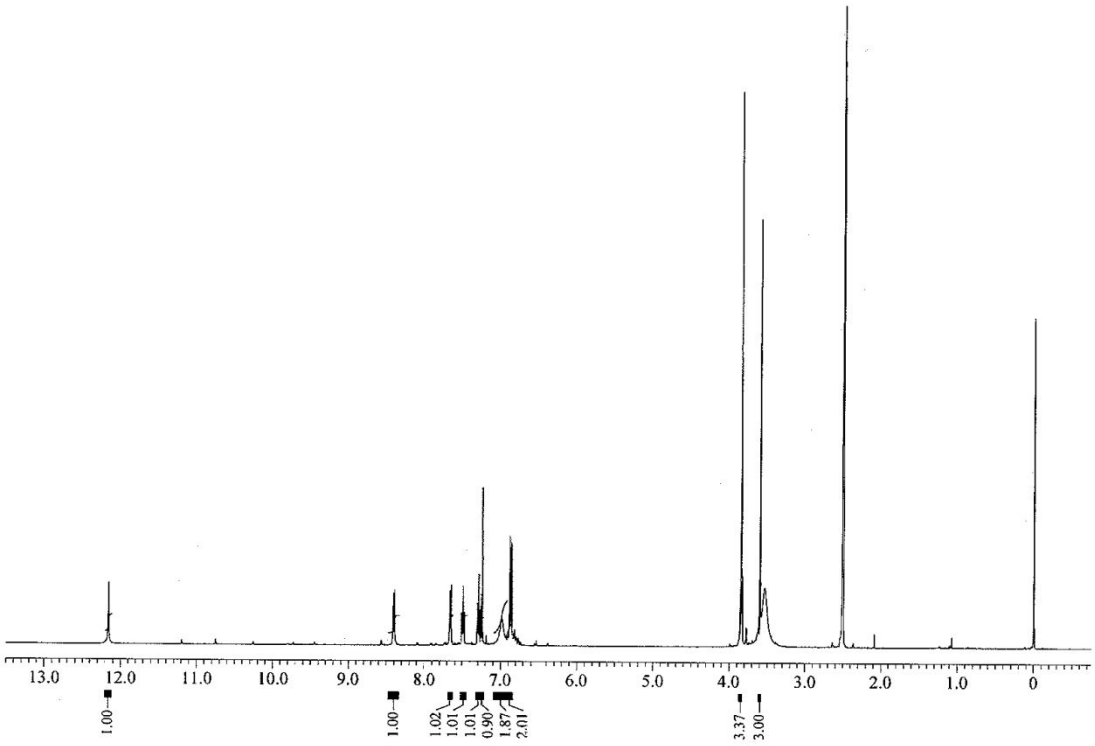

Figure S31: ^{1}H-NMR (300 MHz, DMSO) of Methyl-6-(2-(2,6-difluoro-4-methoxybenzamido)phenyl)-4-amino-3-chloropyridine-2-carboxylate **(18)**.

^{13}C-NMR

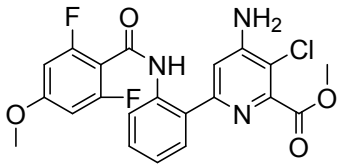

18

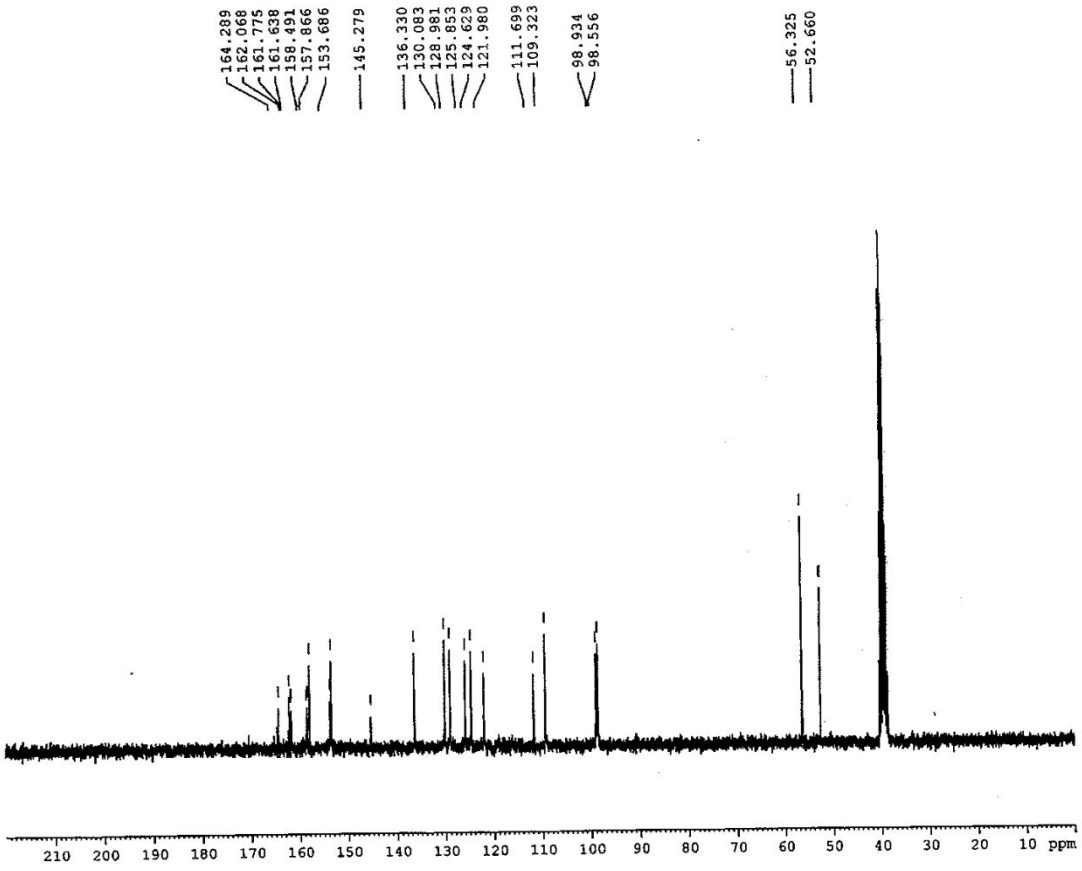

Figure S32: ^{13}C-NMR (75 MHz, DMSO) of Methyl-6-(2-(2,6-difluoro-4-methoxybenzamido)phenyl)-4-amino-3-chloropyridine-2-carboxylate **(18)**.

HRMS

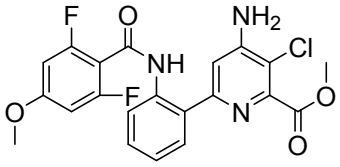

18

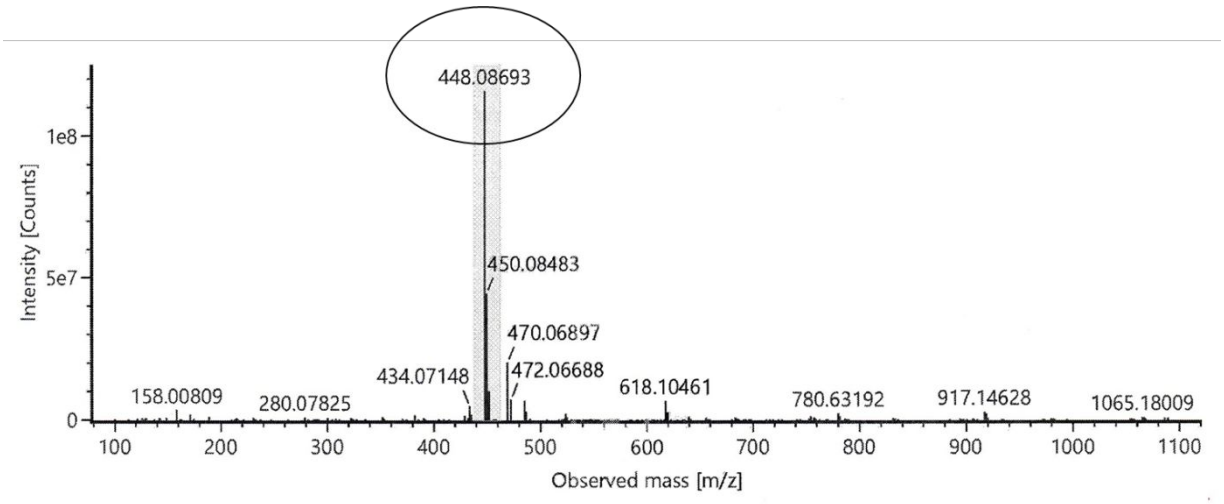

Figure S33: HRMS of Methyl-6-(2-(2,6-difluoro-4-methoxybenzamido)phenyl)-4-amino-3-chloropyridine-2-carboxylate **(18)**.

^{1}H-NMR

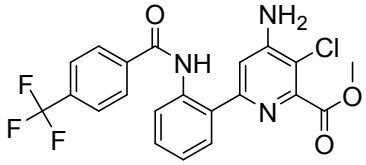

19

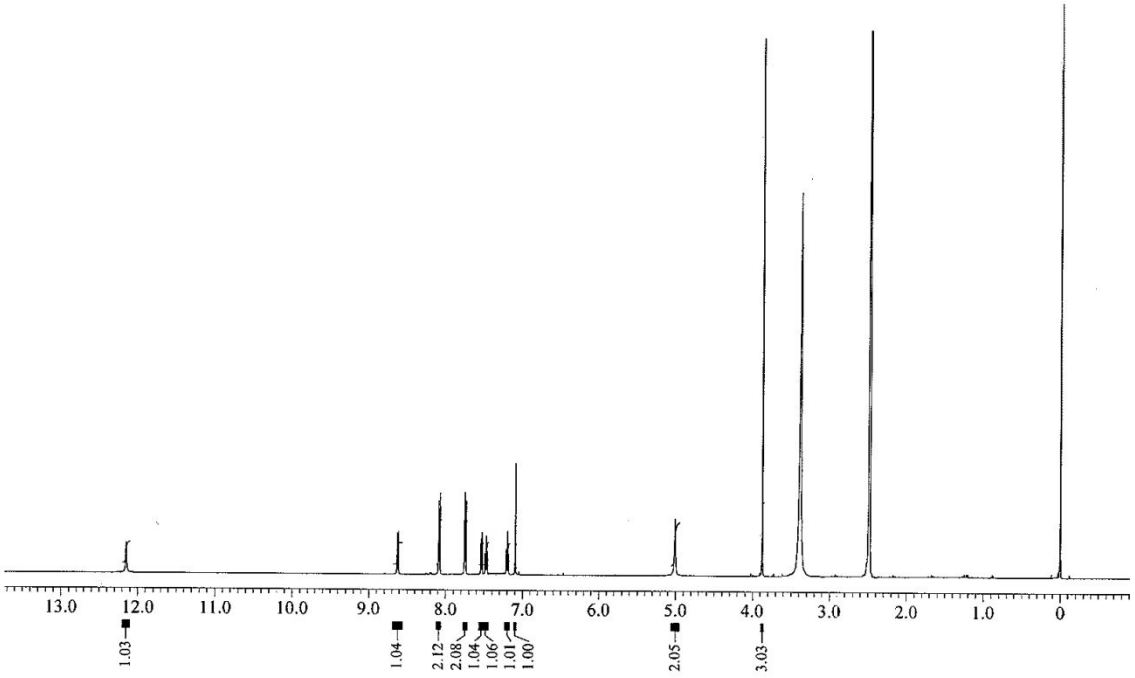

Figure S34: ^{1}H-NMR (300 MHz, DMSO) of Methyl-6-(2-(4-(trifluoromethyl) benzamido) phenyl)-4-amino-3-chloropyridine-2-carboxylate **(19)**.

^{13}C-NMR

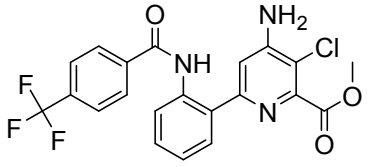

19

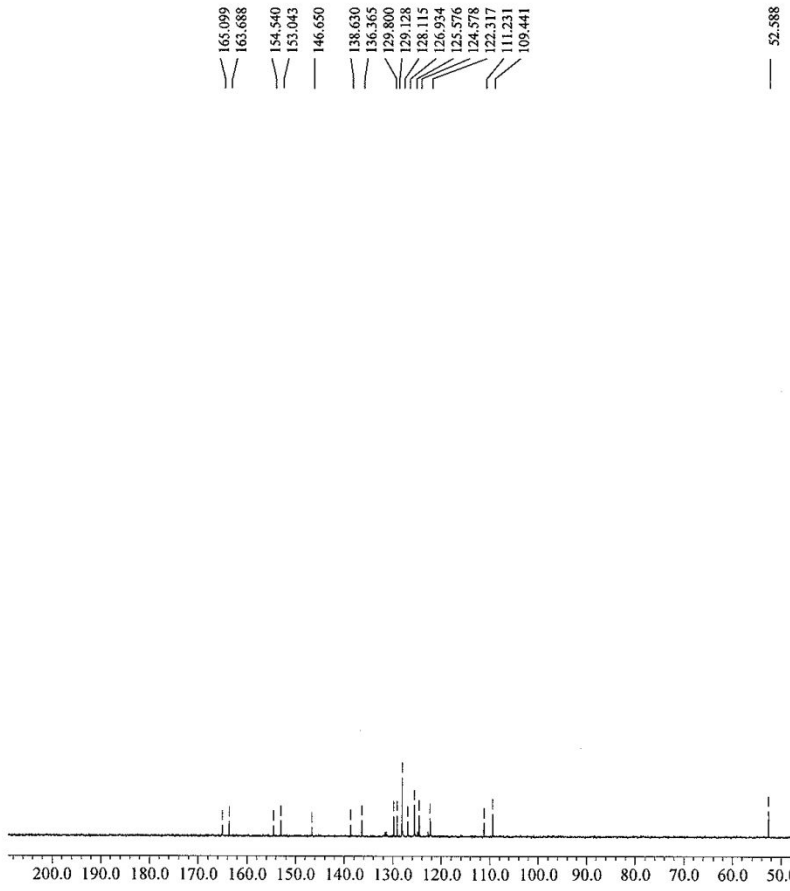

Figure S35: ^{13}C-NMR (75 MHz, DMSO) of Methyl-6-(2-(4-(trifluoromethyl) benzamido) phenyl)-4-amino-3-chloropyridine-2-carboxylate **(19)**.

HRMS

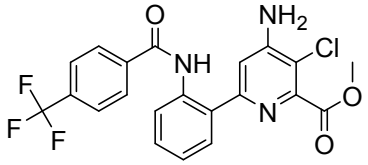

19

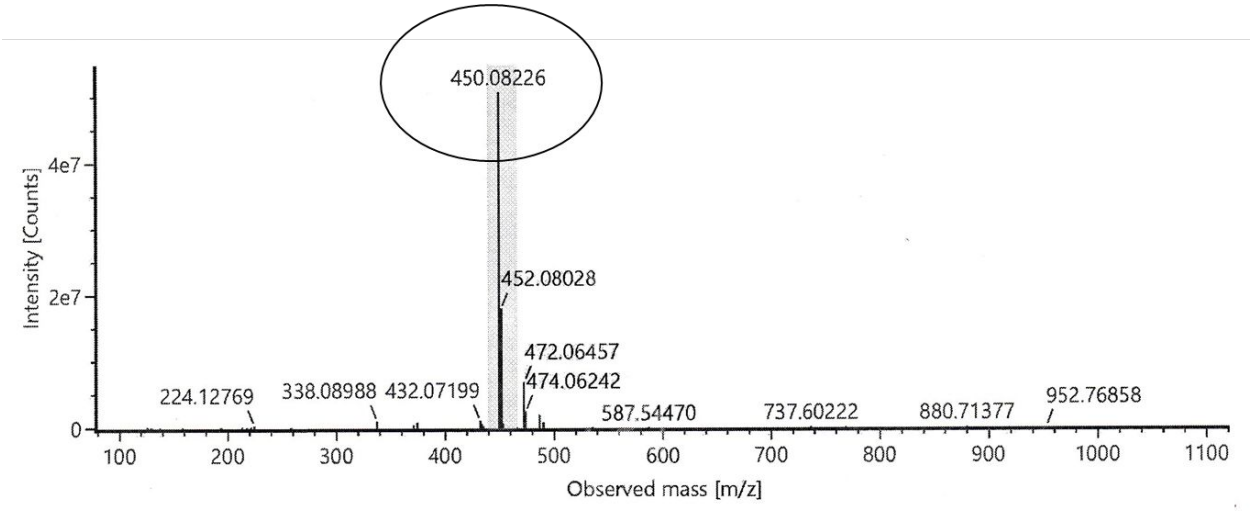

Figure S36: HRMS of Methyl-6-(2-(4-(trifluoromethyl) benzamido) phenyl)-4-amino-3-chloropyridine-2-carboxylate **(19)**.

^{1}H-NMR

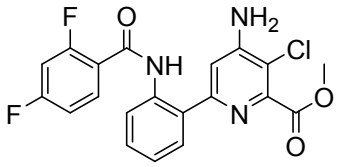

20

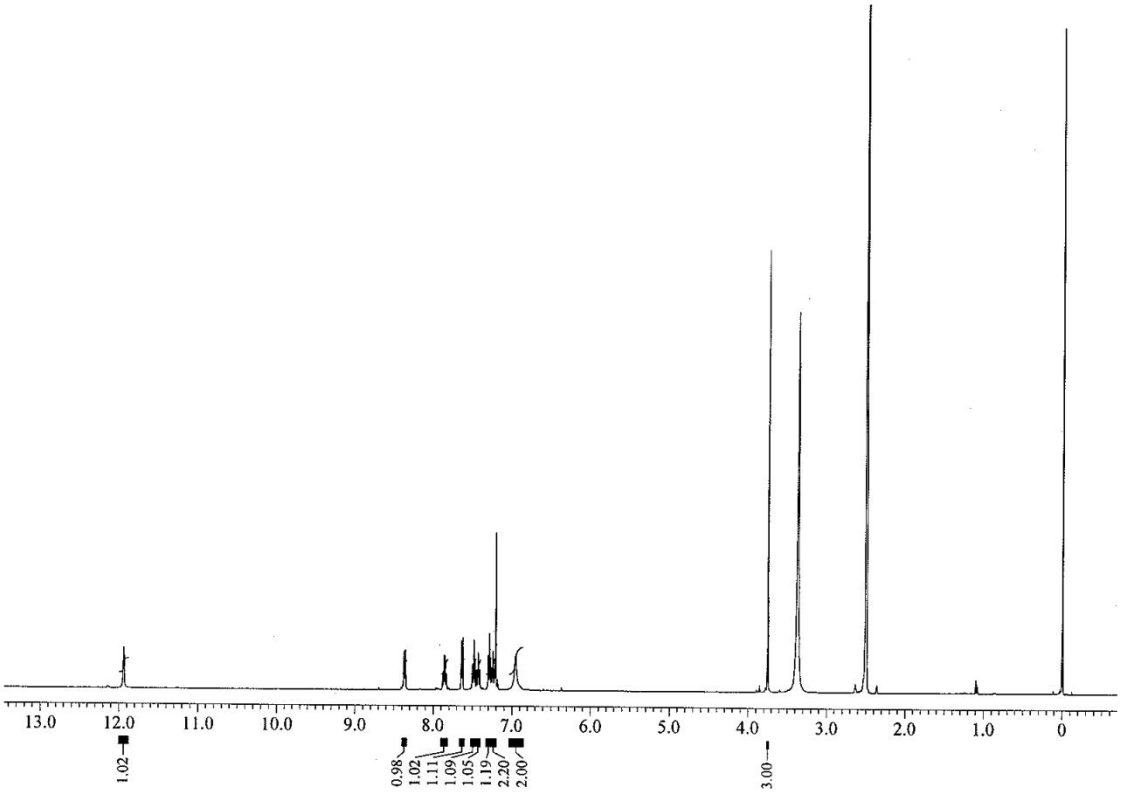

Figure S37: ^{1}H-NMR (300 MHz, DMSO) of Methyl-6-(2-(2,4-difluorobenzamido)phenyl)-4-amino-3-chloropyridine-2-carboxylate **(20)**.

^{13}C-NMR

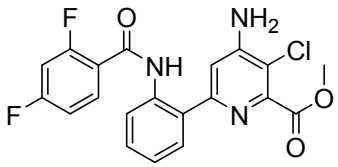

20

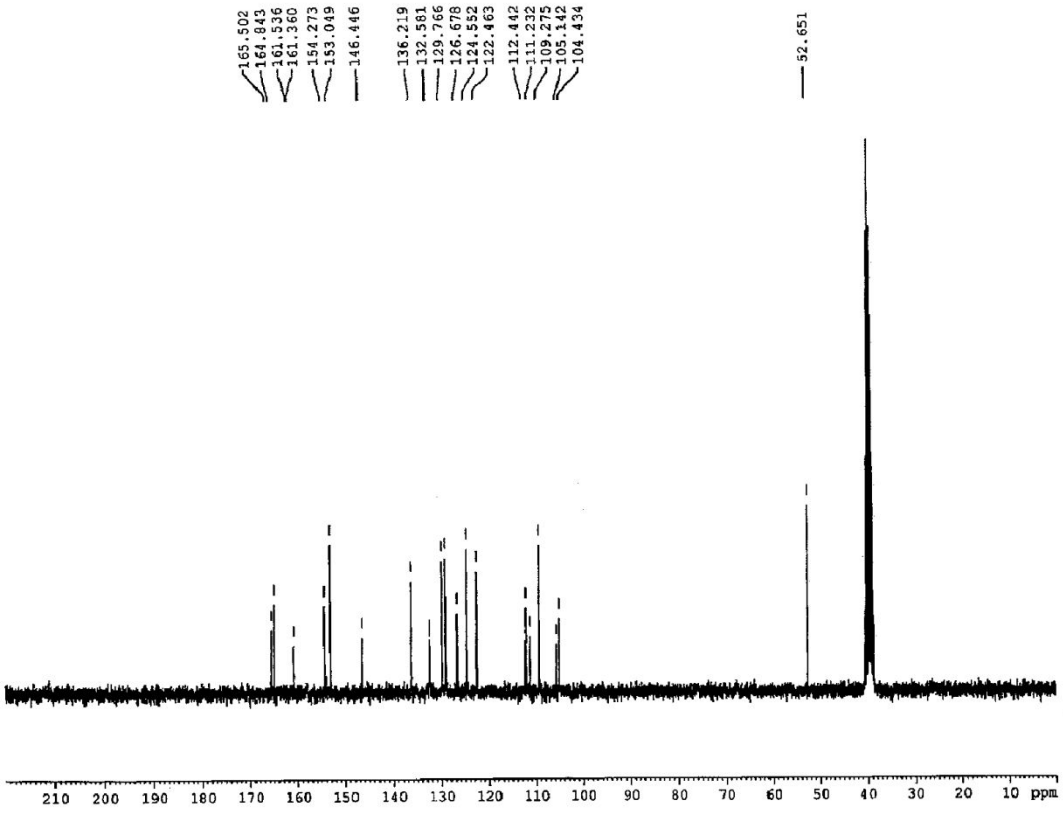

Figure S38: ^{13}C-NMR (75 MHz, DMSO) of Methyl-6-(2-(2,4-difluorobenzamido)phenyl)-4-amino-3-chloropyridine-2-carboxylate **(20)**.

HRMS

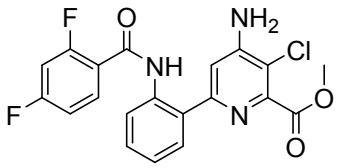

20

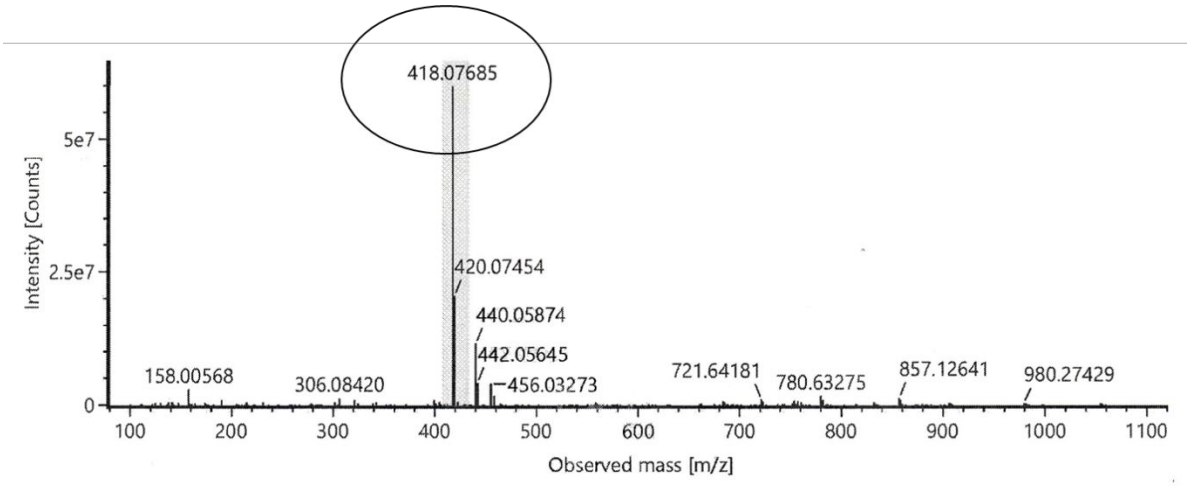

Figure S39: HRMS of Methyl-6-(2-(2,4-difluorobenzamido)phenyl)-4-amino-3-chloropyridine-2-carboxylate **(20)**.

\

^{1}H-NMR

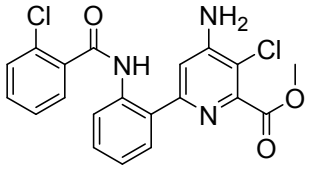

21

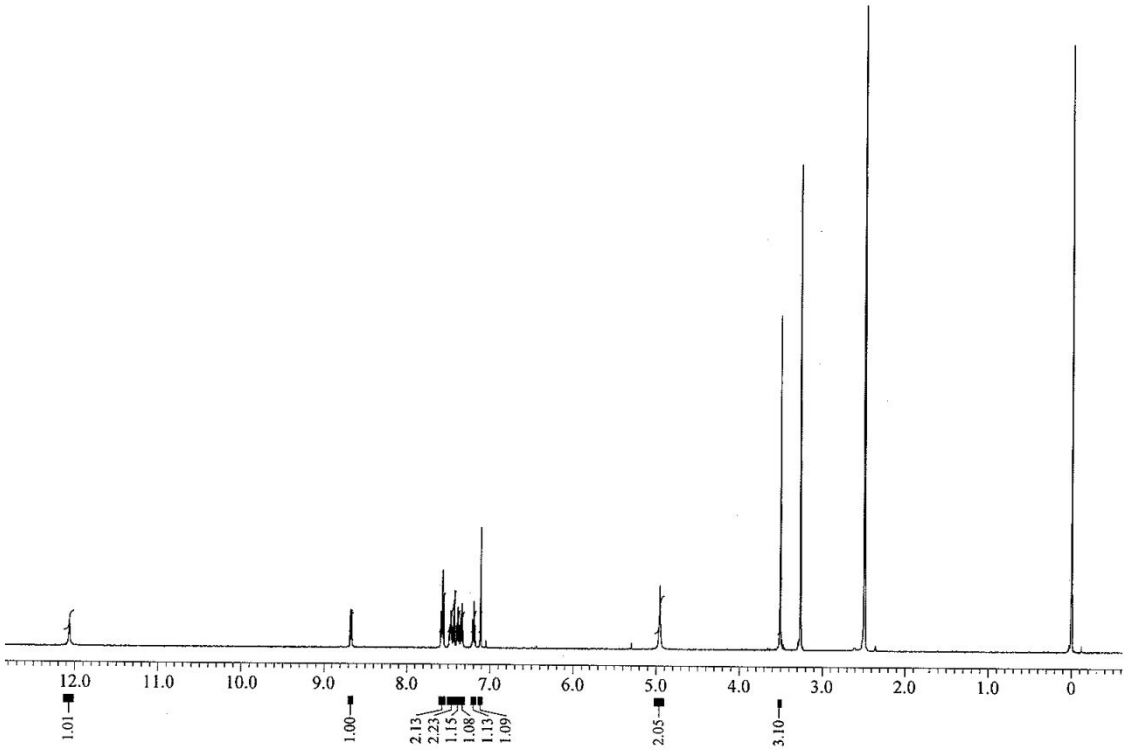

Figure S40: ^{1}H-NMR (300 MHz, DMSO) of Methyl-6-(2-(2-chlorobenzamido) phenyl)-4-amino-3-chloropyridine-2-carboxylate **(21)**.

^{13}C-NMR

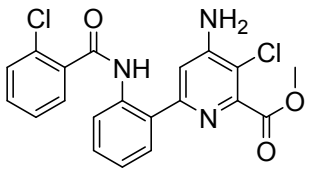

21

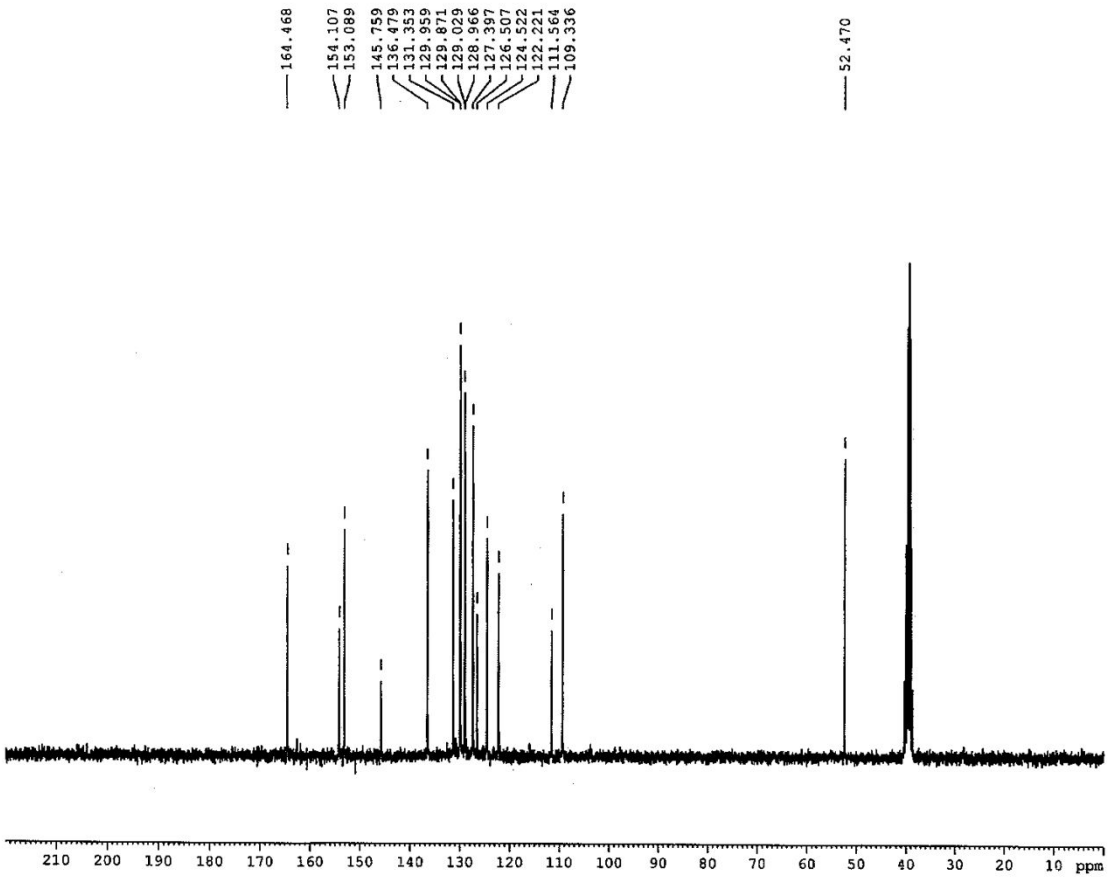

Figure S41: ^{13}C-NMR (75 MHz, DMSO) of Methyl-6-(2-(2-chlorobenzamido) phenyl)-4-amino-3-chloropyridine-2-carboxylate **(21)**.

HRMS

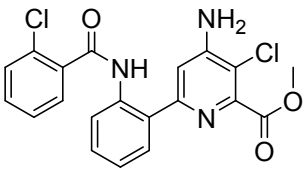

21

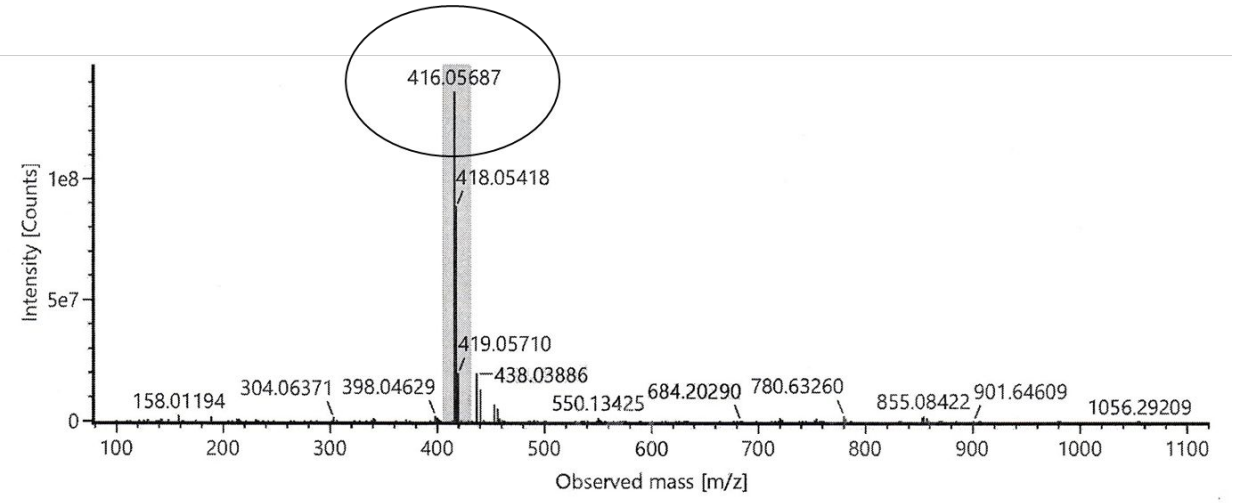

Figure S42: HRMS of Methyl-6-(2-(2-chlorobenzamido) phenyl)-4-amino-3-chloropyridine-2-carboxylate **(21)**.

^{1}H-NMR

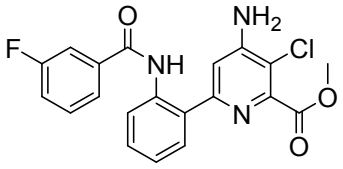

22

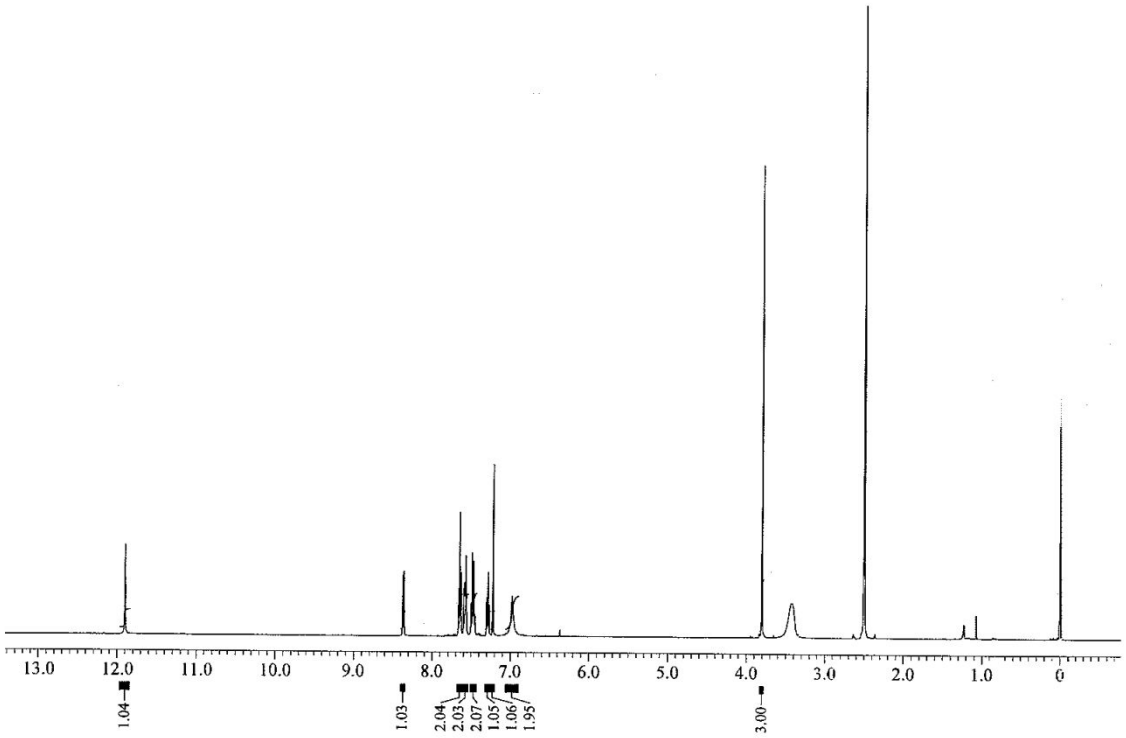

Figure S43: ^{1}H-NMR (300 MHz, DMSO) of Methyl-6-(2-(3-fluorobenzamido) phenyl)-4-amino-3-chloropyridine-2-carboxylate **(22)**.

^{13}C-NMR

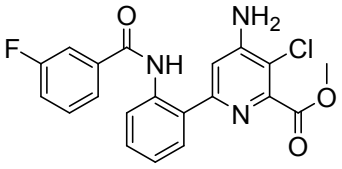

22

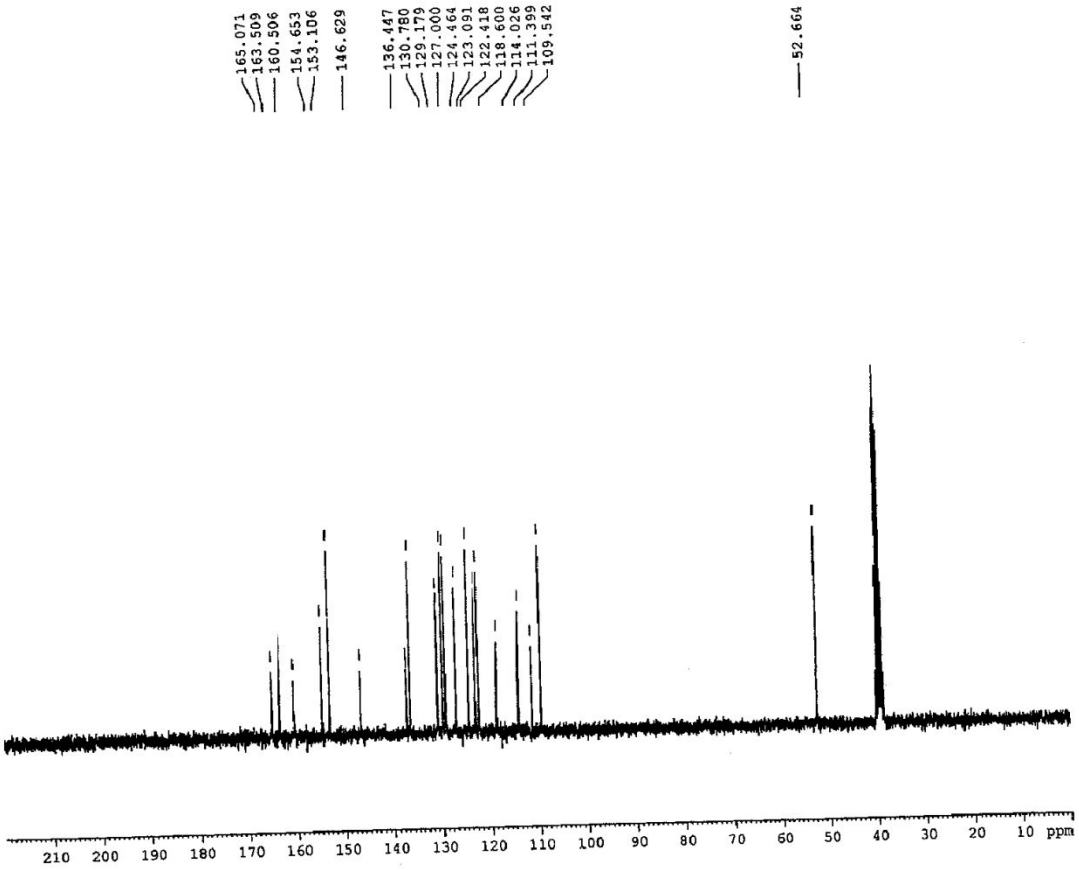

Figure S44: ^{13}C-NMR (75 MHz, DMSO) of Methyl-6-(2-(3-fluorobenzamido) phenyl)-4-amino-3-chloropyridine-2-carboxylate **(22)**.

HRMS

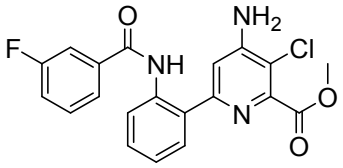

22

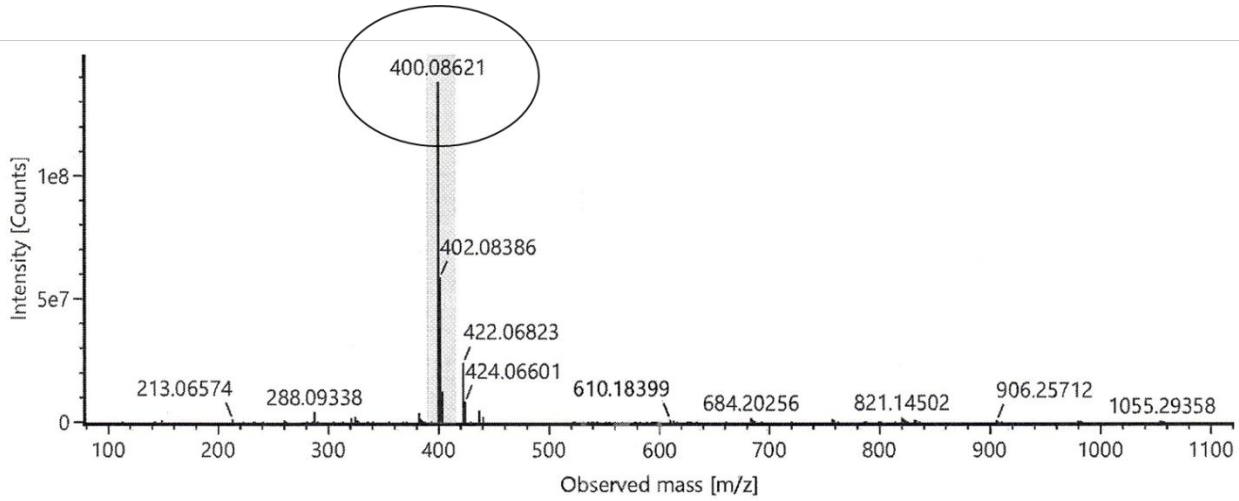

Figure S45: HRMS of Methyl-6-(2-(3-fluorobenzamido) phenyl)-4-amino-3-chloropyridine-2-carboxylate **(22)**.

^{1}H-NMR

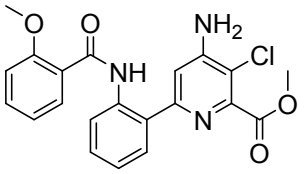

23

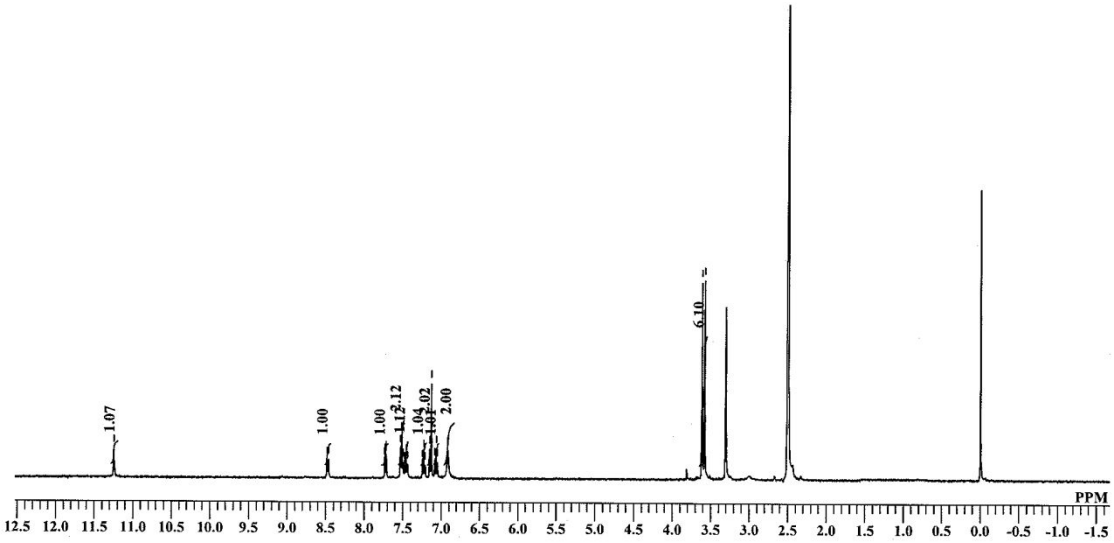

Figure S46: ^{1}H-NMR (300 MHz, DMSO) of Methyl-6-(2-(2-methoxybenzamido) phenyl)-4-amino-3-chloropyridine-2-carboxylate **(23)**.

^{13}C-NMR

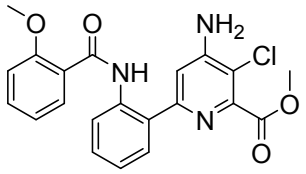

23

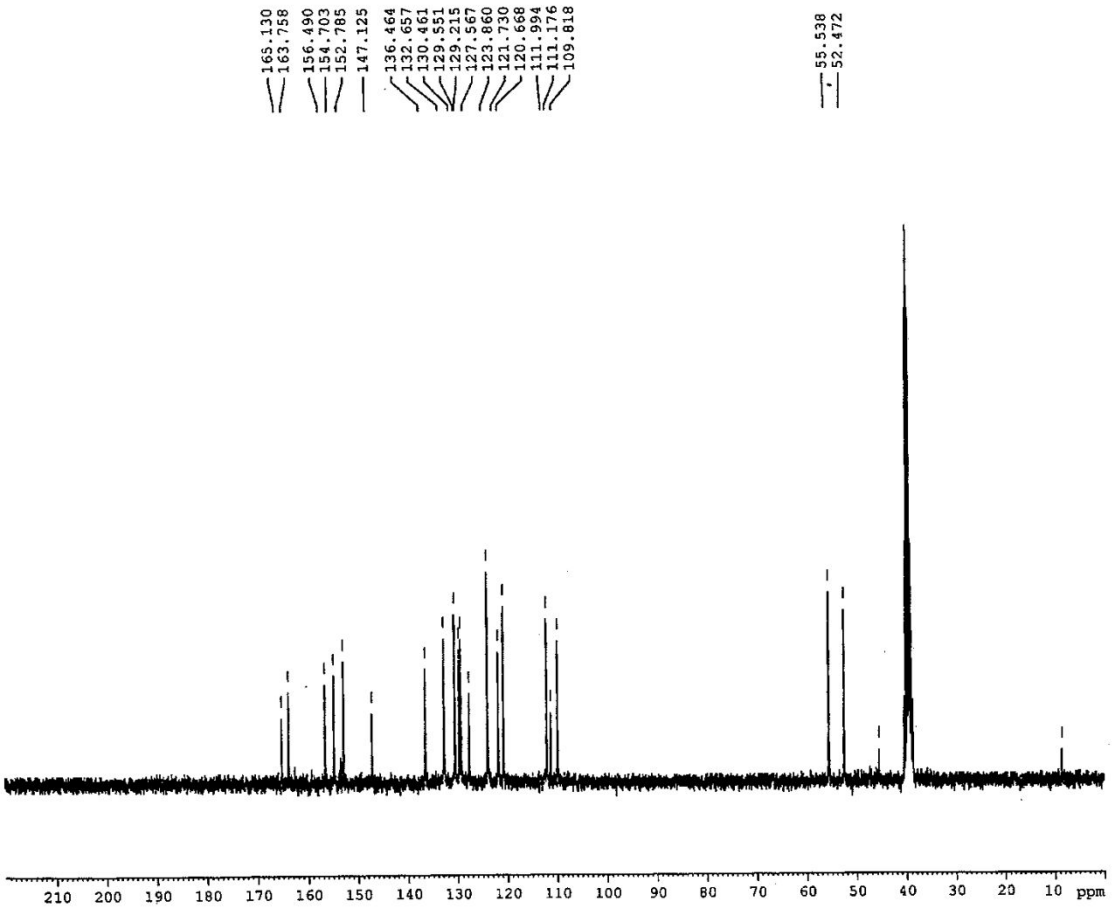

Figure S47: ^{13}C-NMR (75 MHz, DMSO) of Methyl-6-(2-(2-methoxybenzamido) phenyl)-4-amino-3-chloropyridine-2-carboxylate **(23)**.

HRMS

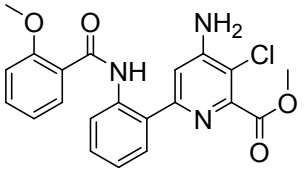

23

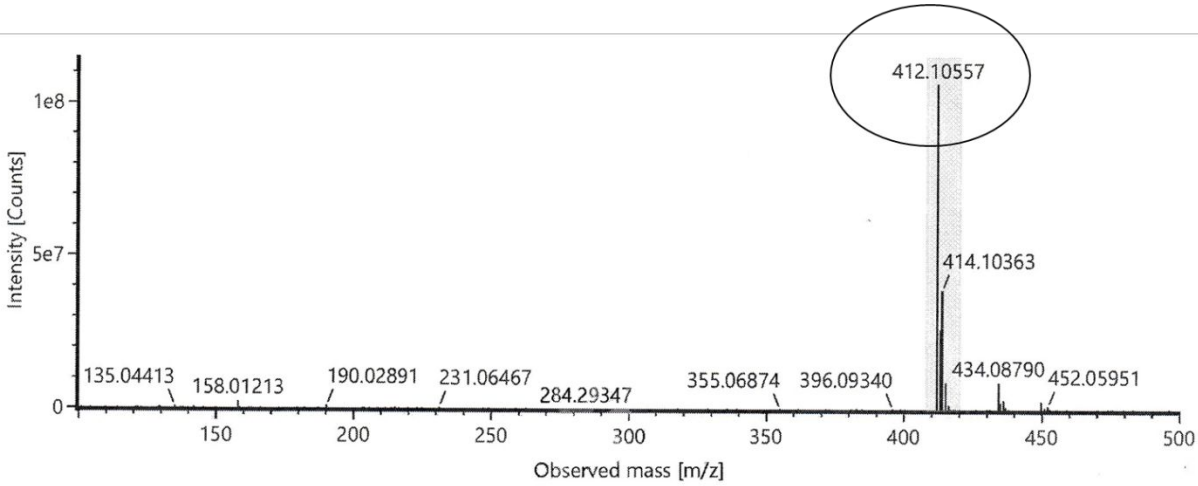

Figure S48: HRMS of Methyl-6-(2-(2-methoxybenzamido) phenyl)-4-amino-3-chloropyridine-2-carboxylate **(23)**.

^{1}H-NMR

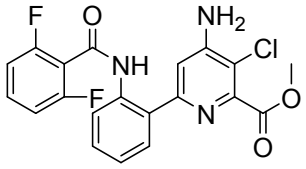

24

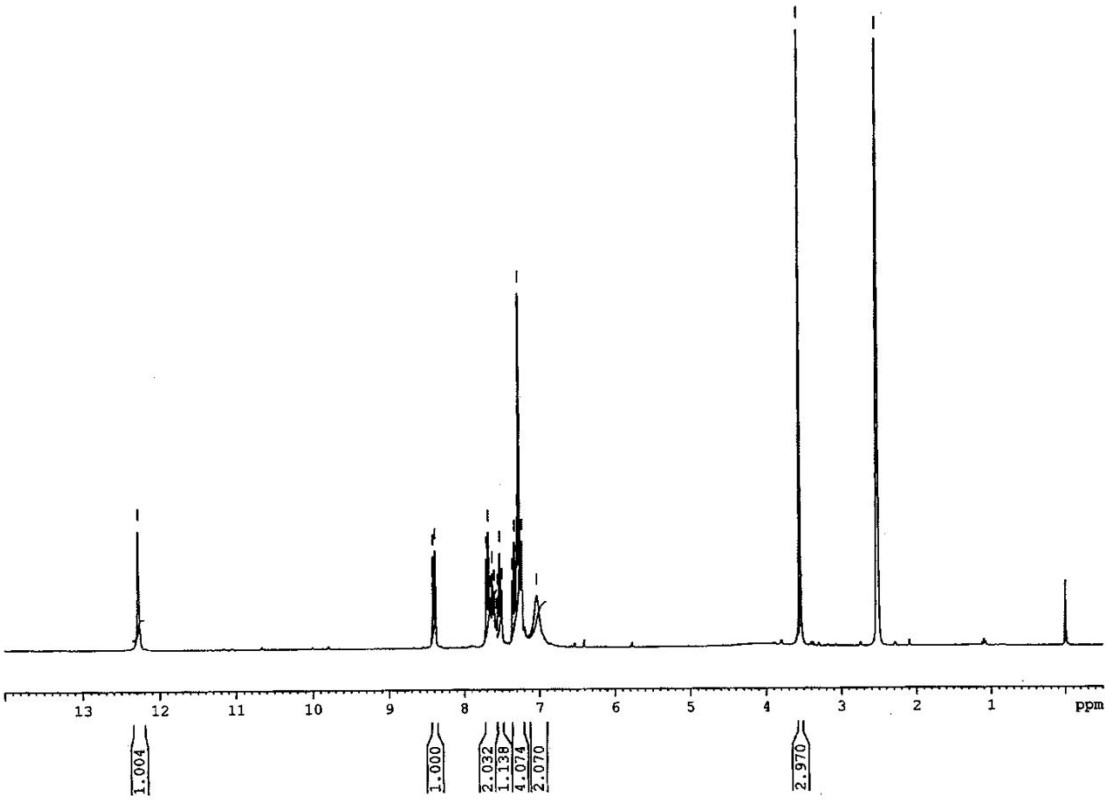

Figure S49: ^{1}H-NMR (300 MHz, DMSO) of Methyl-6-(2-(2,6-difluorobenzamido)phenyl)-4-amino-3-chloropyridine-2-carboxylate **(24)**.

^{13}C-NMR

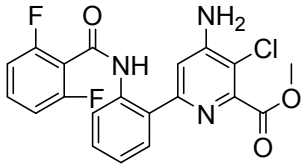

24

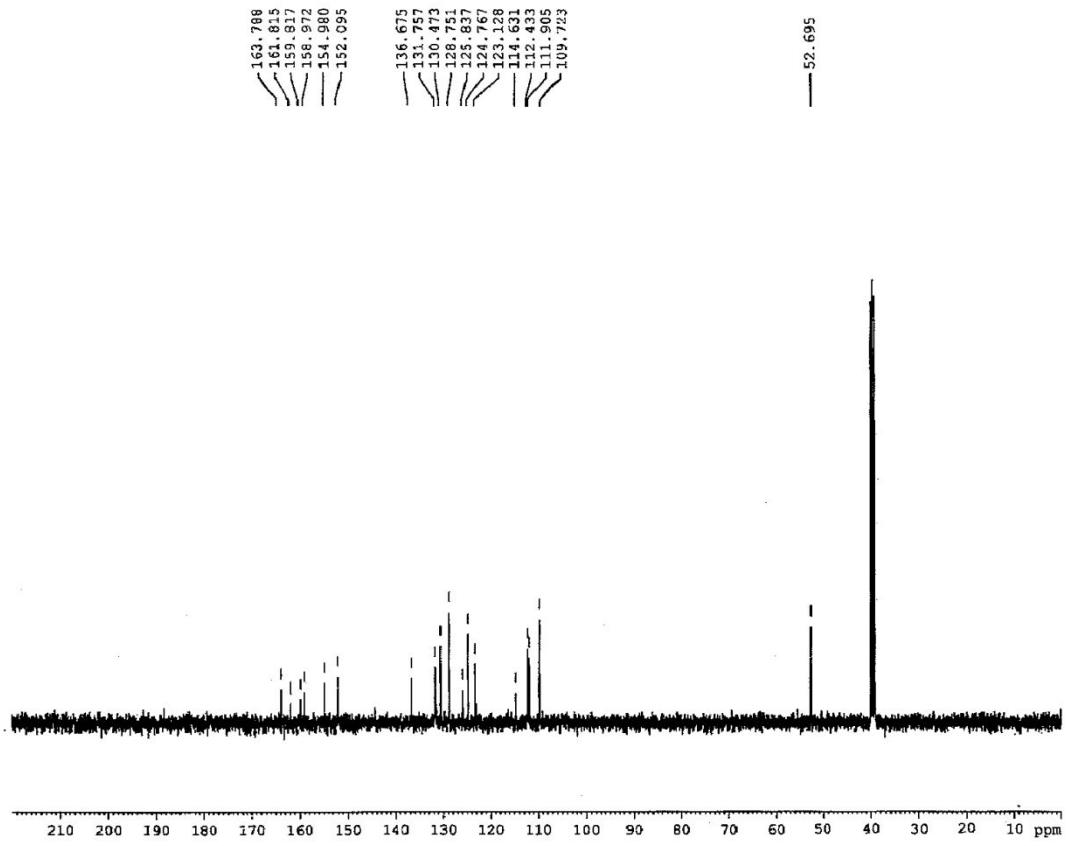

Figure S50: ^{13}C-NMR (75 MHz, DMSO) of Methyl-6-(2-(2,6-difluorobenzamido)phenyl)-4-amino-3-chloropyridine-2-carboxylate **(24)**.

HRMS

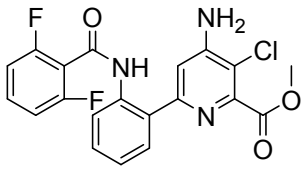

24

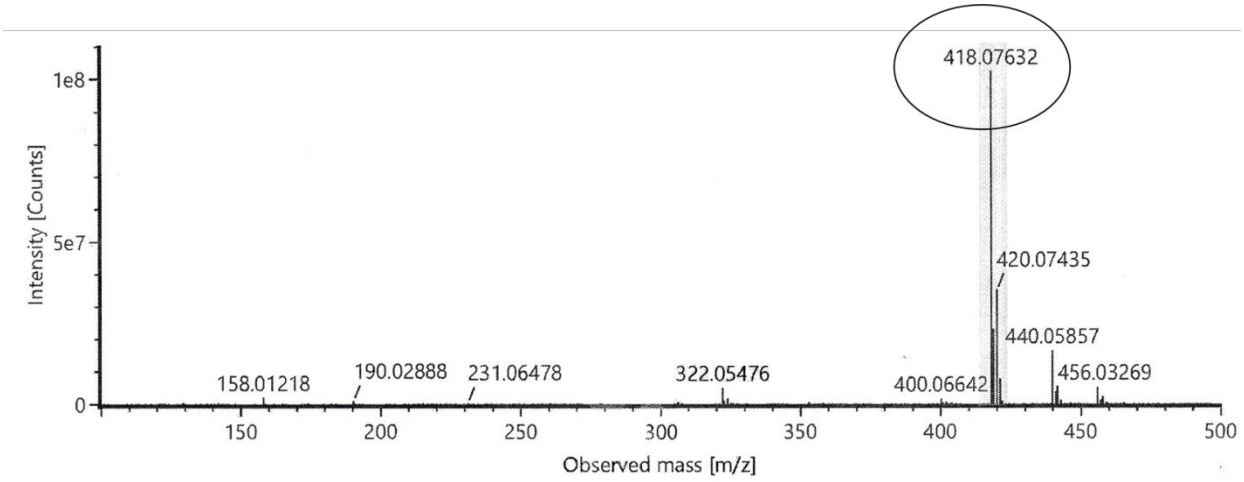

Figure S51: HRMS of Methyl-6-(2-(2,6-difluorobenzamido)phenyl)-4-amino-3-chloropyridine-2-carboxylate **(24)**.

^{1}H-NMR

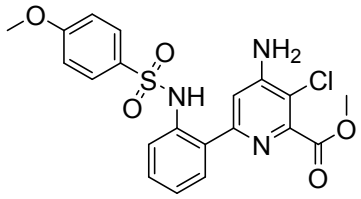

25

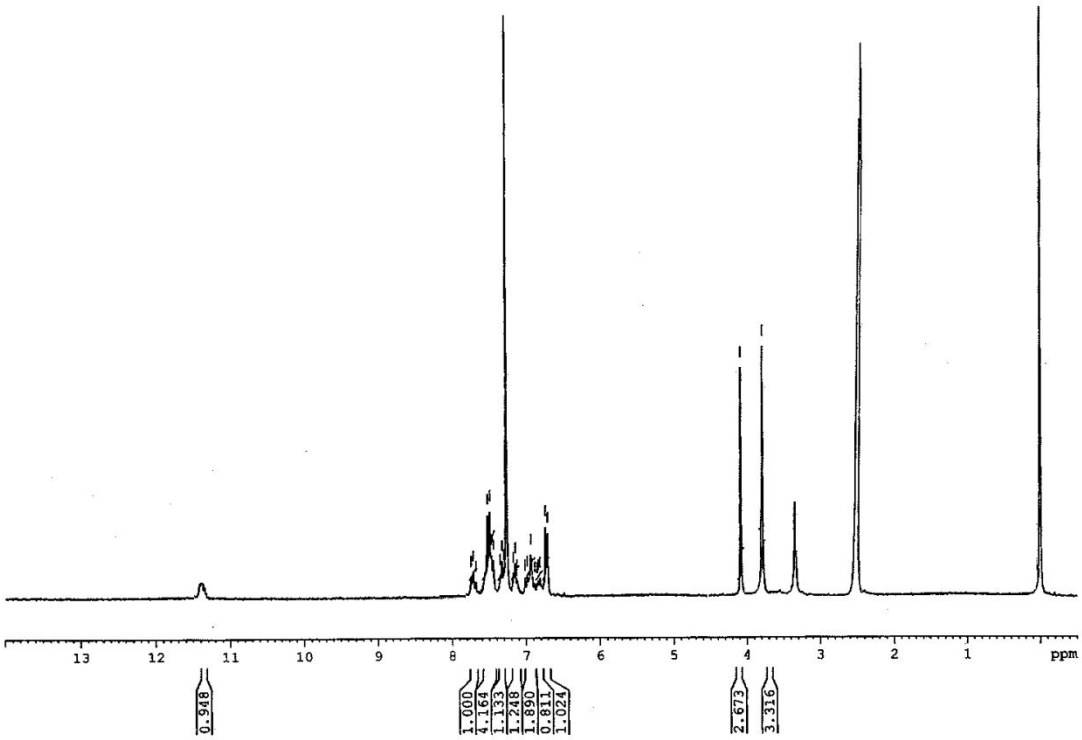

Figure S52: ^{1}H-NMR (300 MHz, DMSO) of Methyl-4-amino-3-chloro-6-(2-((4-methoxyphenyl) sulfonamido) phenyl) picolinate **(25)**.

^{13}C-NMR

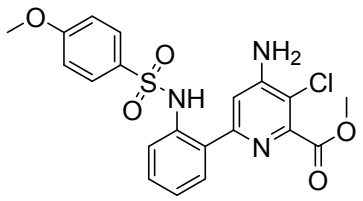

25

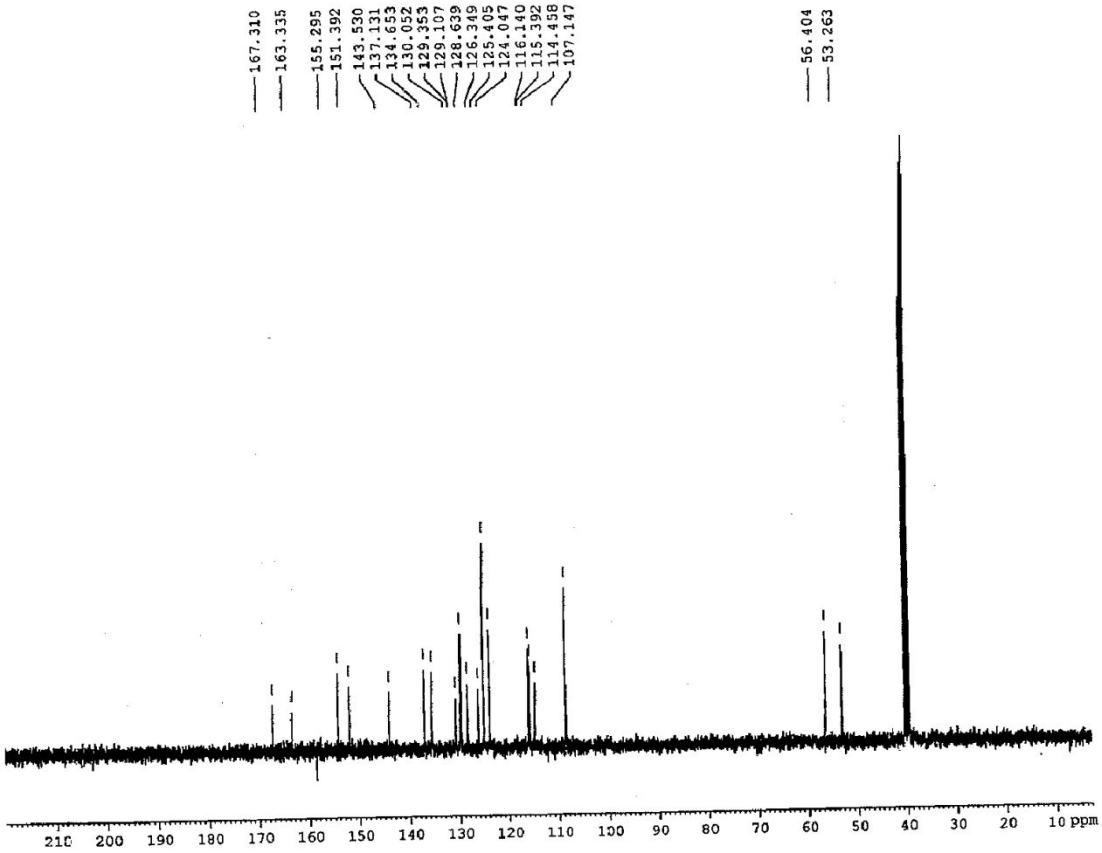

Figure S53: ^{13}C-NMR (75 MHz, DMSO) of Methyl-4-amino-3-chloro-6-(2-((4-methoxyphenyl) sulfonamido) phenyl) picolinate **(25)**.

HRMS

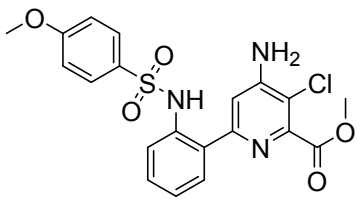

25

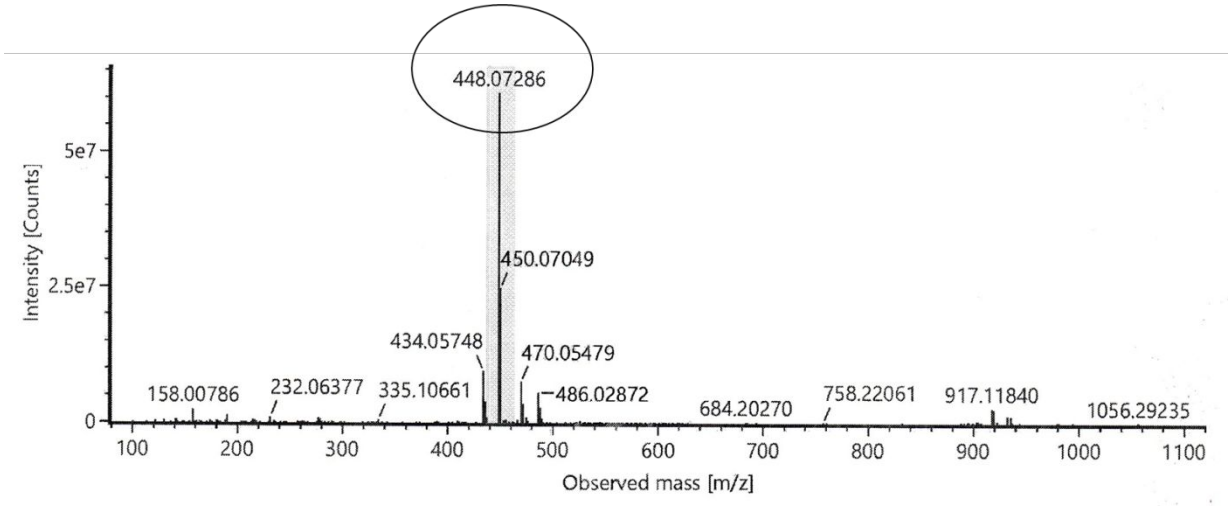

Figure S54: HRMS of Methyl-4-amino-3-chloro-6-(2-((4-methoxyphenyl) sulfonamido) phenyl) picolinate **(25)**.

^{1}H-NMR

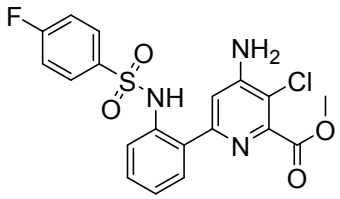

26

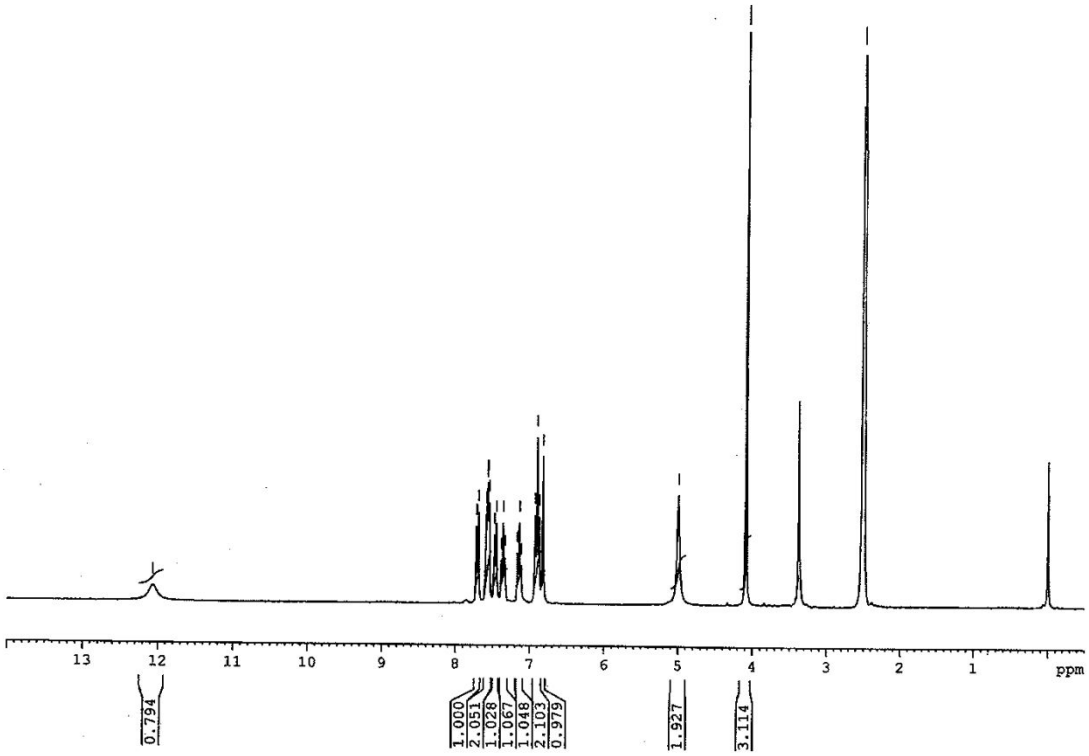

Figure S55: ^{1}H-NMR (300 MHz, DMSO) of Methyl-4-amino-3-chloro-6-(2-((4-fluorophenyl) sulfonamido) phenyl) picolinate **(26)**.

^{13}C-NMR

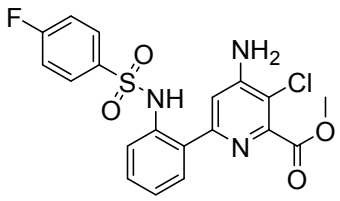

26

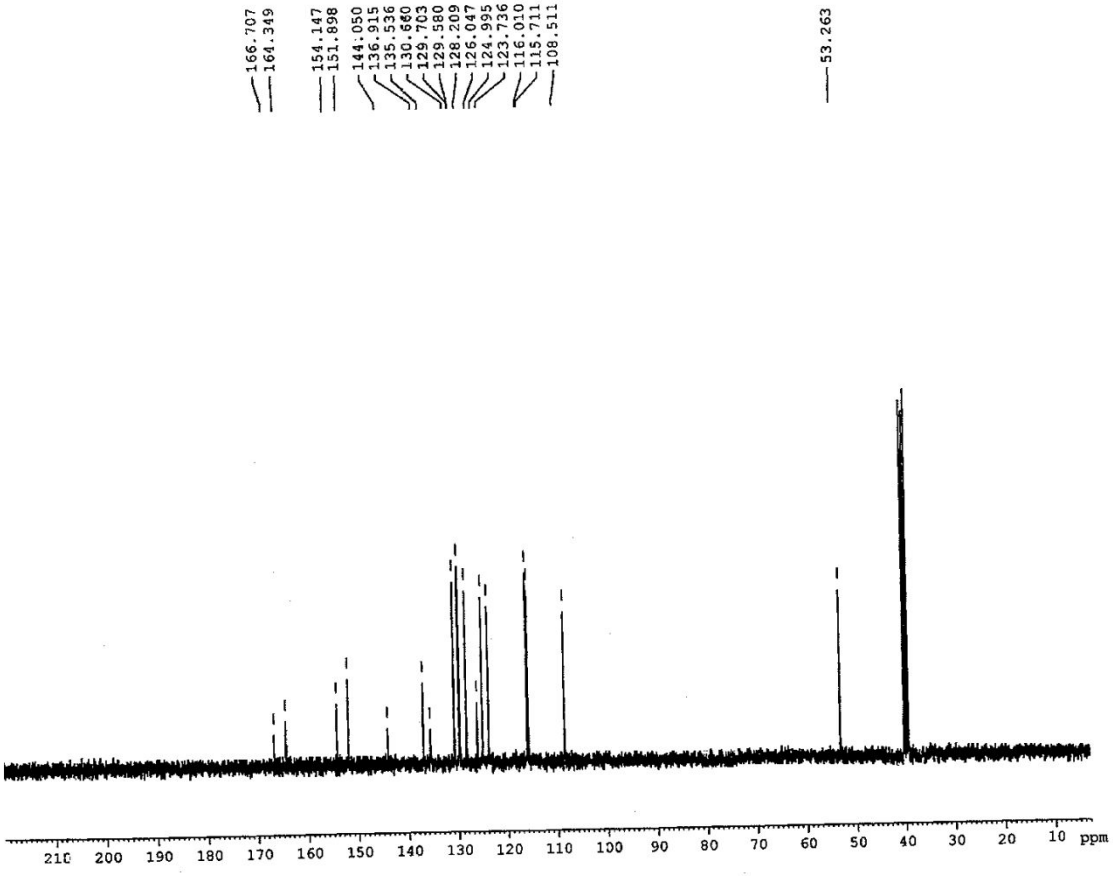

Figure S56: ^{13}C-NMR (75 MHz, DMSO) of Methyl-4-amino-3-chloro-6-(2-((4-fluorophenyl) sulfonamido) phenyl) picolinate **(26)**.

HRMS

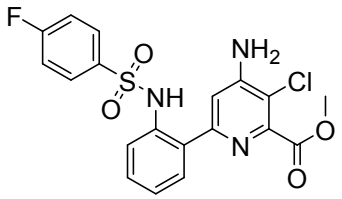

26

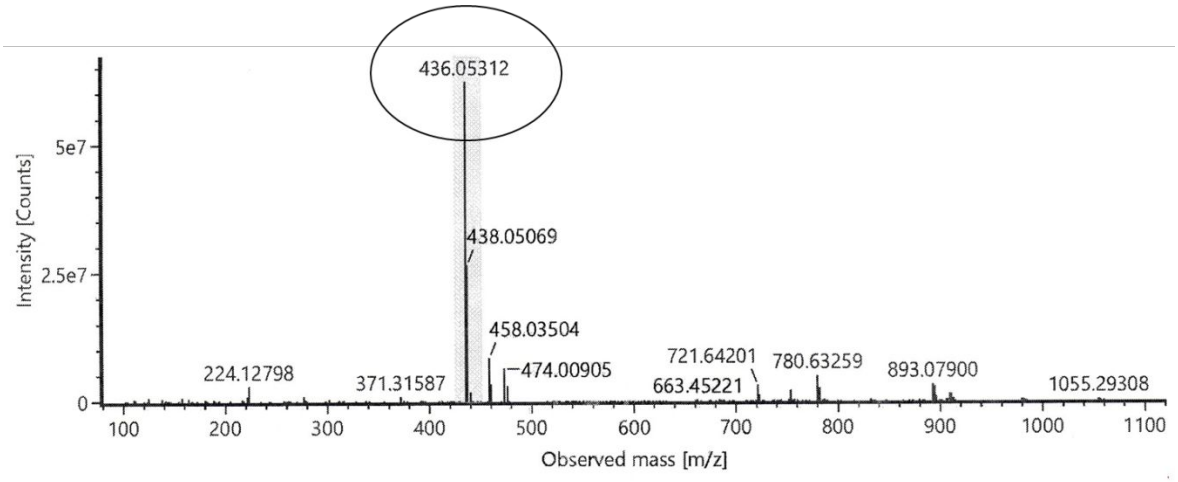

Figure S57: HRMS of Methyl-4-amino-3-chloro-6-(2-((4-fluorophenyl) sulfonamido) phenyl) picolinate **(26)**.

^{1}H-NMR

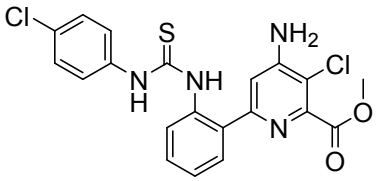

27

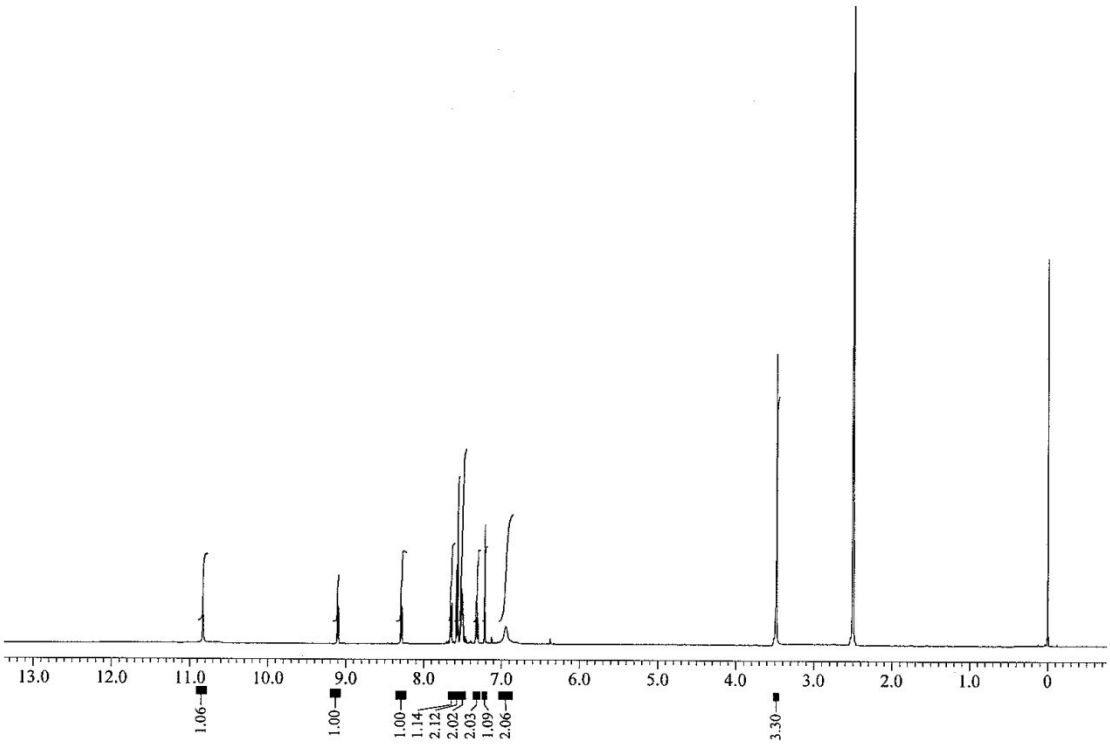

Figure S58: ^{1}H-NMR (300 MHz, DMSO) of Methyl-4-amino-3-chloro-6-(2-(3-(4-chlorophenyl) thioureido) phenyl) pyridine-2-carboxylate **(27)**.

^{13}C-NMR

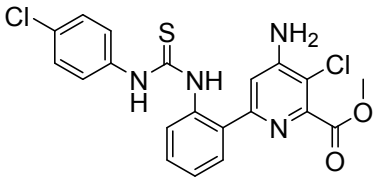

27

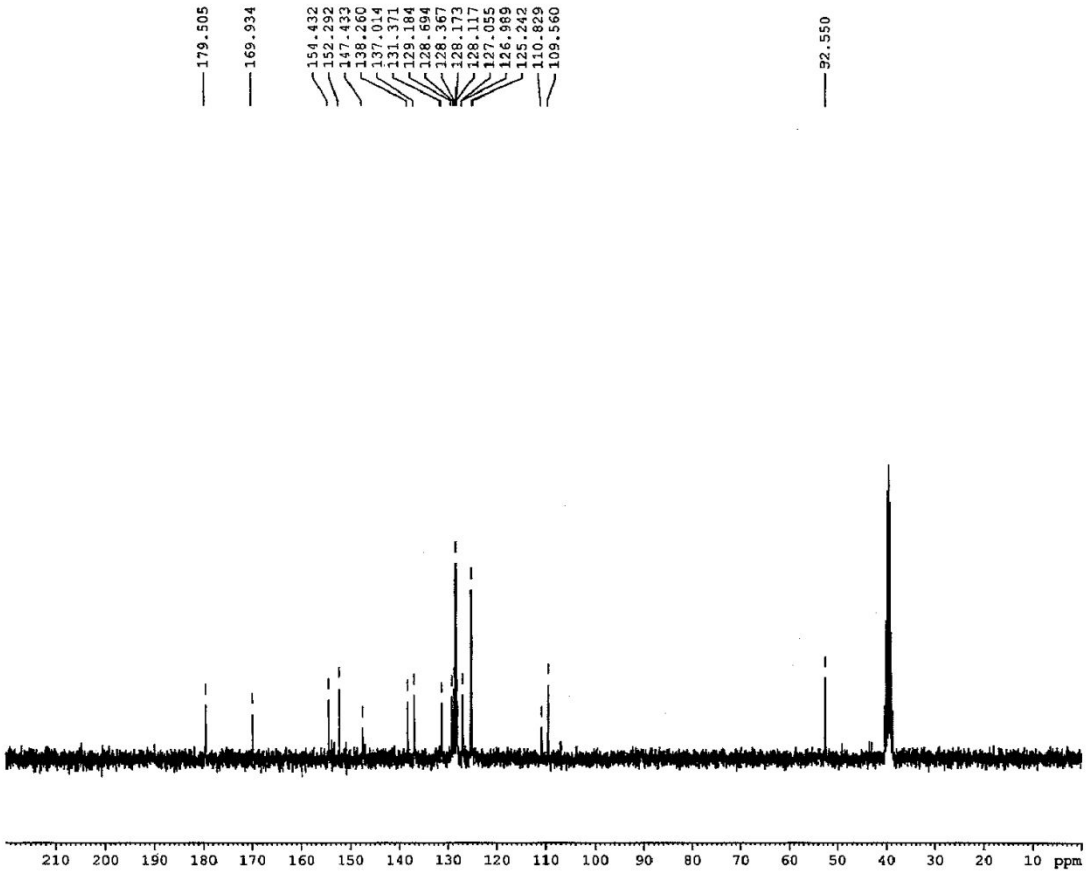

Figure S59: ^{13}C-NMR (75 MHz, DMSO) of Methyl-4-amino-3-chloro-6-(2-(3-(4-chlorophenyl) thioureido) phenyl) pyridine-2-carboxylate **(27)**.

HRMS

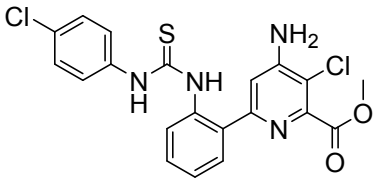

27

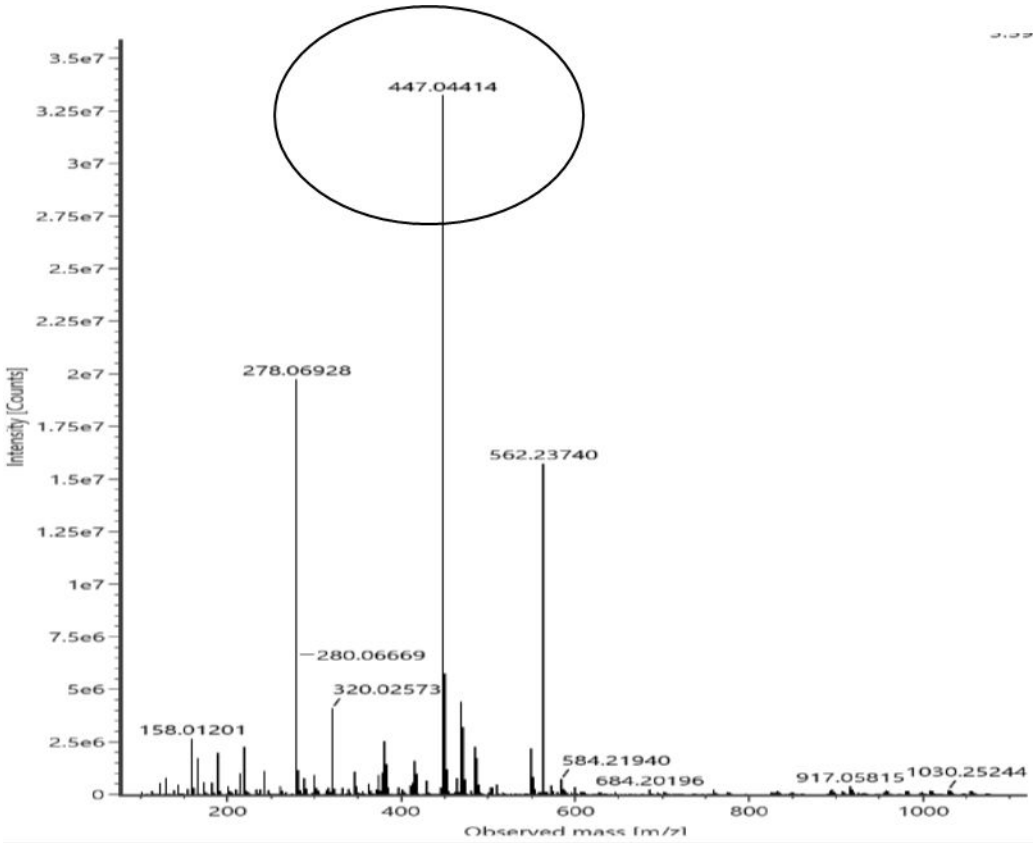

Figure S60: HRMS of Methyl-4-amino-3-chloro-6-(2-(3-(4-chlorophenyl) thioureido) phenyl) pyridine-2-carboxylate **(27)**.

^{1}H-NMR

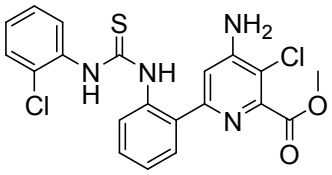

28

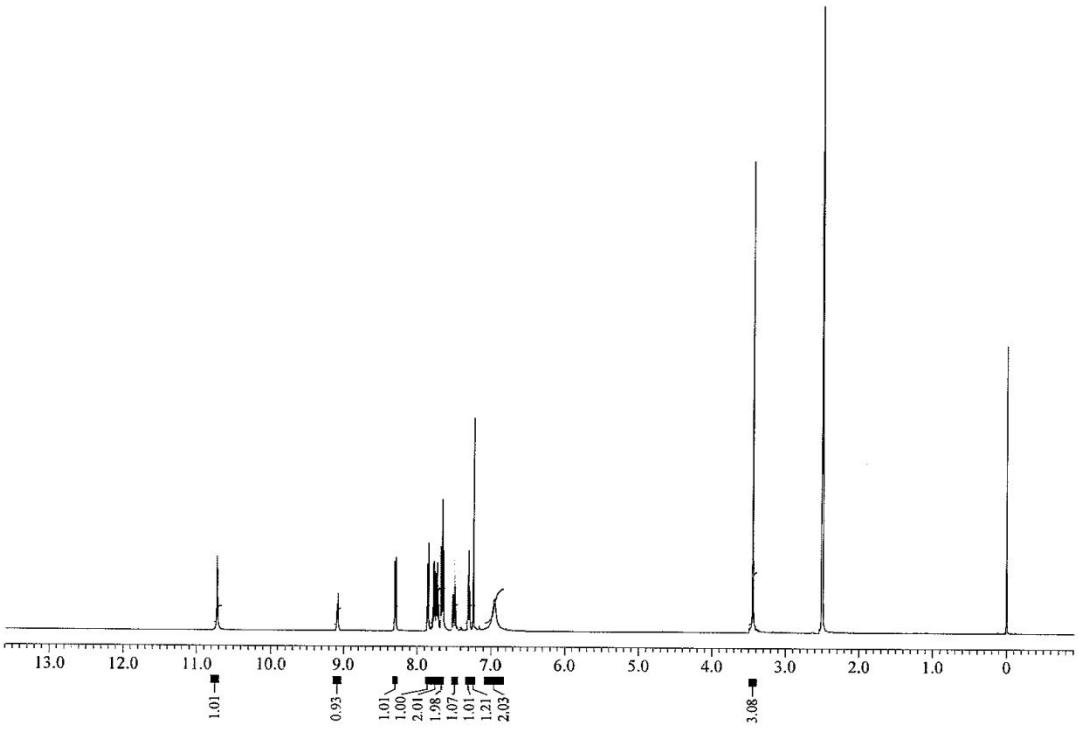

Figure S61: ^{1}H-NMR (300 MHz, DMSO) of Methyl-4-amino-3-chloro-6-(2-(3-(2-chlorophenyl) thioureido) phenyl) pyridine-2-carboxylate **(28)**.

^{13}C-NMR

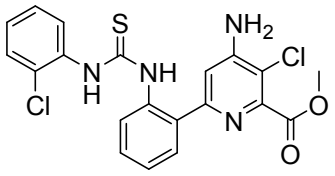

28

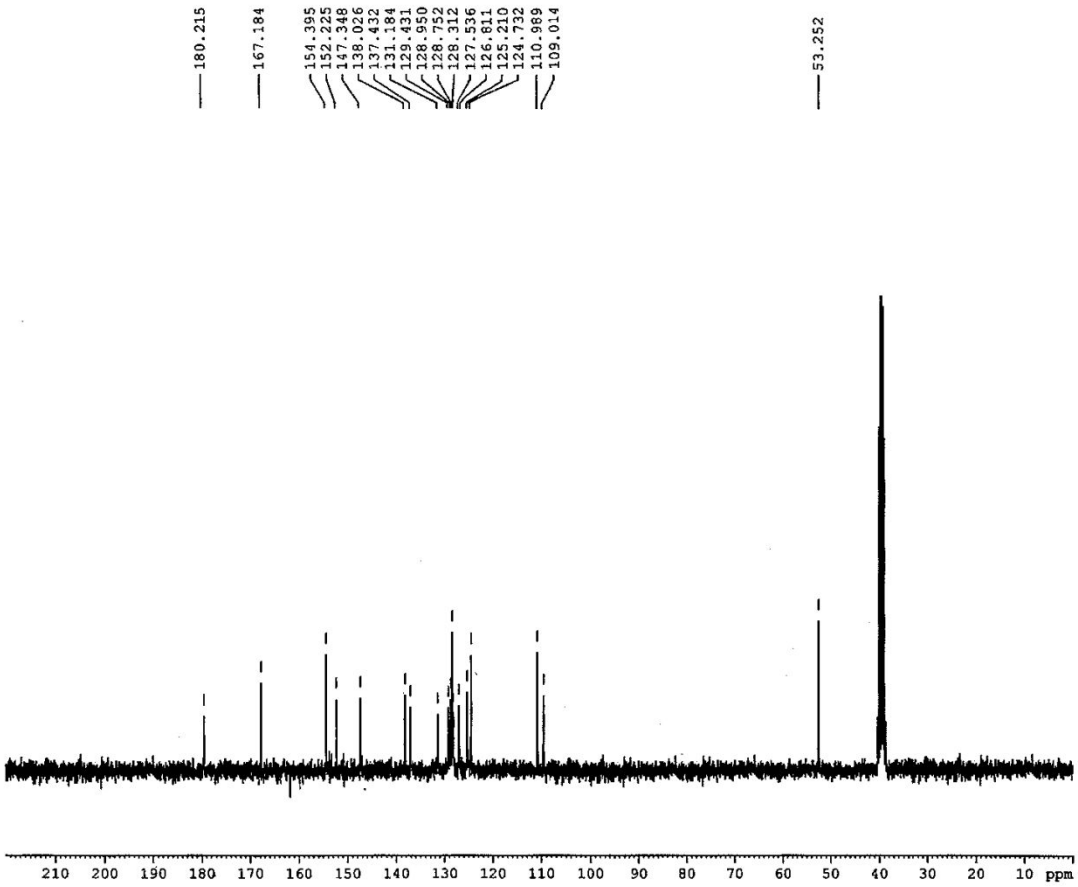

Figure S62: ^{13}C-NMR (75 MHz, DMSO) of Methyl-4-amino-3-chloro-6-(2-(3-(2-chlorophenyl) thioureido) phenyl) pyridine-2-carboxylate **(28)**.

HRMS

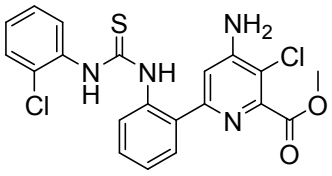

28

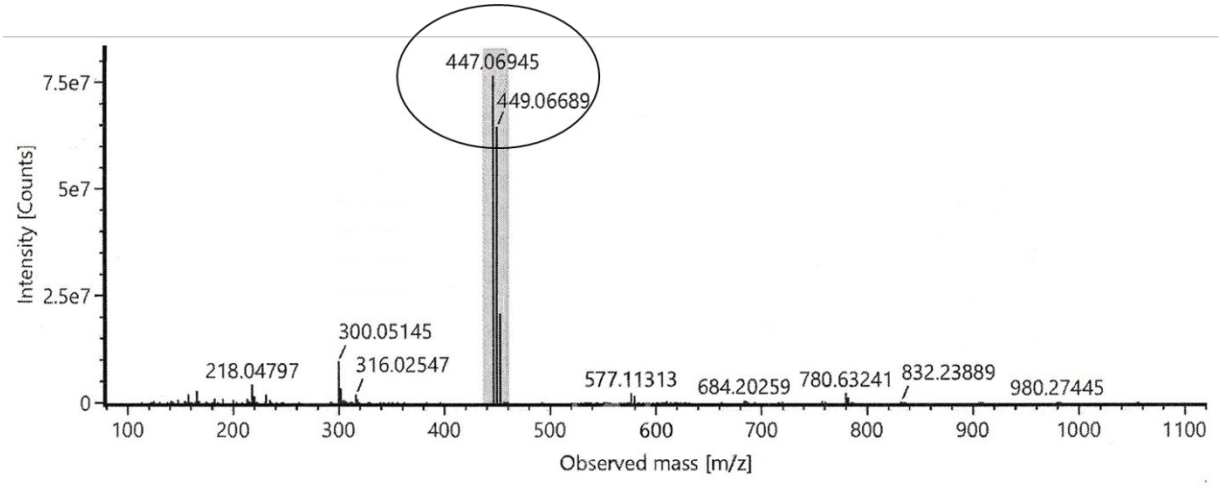

Figure S63: HRMS of Methyl-4-amino-3-chloro-6-(2-(3-(2-chlorophenyl) thioureido) phenyl) pyridine-2-carboxylate **(28)**.

^{1}H-NMR

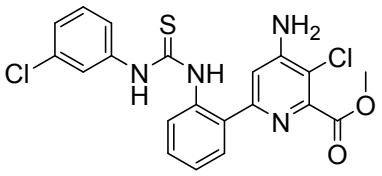

29

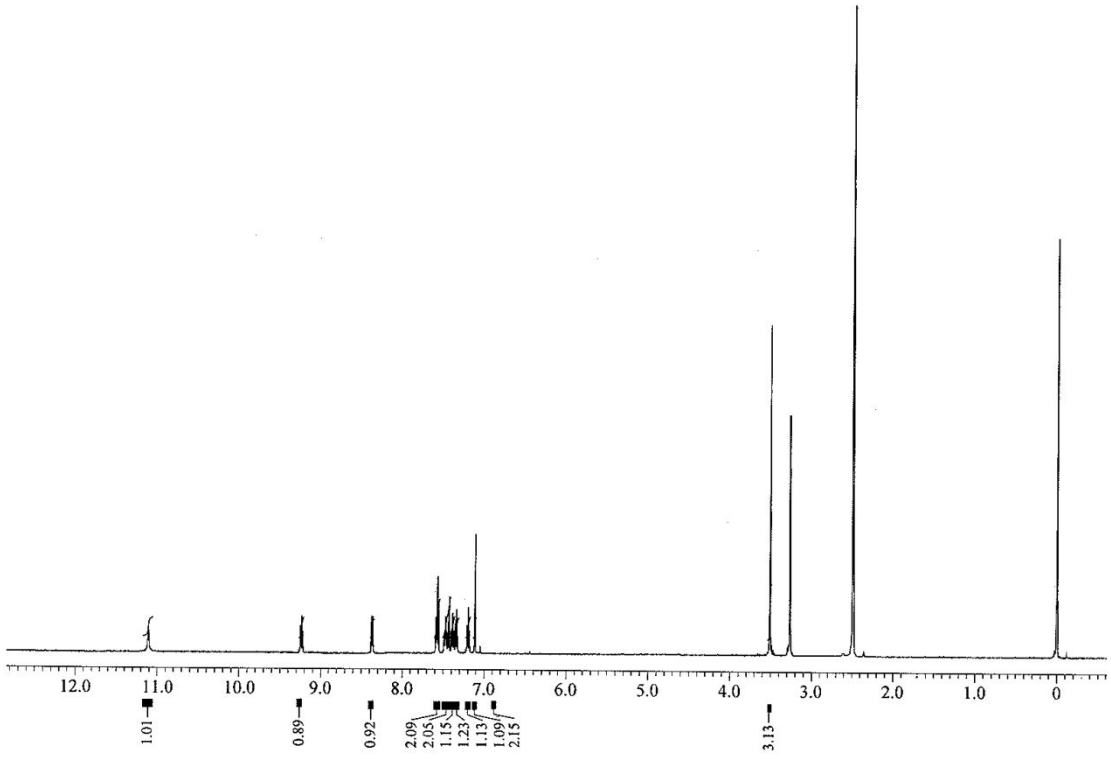

Figure S64: ^{1}H-NMR (300 MHz, DMSO) of Methyl-4-amino-3-chloro-6-(2-(3-(3-chlorophenyl) thioureido) phenyl) pyridine-2-carboxylate **(29)**.

^{13}C-NMR

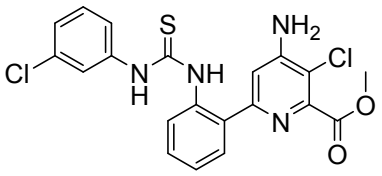

29

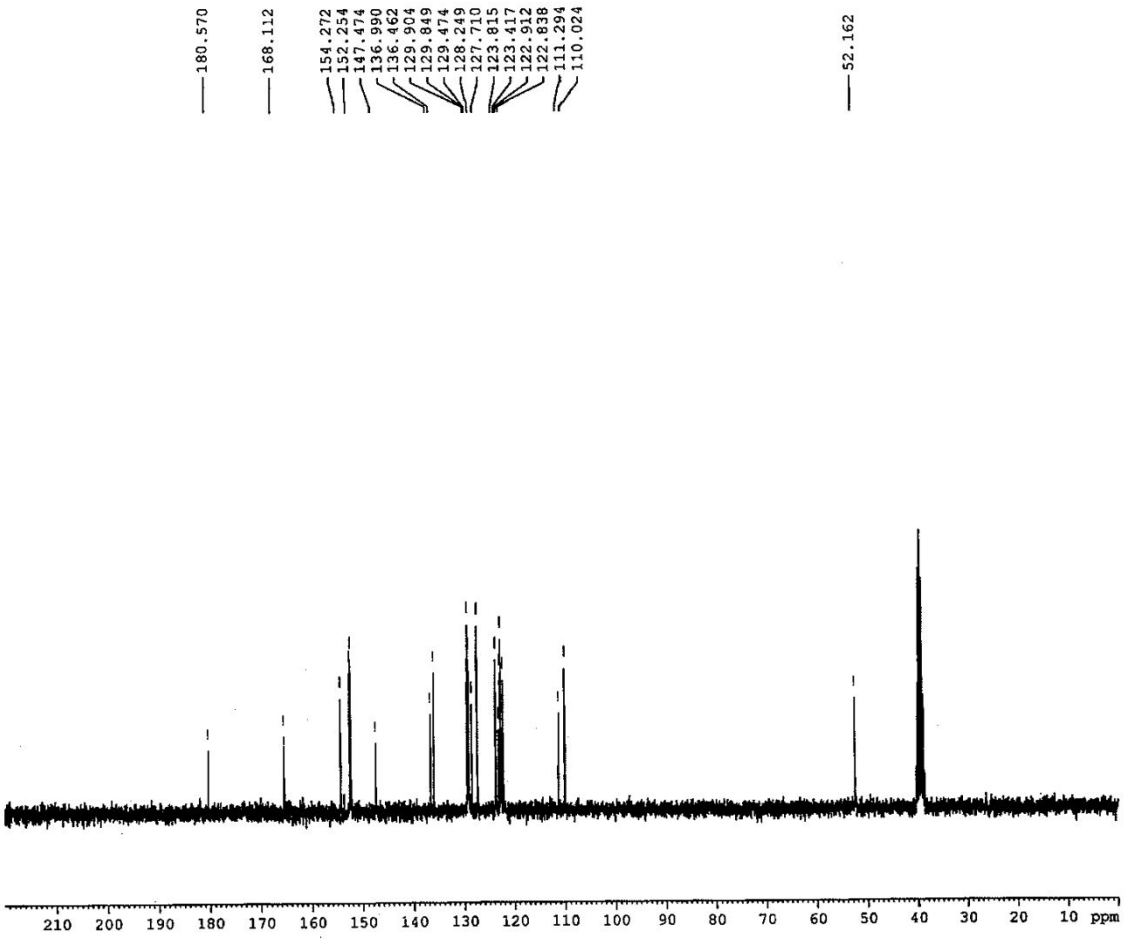

Figure S65: ^{13}C-NMR (75 MHz, DMSO) of Methyl-4-amino-3-chloro-6-(2-(3-(3-chlorophenyl) thioureido) phenyl) pyridine-2-carboxylate **(29)**.

HRMS

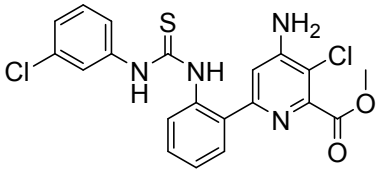

29

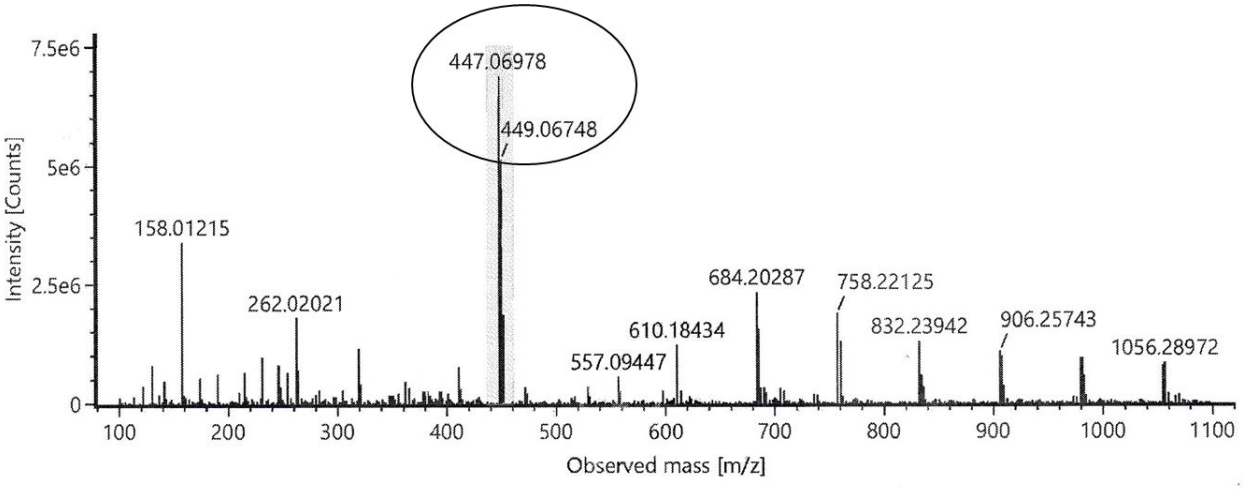

Figure S66: HRMS of Methyl-4-amino-3-chloro-6-(2-(3-(3-chlorophenyl) thioureido) phenyl) pyridine-2-carboxylate **(29)**.

^{1}H-NMR

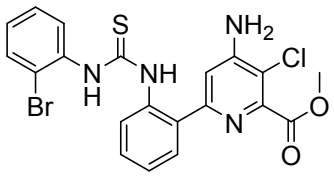

30

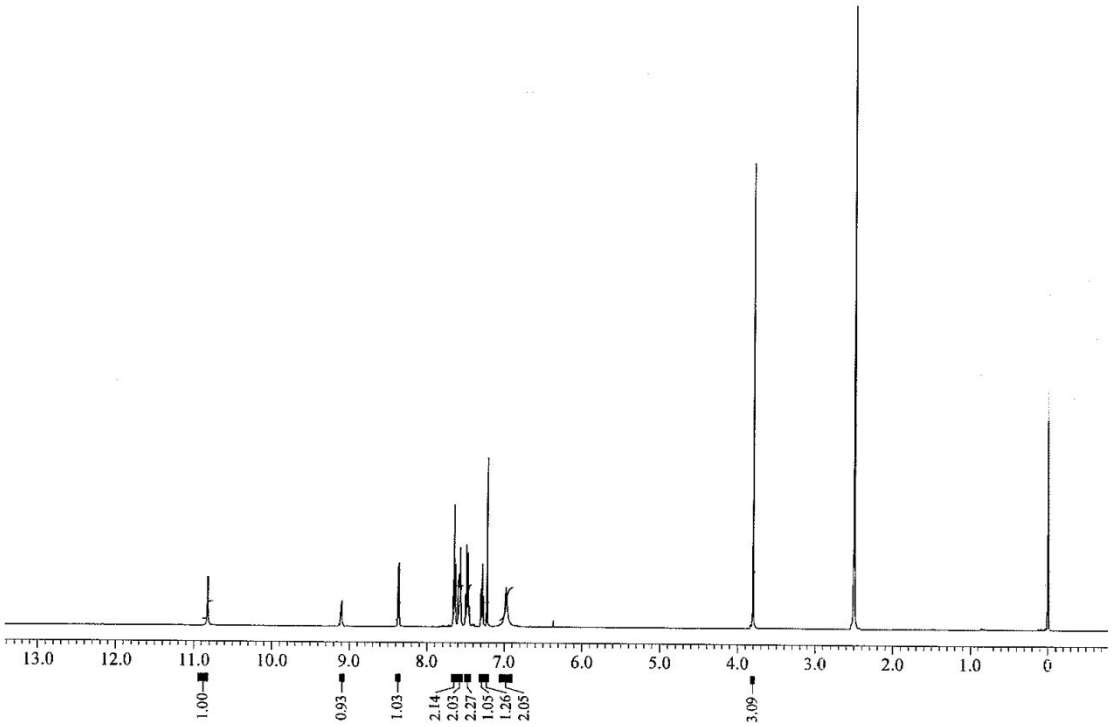

Figure S67: ^{1}H-NMR (300 MHz, DMSO) of Methyl-4-amino-6-(2-(3-(2-bromophenyl) thioureido) phenyl)-3-chloropyridine-2-carboxylate **(30)**.

^{13}C-NMR

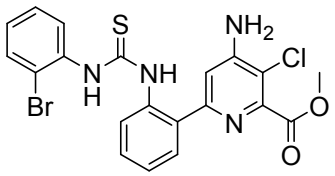

30

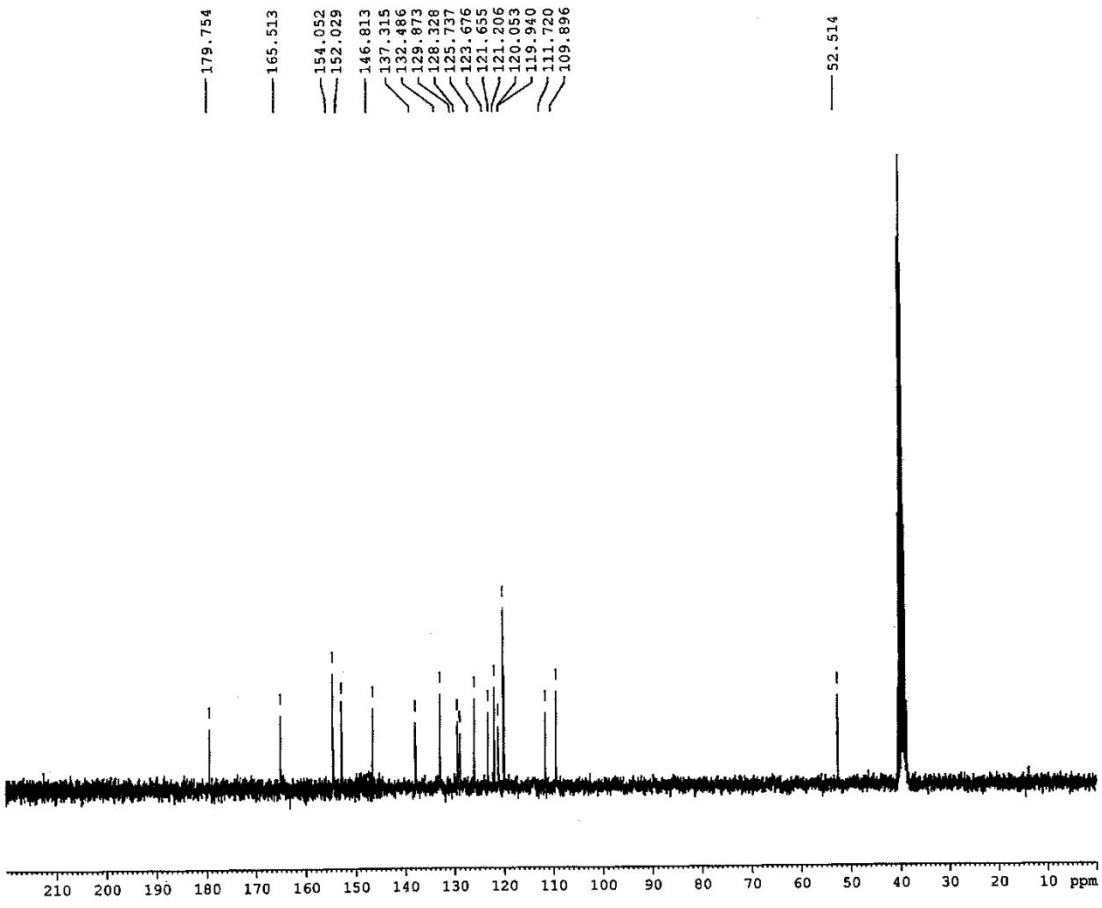

Figure S68: ^{13}C-NMR (75 MHz, DMSO) of Methyl-4-amino-6-(2-(3-(2-bromophenyl) thioureido) phenyl)-3-chloropyridine-2-carboxylate **(30)**.

HRMS

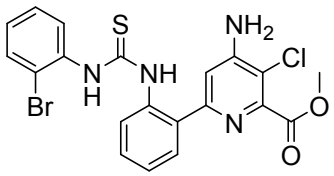

30

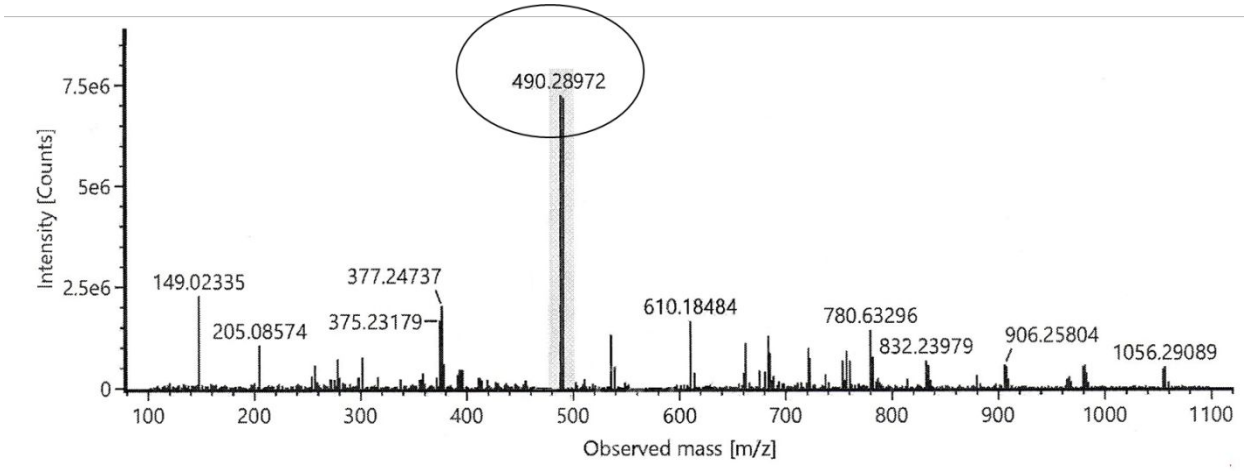

Figure S69: HRMS of Methyl-4-amino-6-(2-(3-(2-bromophenyl) thioureido) phenyl)-3-chloropyridine-2-carboxylate **(30)**.

^{1}H-NMR

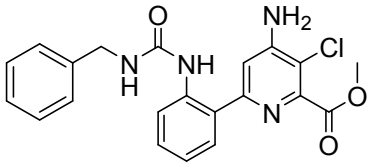

31

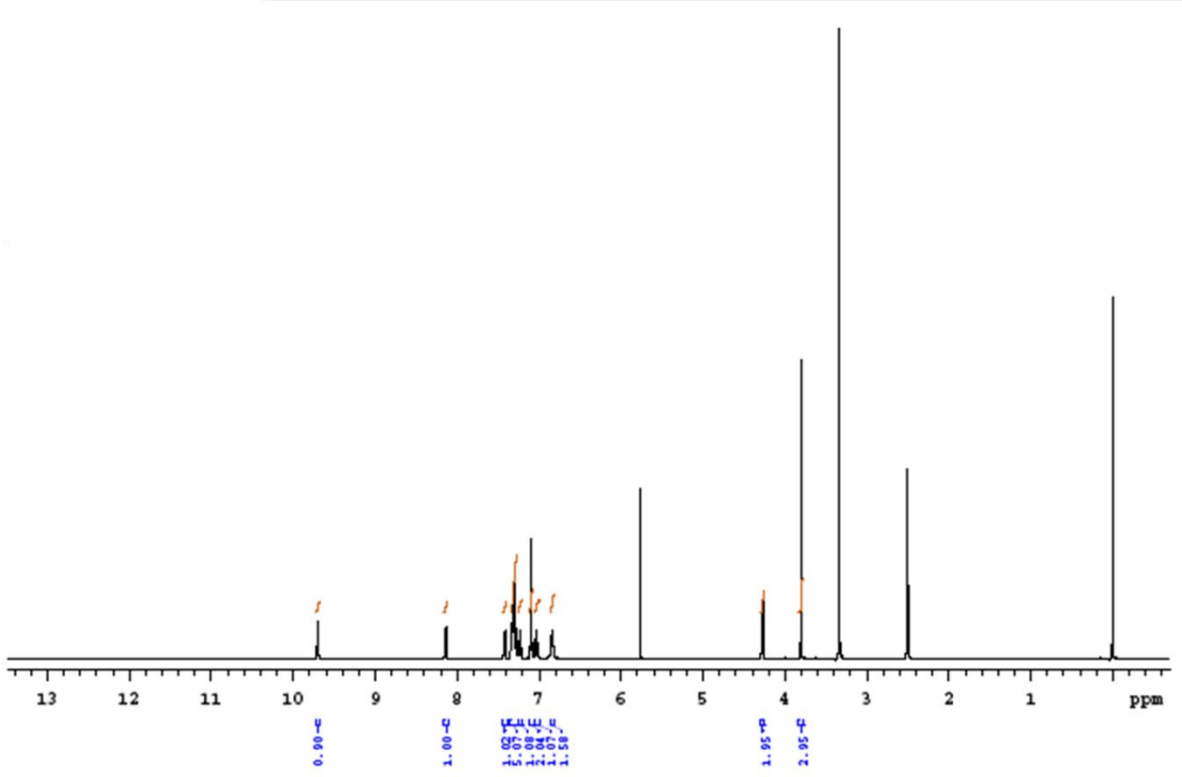

Figure S70: ^{1}H-NMR (400 MHz, DMSO) of Methyl-4-amino-6-(2-(3-benzylureido) phenyl)-3-chloropyridine-2-carboxylate **(31)**.

^{13}C-NMR

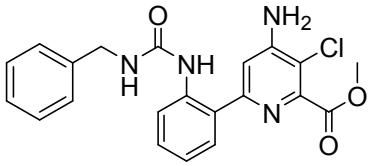

31

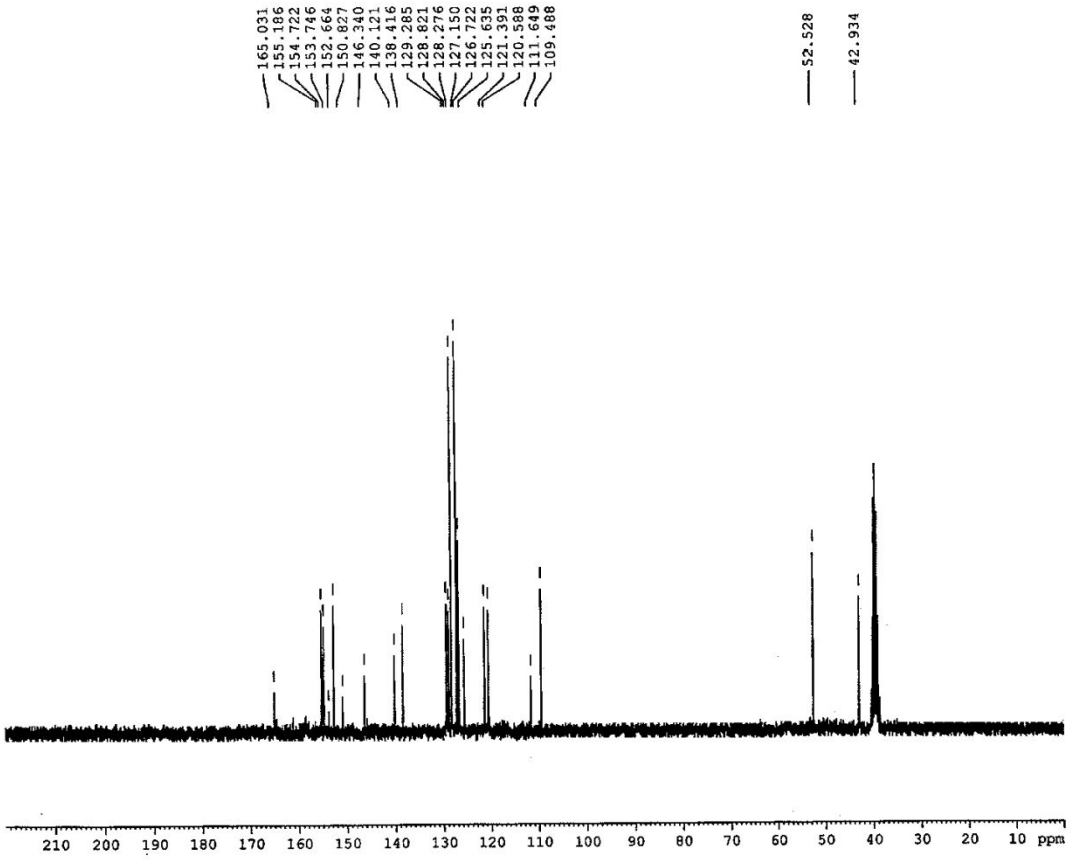

Figure S71**:** ^{13}C-NMR (75 MHz, DMSO) of Methyl-4-amino-6-(2-(3-benzylureido) phenyl)-3-chloropyridine-2-carboxylate **(31)**.

HRMS

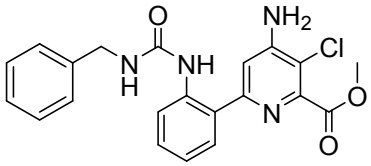

31

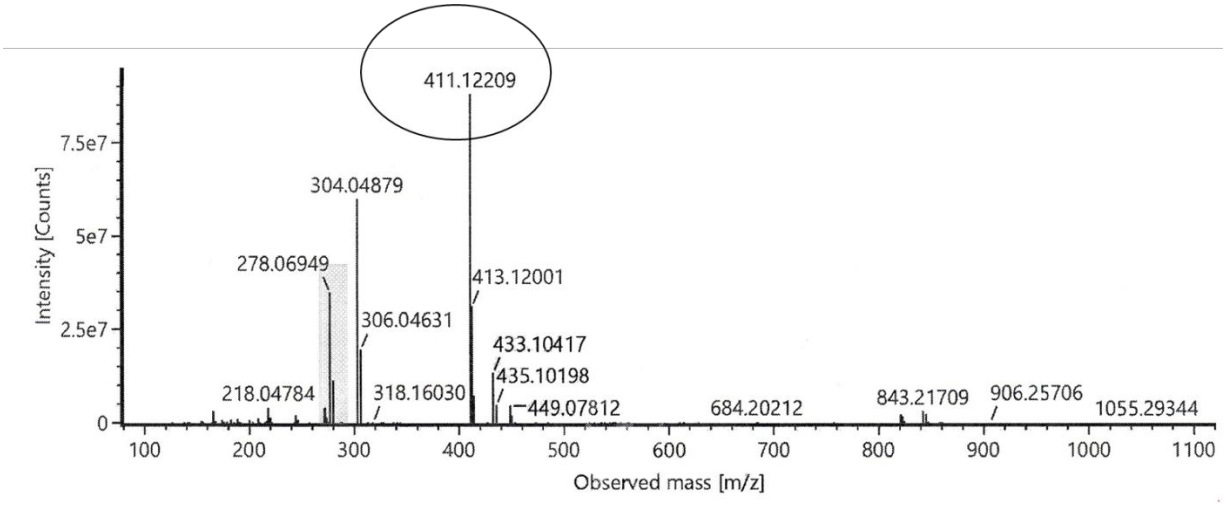

Figure S72: HRMS of Methyl-4-amino-6-(2-(3-benzylureido) phenyl)-3-chloropyridine-2-carboxylate **(31)**.

^{1}H-NMR

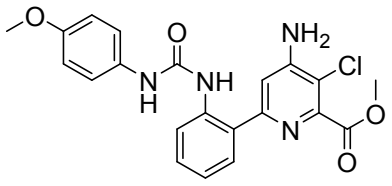

32

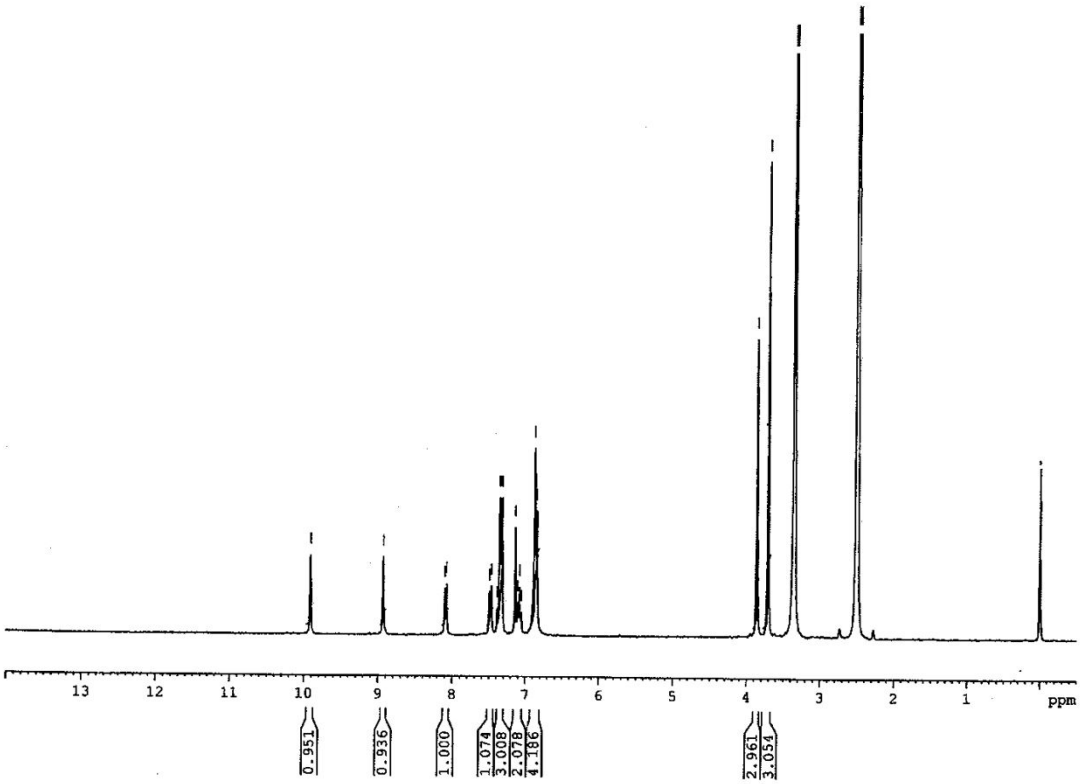

Figure S73: ^{1}H-NMR (300 MHz, DMSO) of Methyl-4-amino-3-chloro-6-(2-(3-(4-methoxyphenyl) ureido) phenyl) pyridine-2-carboxylate **(32)**.

^{13}C-NMR

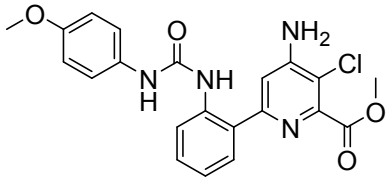

32

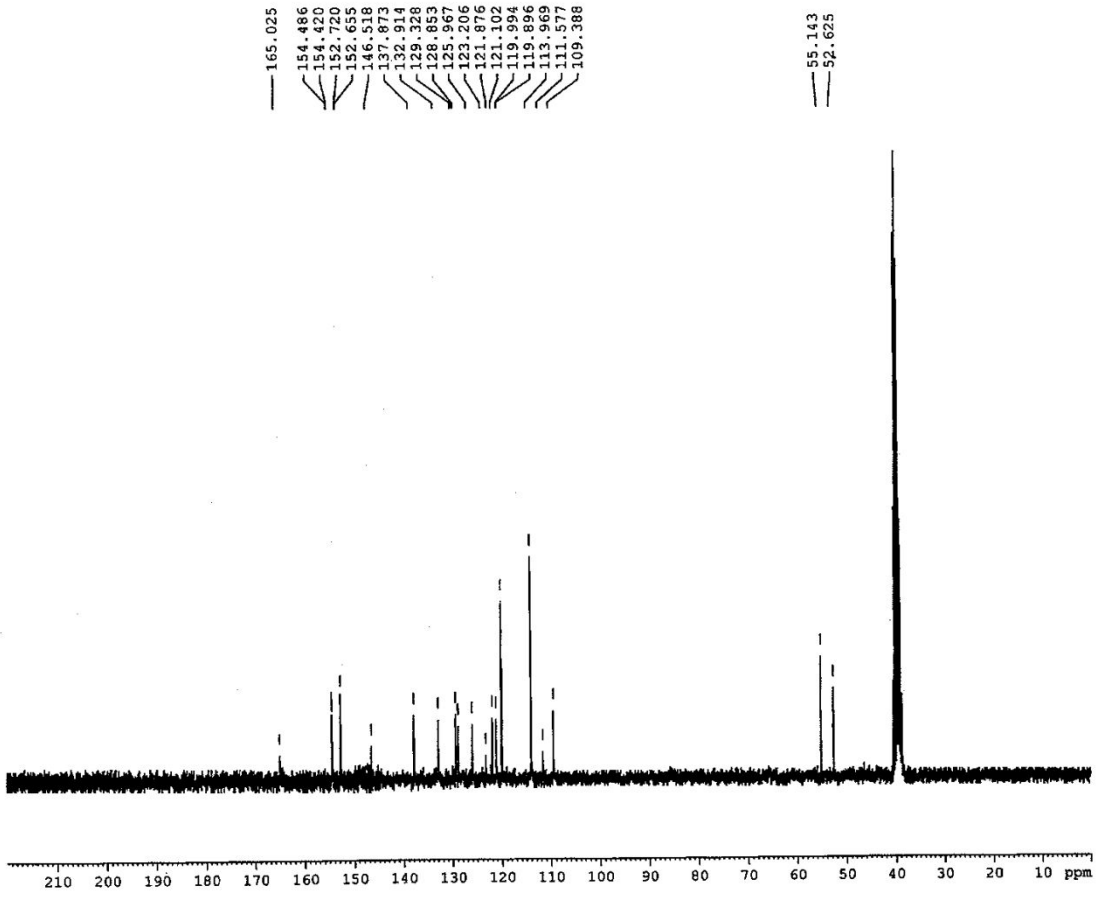

Figure S74: ^{13}C-NMR (75 MHz, DMSO) of Methyl-4-amino-3-chloro-6-(2-(3-(4-methoxyphenyl) ureido) phenyl) pyridine-2-carboxylate **(32)**.

HRMS

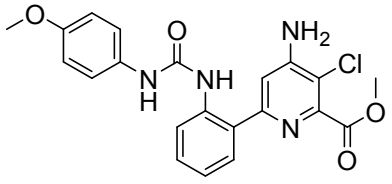

32

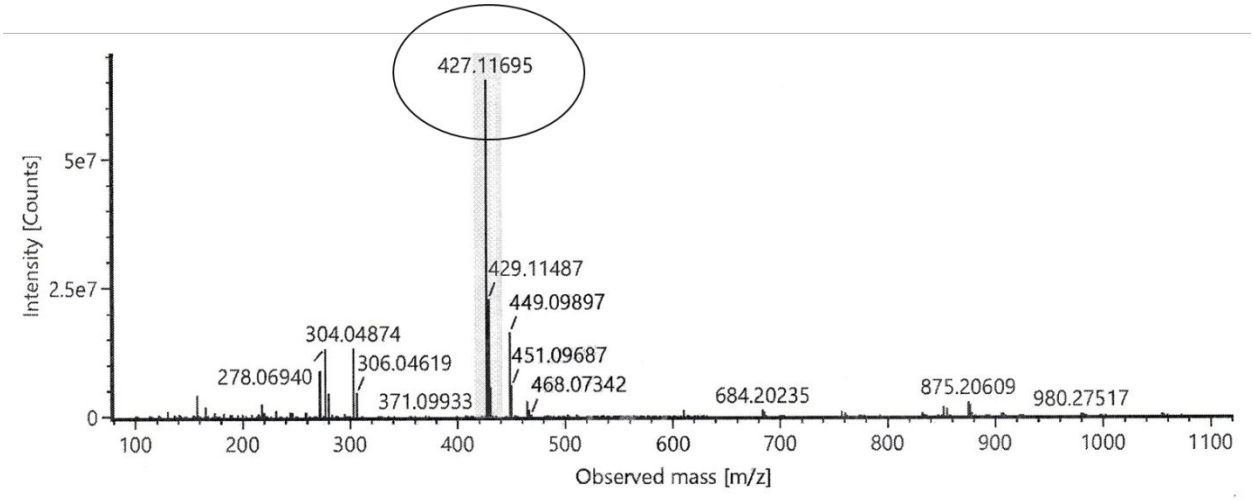

Figure S75: HRMS of Methyl-4-amino-3-chloro-6-(2-(3-(4-methoxyphenyl) ureido) phenyl) pyridine-2-carboxylate **(32)**.

^{1}H-NMR

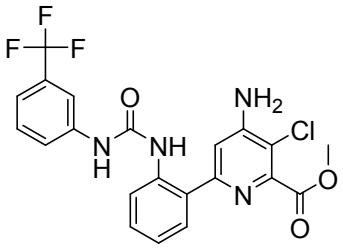

33

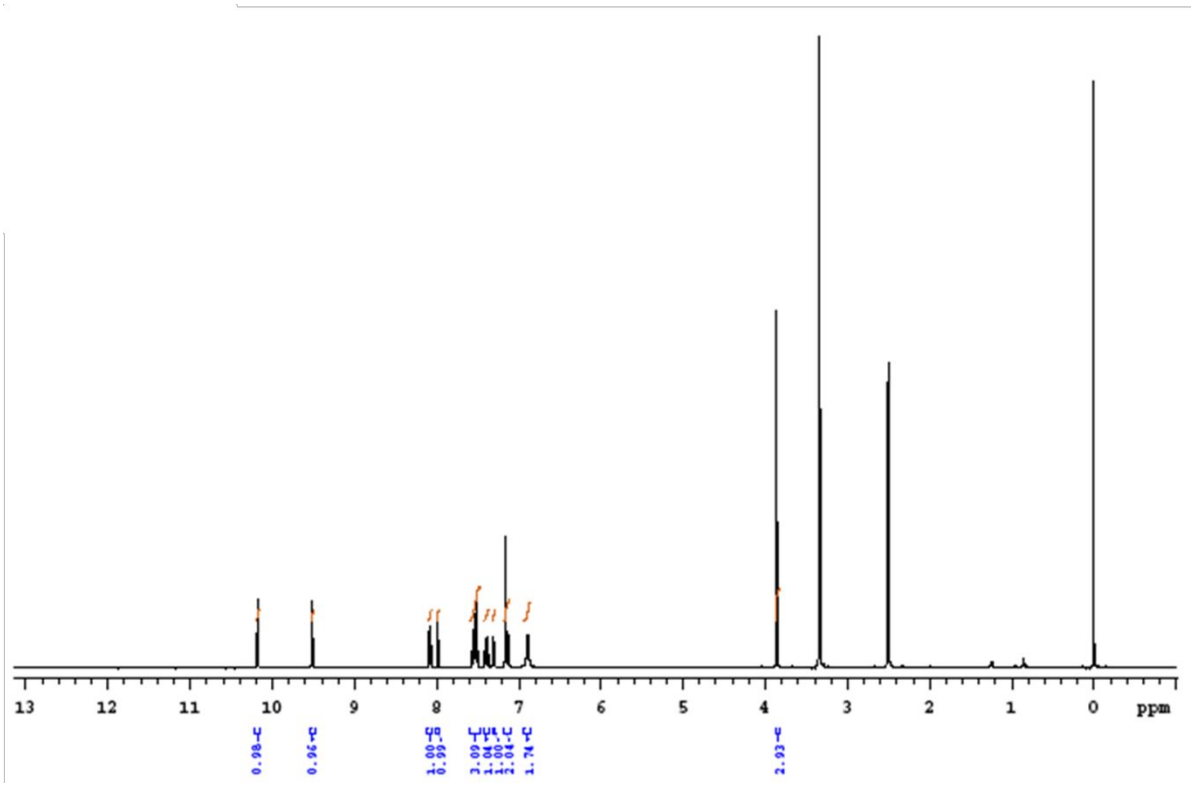

Figure S76: ^{1}H-NMR (400 MHz, DMSO) of Methyl-4-amino-3-chloro-6-(2-(3-(3-(trifluoromethyl) phenyl) ureido) phenyl) pyridine-2-carboxylate **(33)**.

^{13}C-NMR

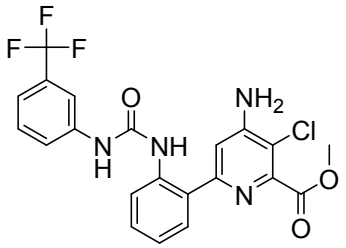

33

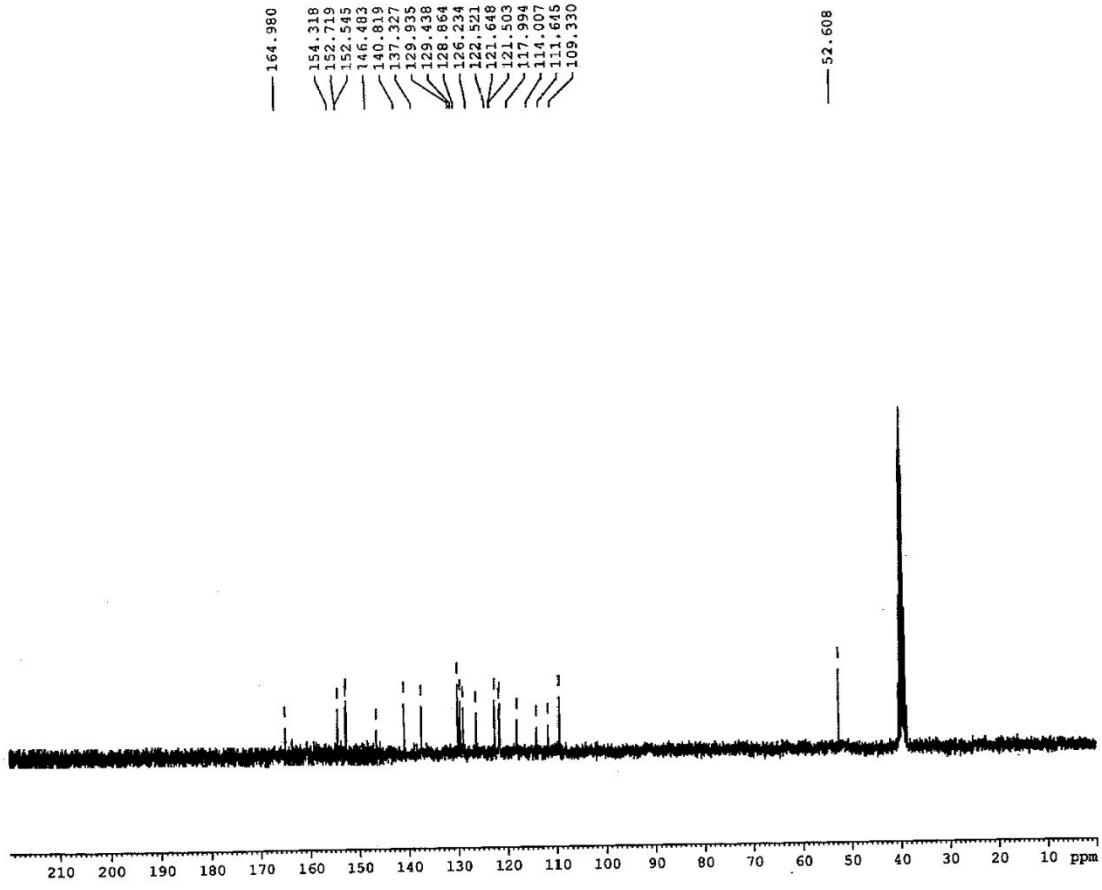

Figure S77: ^{13}C-NMR (75 MHz, DMSO) of Methyl-4-amino-3-chloro-6-(2-(3-(3-(trifluoromethyl) phenyl) ureido) phenyl) pyridine-2-carboxylate **(33)**.

HRMS

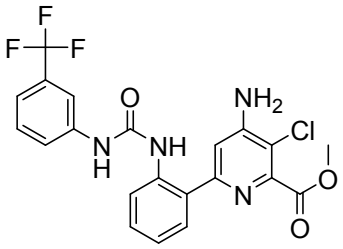

33

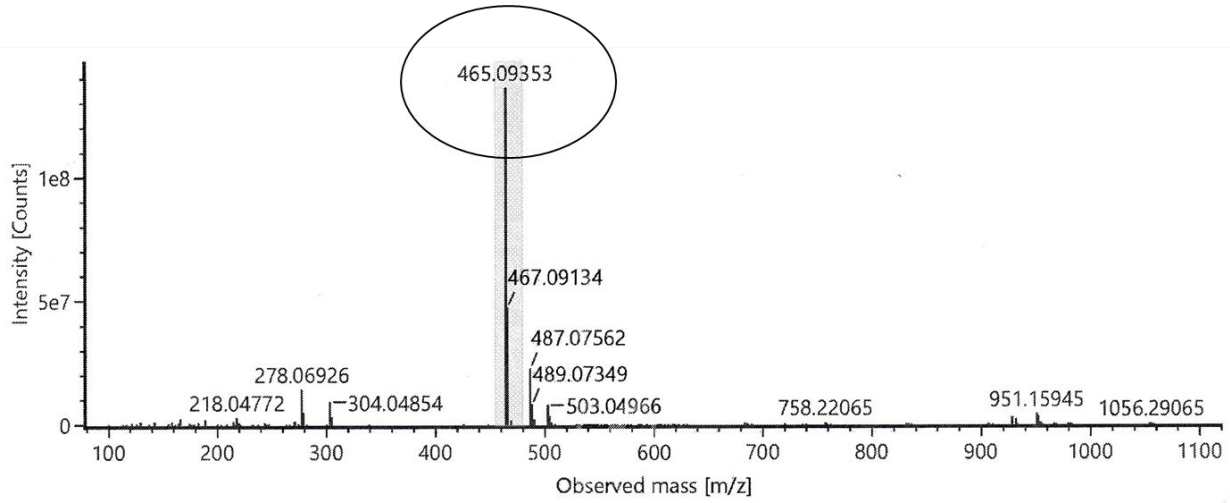

Figure S78: HRMS of Methyl-4-amino-3-chloro-6-(2-(3-(3-(trifluoromethyl) phenyl) ureido) phenyl) pyridine-2-carboxylate **(33)**.

^{1}H-NMR

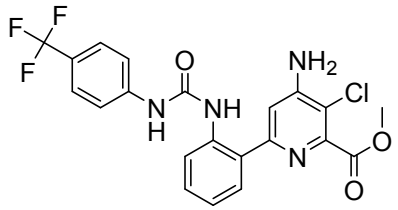

34

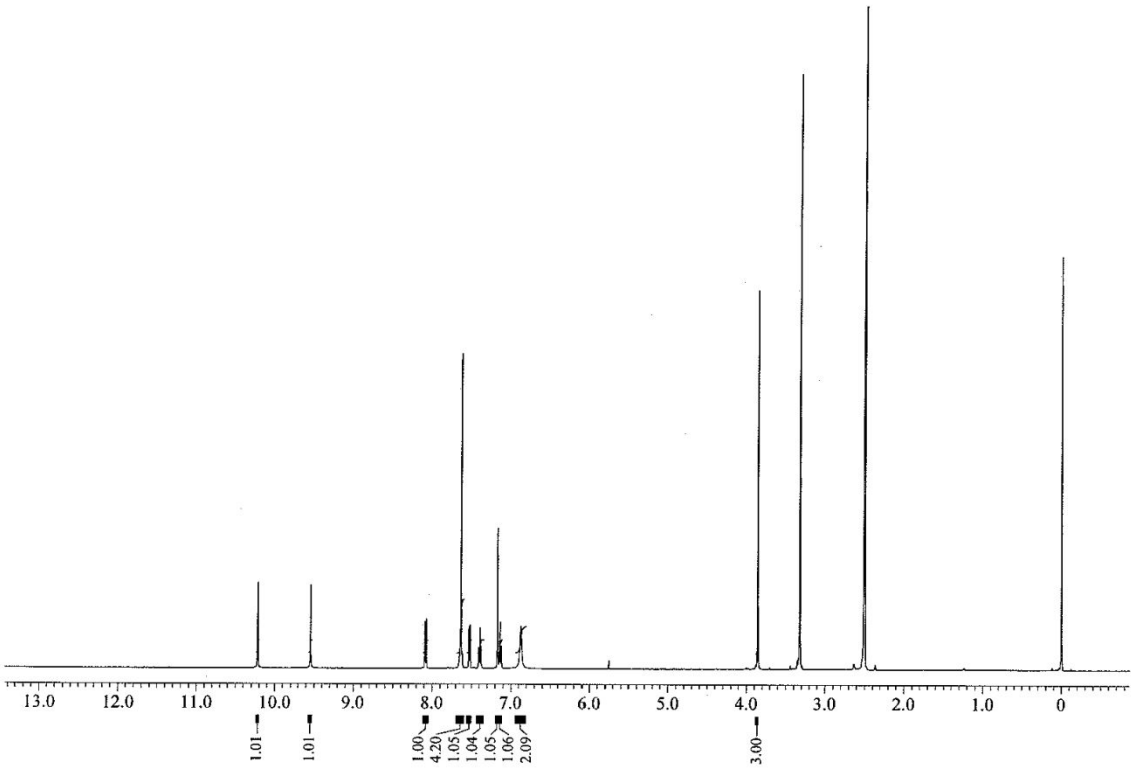

Figure S79: ^{1}H-NMR (300 MHz, DMSO) of Methyl-4-amino-3-chloro-6-(2-(3-(4-(trifluoromethyl) phenyl) ureido) phenyl) pyridine-2-carboxylate **(34)**.

^{13}C-NMR

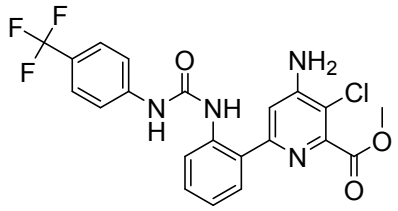

34

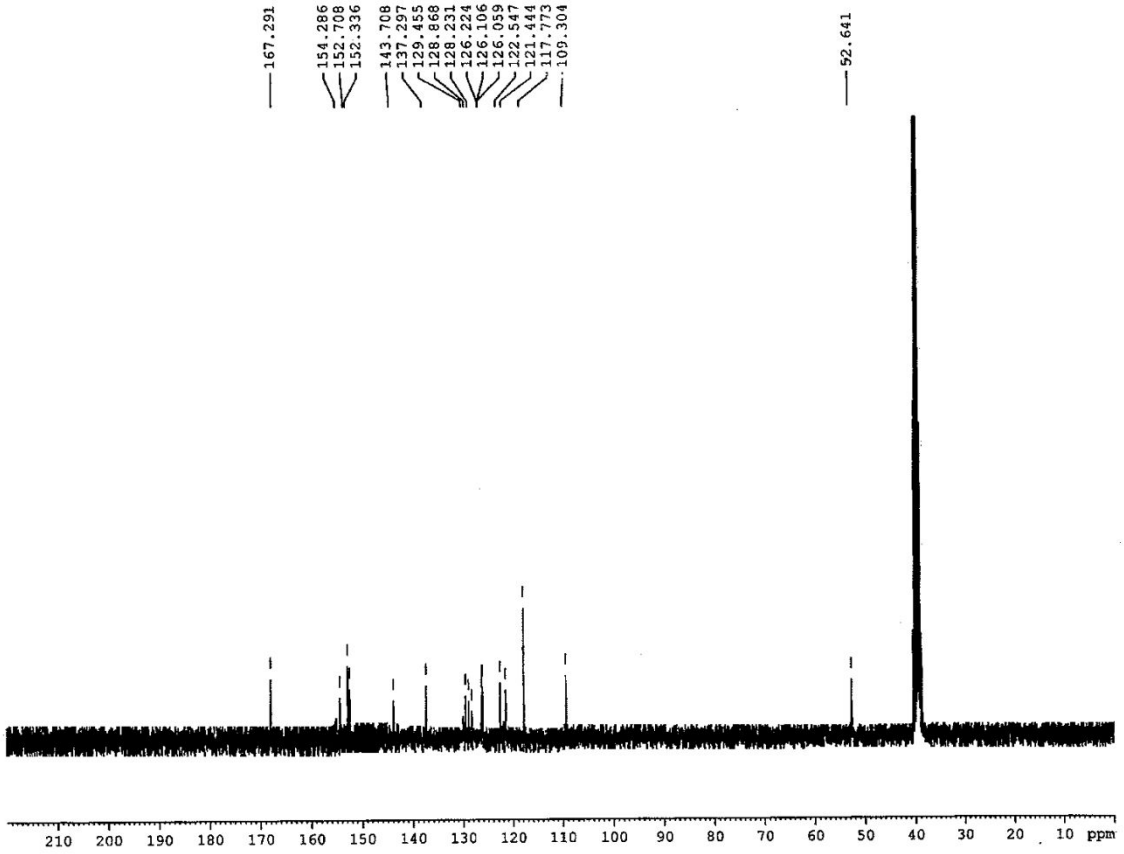

Figure S80: ^{13}C-NMR (75 MHz, DMSO) of Methyl-4-amino-3-chloro-6-(2-(3-(4-(trifluoromethyl) phenyl) ureido) phenyl) pyridine-2-carboxylate **(34)**.

HRMS

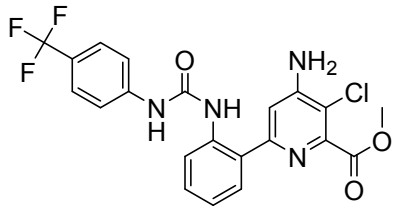

34

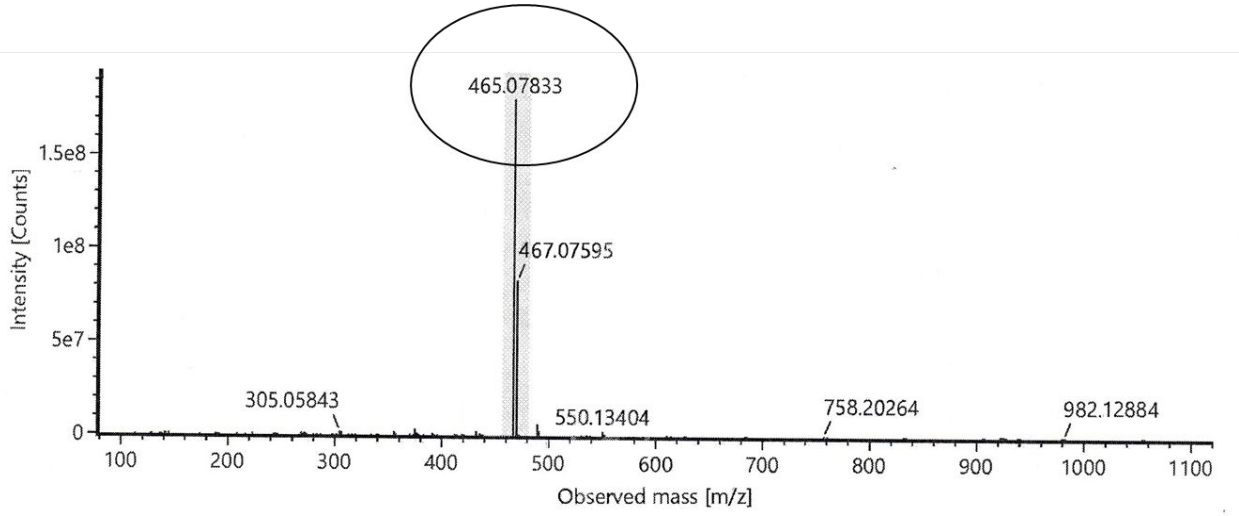

Figure S81: HRMS of Methyl-4-amino-3-chloro-6-(2-(3-(4-(trifluoromethyl) phenyl) ureido) phenyl) pyridine-2-carboxylate **(34)**.

^{1}H-NMR

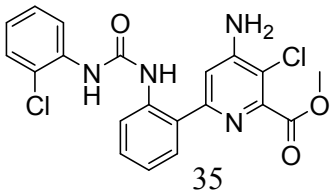

35

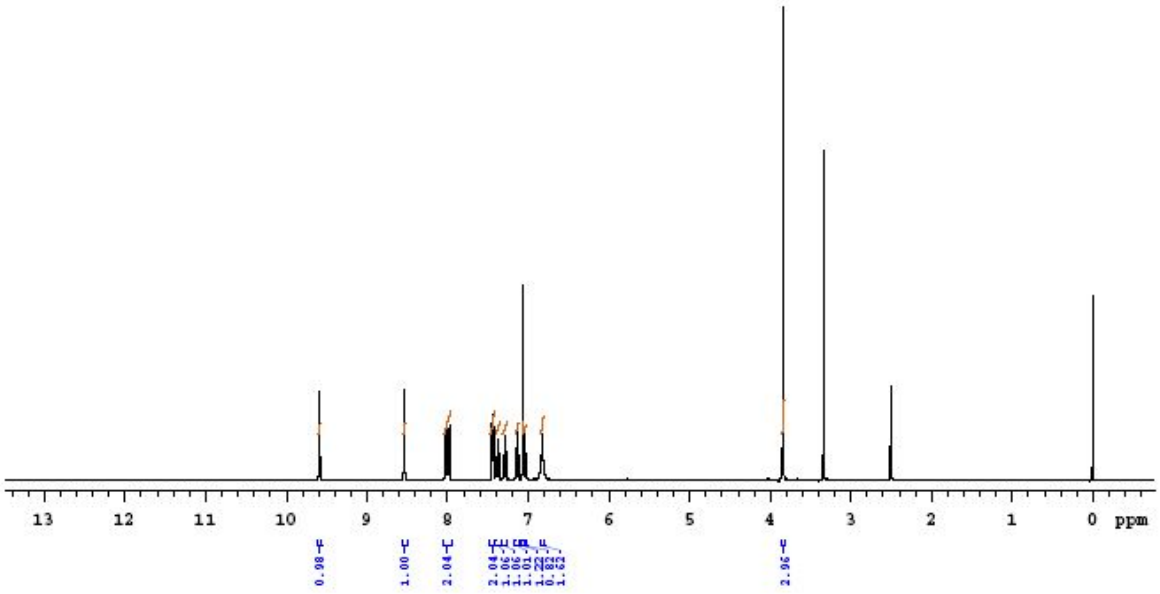

Figure S82: ^{1}H-NMR (400 MHz, DMSO) of Methyl-4-amino-3-chloro-6-(2-(3-(2-chlorophenyl) ureido) phenyl) pyridine-2-carboxylate **(35)**.

^{13}C-NMR

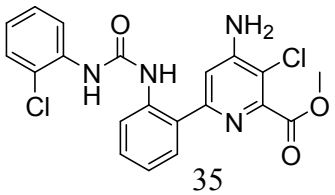

35

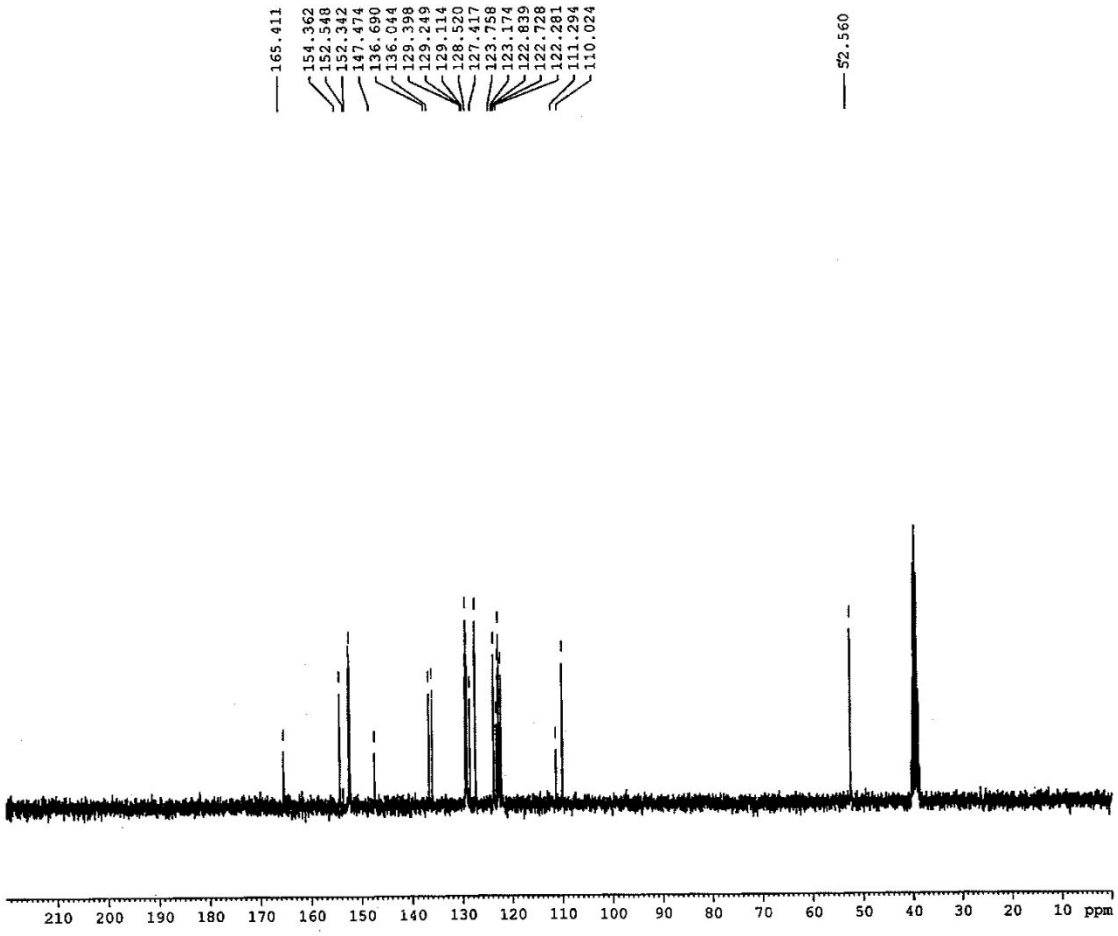

Figure S83: ^{13}C-NMR (75 MHz, DMSO) of Methyl-4-amino-3-chloro-6-(2-(3-(2-chlorophenyl) ureido) phenyl) pyridine-2-carboxylate **(35)**.

HRMS

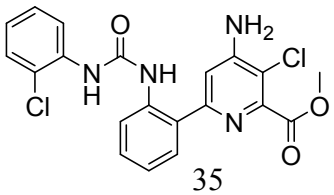

35

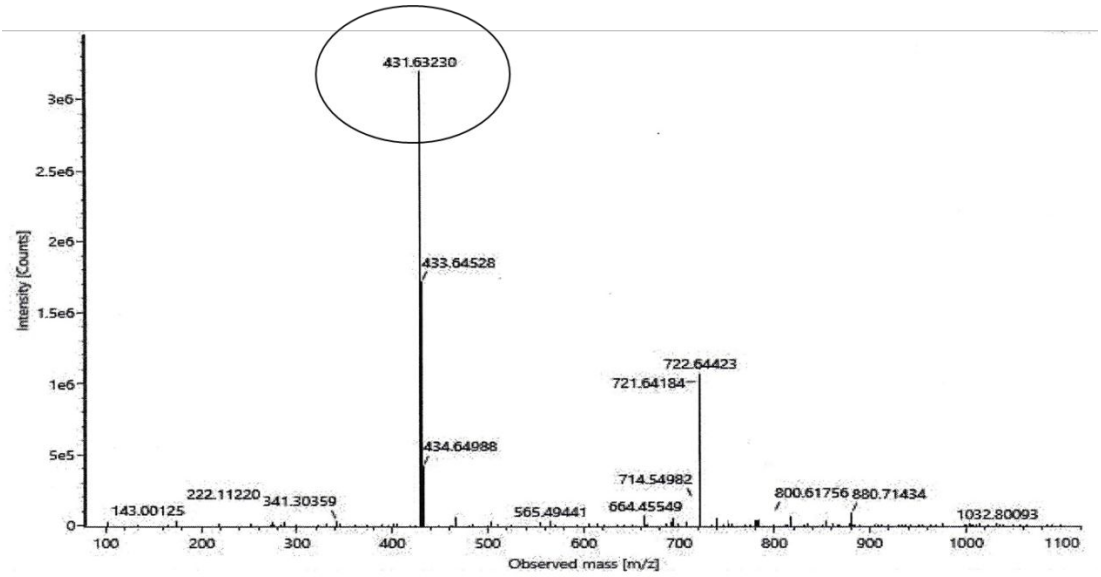

Figure S84: HRMS of Methyl-4-amino-3-chloro-6-(2-(3-(2-chlorophenyl) ureido) phenyl) pyridine-2-carboxylate **(35)**.

^{1}H-NMR

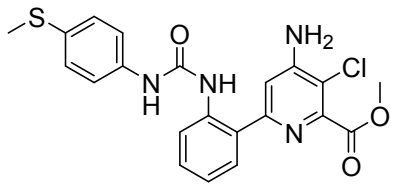

36

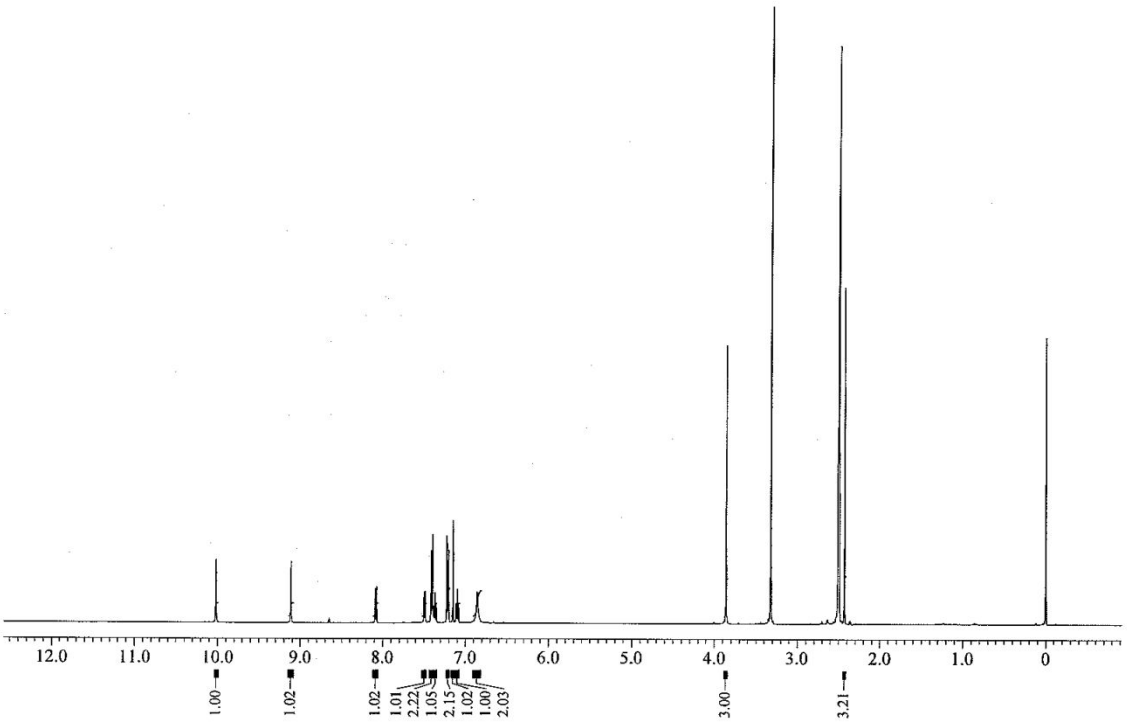

Figure S85: ^{1}H-NMR (300 MHz, DMSO) of Methyl-4-amino-3-chloro-6-(2-(3-(4-(methylthio) phenyl) ureido) phenyl) pyridine-2-carboxylate **(36)**.

^{13}C-NMR

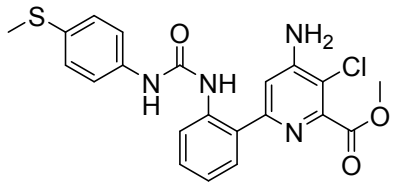

36

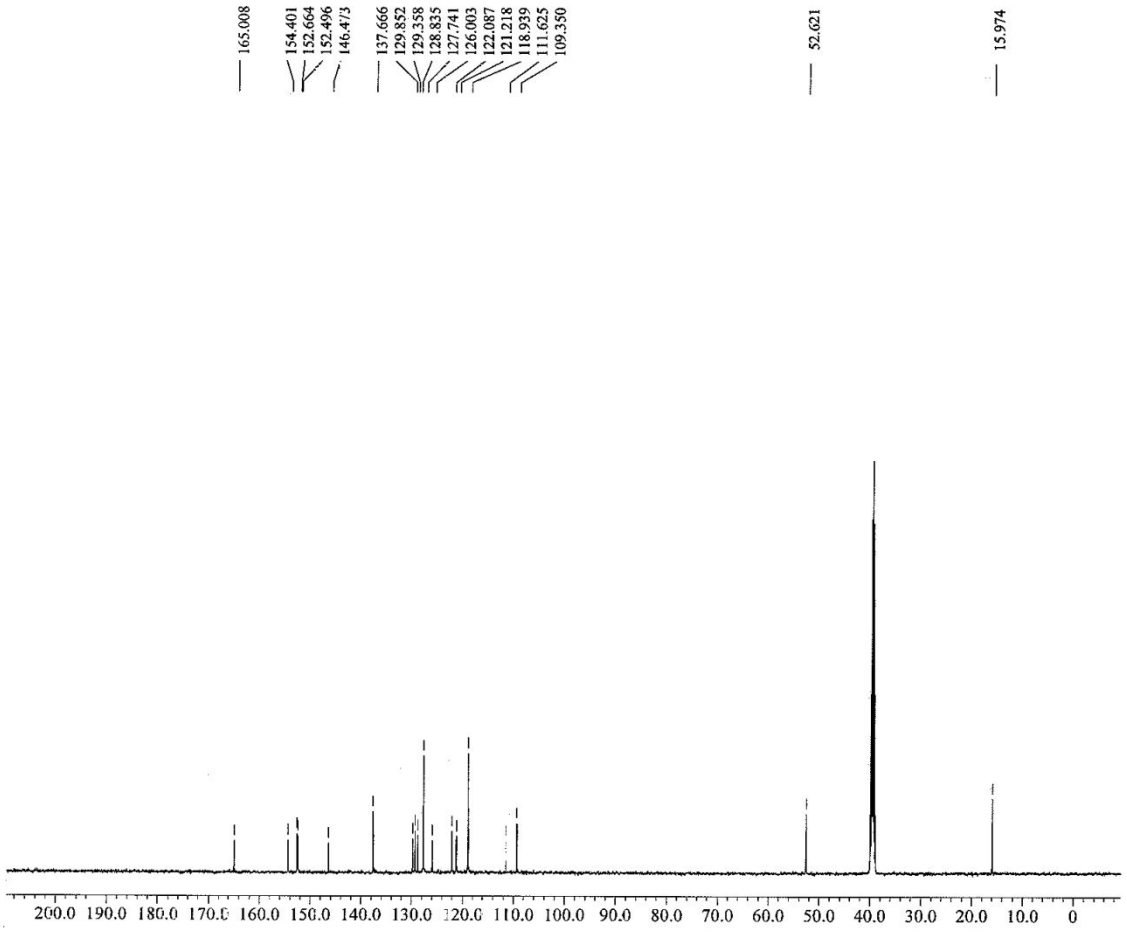

Figure S86: ^{13}C-NMR (75 MHz, DMSO) of Methyl-4-amino-3-chloro-6-(2-(3-(4-(methylthio) phenyl) ureido) phenyl) pyridine-2-carboxylate **(36)**.

HRMS

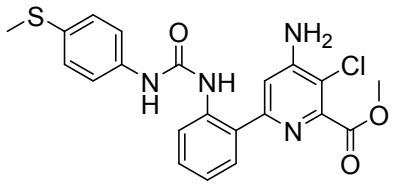

36

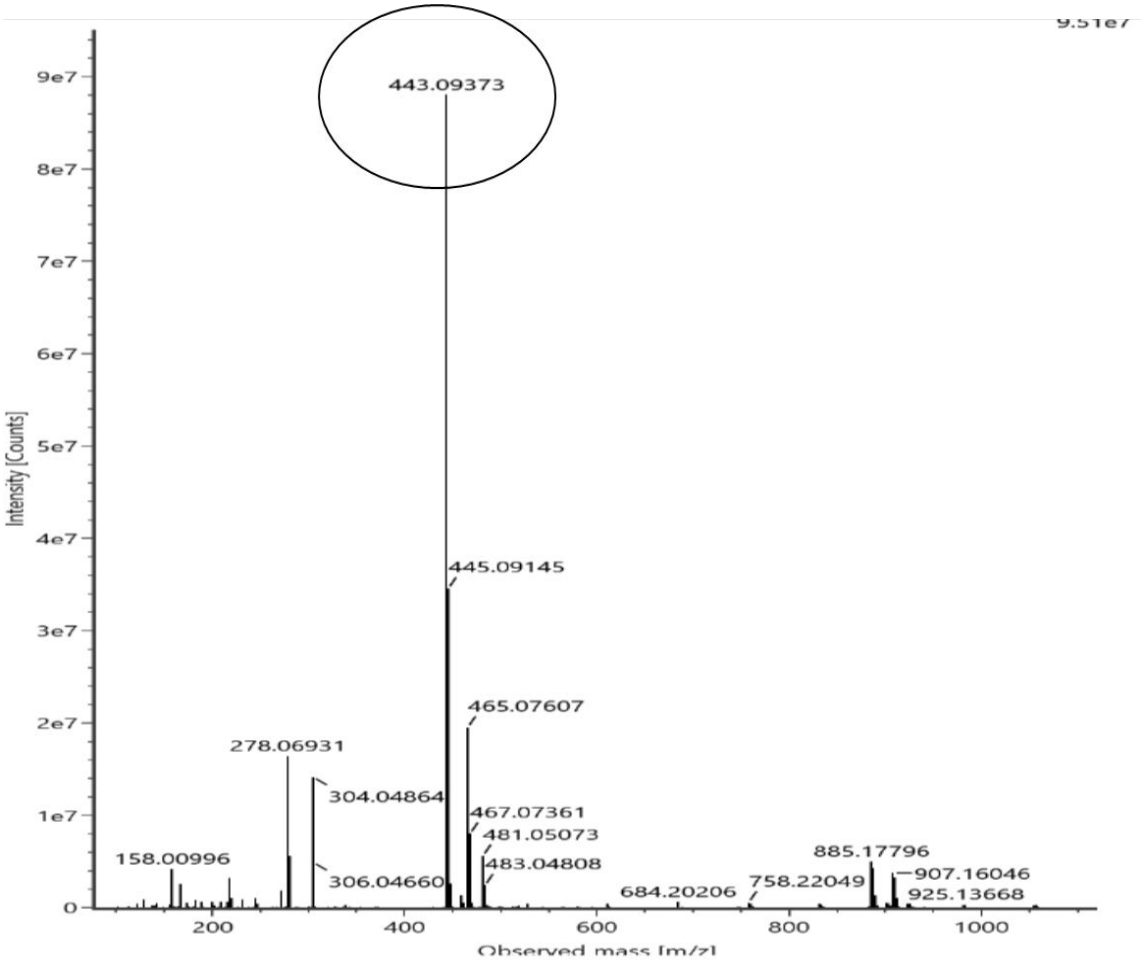

Figure S87: HRMS of Methyl-4-amino-3-chloro-6-(2-(3-(4-(methylthio) phenyl) ureido) phenyl) pyridine-2-carboxylate **(36)**.

^{1}H-NMR

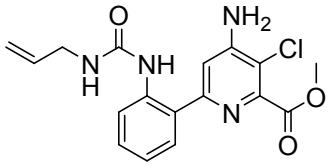

37

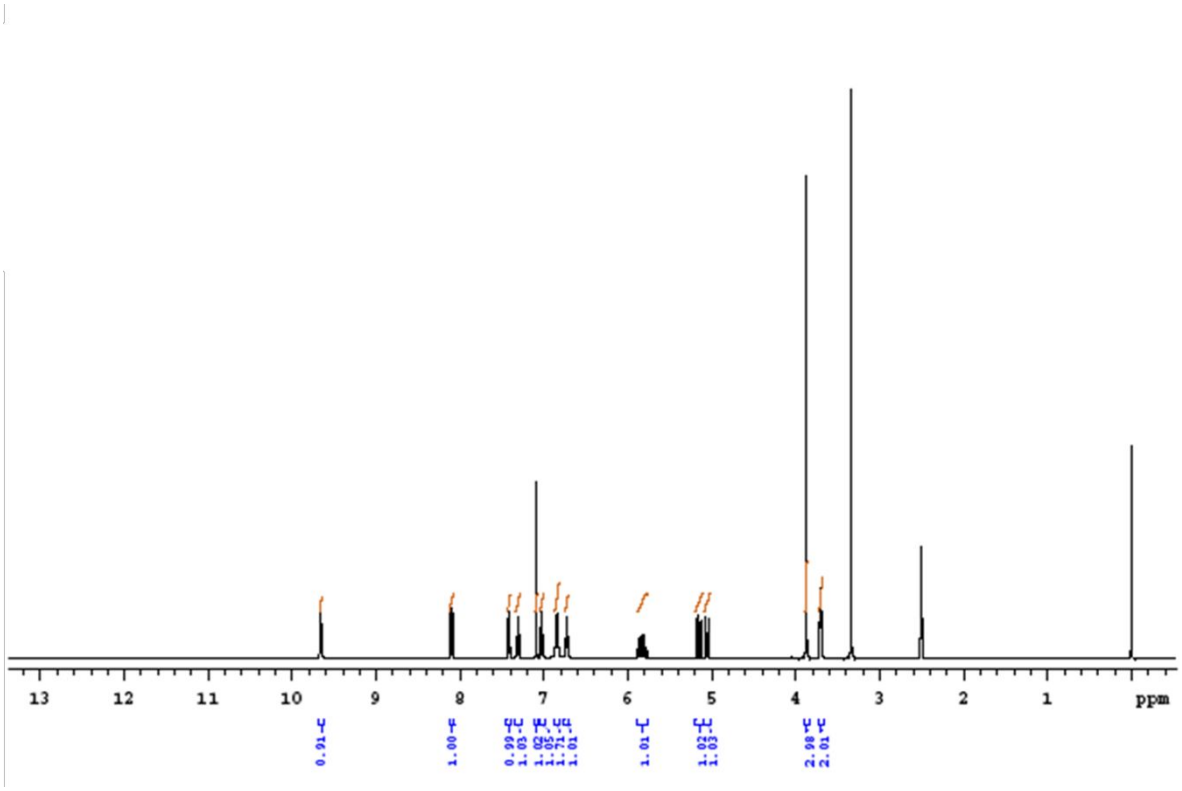

Figure S88: ^{1}H-NMR (400 MHz, DMSO) of Methyl 6-(2-(3-allylureido) phenyl)-4-amino-3-chloropyridine-2-carboxylate**(37)**.

^{13}C-NMR

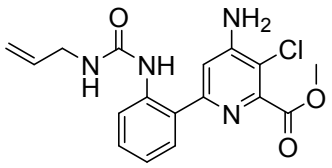

37

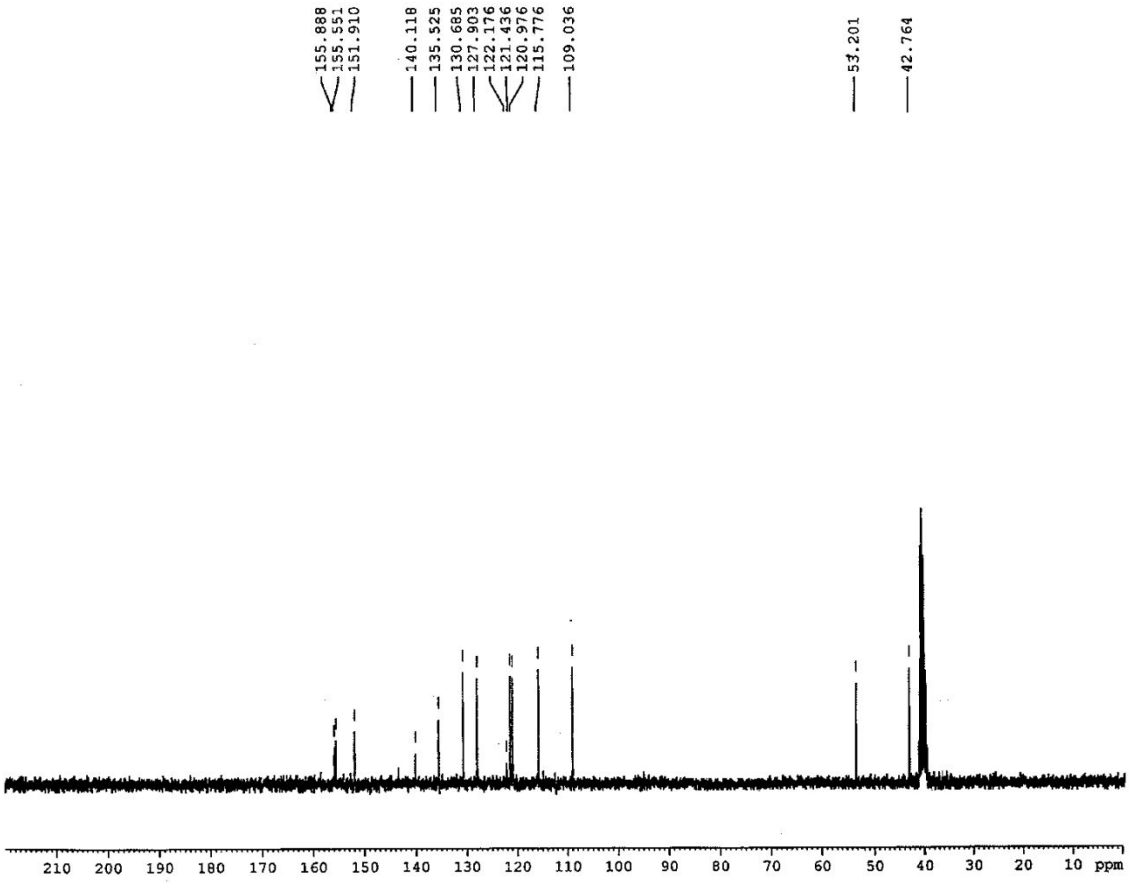

Figure S89: ^{13}C-NMR (75 MHz, DMSO) of Methyl 6-(2-(3-allylureido) phenyl)-4-amino-3-chloropyridine-2-carboxylate**(37)**.

HRMS

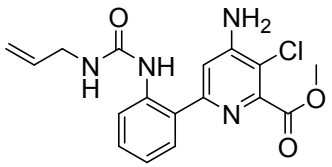

37

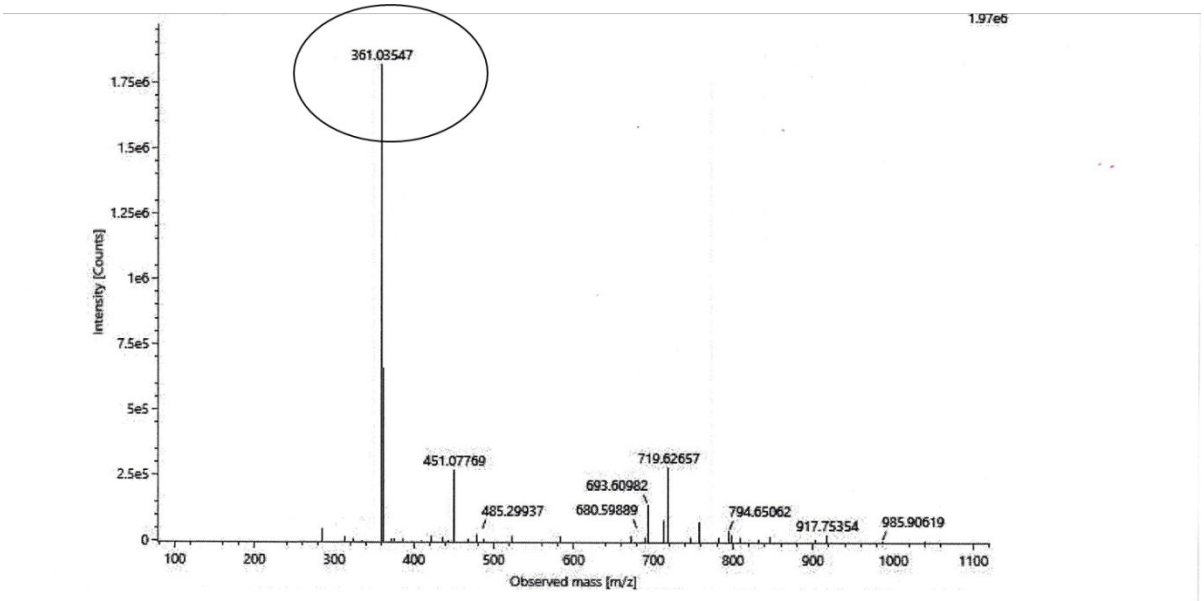

Figure S90: HRMS of Methyl 6-(2-(3-allylureido) phenyl)-4-amino-3-chloropyridine-2-carboxylate**(37)**.